Application Of The Gauge/Gravity Duality In Physical Systems

Thesis submitted for the degree of
Doctor of Philosophy (Science)
in Physics (Theoretical)

by

Ankur Srivastav

Department of Physics

University of Calcutta

2023

Dedicated to my mother.

Acknowledgments

First of all, I would like to acknowledge my supervisor, Dr. Sunandan Gangopadhyay, for his careful doctoral guidance, without which this thesis would not have been shaped in its present form. I am indebted to him for his continuous support, vigorous encouragement, and active involvement in the research supervision. I am also grateful to the thesis advisory committee members for their critical feedback on my research work, which has been immensely useful.

I would like to acknowledge Mr. Akhil Srivastava, who seeded my interest in mathematics; Mr. Brijesh Jha, who first sparked my interest in physics; and Mr. Vishal Deoarshi (Trajectory Educations), who guided me for various competitive exams in physics. I shall always be indebted to Prof. Subhrangshu Sekhar Manna (SNBNCBS, Kolkata) for his exceptional teaching and humble guidance during my master's degree research projects in computational physics, which has left a cherishable impact on my life. I am also thankful to Late Prof. Ranjana Prakash (University of Allahabad), Prof. Geeta Watal (University of Allahabad), Dr. Sanjeev Kant Soni (S.G.T.B. Khalsa College, University of Delhi), Dr. Deepak Chandra (S.G.T.B. Khalsa College, University of Delhi), and Dr. Ravi S. Bhattacharjee (S.G.T.B. Khalsa College, University of Delhi) for their strong academic influence on me, which motivated me to build my career in academia. I am extremely grateful to my master's degree teachers at SNBNCBS who prepared me well for pursuing this doctoral work. I would especially like to acknowledge Prof. Samir Kumar Paul, Prof. Amitabha Lahiri, and Dr. Sakuntala Chatterjee.

I extend my gratitude to my parents and other family members, who have been a great personal support throughout my doctoral journey. Moral support from my sister, Dr. Manjari Shrivastava, is specifically acknowledged. I am also thankful to my friends and colleagues at SNBNCBS who made this journey a little more sparkling. I would especially like to acknowledge my friend, Mr. Achintya Low, for being with me in every up and down over the years, without whom it would have been impossible to complete this journey. My friends and colleagues, Dr. Debabrata Ghorai (Hanyang University, Republic of Korea), Mrs. Rituparna Mandal (University of Hyderabad), Mrs. Megha Dave (Albert Einstein Institute, Hannover), Mr. Neeraj

Kumar (SNBNCBS), and Mr. Anish Das (SNBNCBS), deserve special thanks as fruitful discussions with them were indispensable. I would also like to thank my other colleagues and friends from the Integrated-Ph.D. 2016 batch, especially Ms. Anwesha Chakraborty and Mr. Sayan Routh.

I acknowledge Mrs. Rituparna Mandal, Mr. Neeraj Kumar, Mr. Saurav Kantha, and Dr. Debabrata Ghorai for proofreading some parts of this thesis and sharing their valuable comments. I am thankful to Mr. Atul Rathore as well for assisting me in the translation of the thesis abstract in my mother tongue. I also acknowledge S. N. Bose National Centre for Basic Sciences for providing me with a generous fellowship and a nice research environment. I would like to extend many thanks to the non-academic staff of SNBNCBS for assisting me effectively during my tenure at the institute.

Finally, I want to lovingly acknowledge my wife, Mrs. Megha Dave, for her unconditional support for my dreams, even when it cost us more than four years of physical separation.

Abstract

For the past few years, applied gauge/gravity duality (also known as applied holography) is gaining a lot of attention from physicists working in various research fields. It has become a truly interdisciplinary research topic with applications ranging from quantum matter to cosmology. After its discovery (in the superstring theory) in 1997 by Maldacena in the form of AdS/CFT correspondence [4], it was soon generalised in a wider context for low energy physics without invoking any string theory. Although gauge/gravity duality is still a conjecture, it has provided us with a lot of working toy models for various physical problems such as quantum chromodynamics (QCD), strongly coupled quantum matter, early Universe cosmology etc. Basically, the gauge/gravity duality provides an exact correspondence between a certain gravity theory in $(d+1)$-dimensions and a certain quantum field theory at its d-dimensional boundary. In its most popular version, known as AdS/CFT correspondence, a gravity theory in Anti de-Sitter spacetime is dual to a conformal field theory (CFT) defined on its asymptotic boundary. However, in almost all the practical applications, the gauge/gravity duality is usually considered in a larger context where various deformations on the boundary CFT structure are captured as various deformations in the gravity theory away from the asymptotic boundary.

In this thesis, we shall limit ourselves to the applications of the gauge/gravity duality to physical systems in strongly coupled quantum matter. In 2008, Hartnoll et.al. first proposed a holographic toy model for high temperature superconductors [51]. Since then this model has been explored in various phenomenological settings. We have also utilised this duality to study few holographic models for high temperature layered superconductors [86, 98], vortices in unconventional superfluids [124, 125] and thermoelectric transport properties of Graphene in the Dirac fluid regime [141]. We have especially focused our attention on the Born-Infeld electrodynamics and rotating holographic systems purely from phenomenological perspective. We have analytically obtained condensation operator value and the critical temperature for holographic superconductor models and discovered novel vortex solutions for holographic superfluids. We have further discussed dissipative effects in these holographic superfluids in the presence of Lifshitz scaling and found some intriguing results. Finally, we have also studied a holographic lattice model, in

which we have obtained Born-Infeld corrections to all the thermoelectric transport coefficients and used these results to discuss a two gauge current model [135], which is recently shown to exhibit properties of the Graphene in the Dirac fluid regime.

Abstract in Mother Tongue

पिछले कुछ वर्षों में गेज एवं गुरुत्व में द्वैत के अनुप्रयोगों ने विभिन्न अनुसंधानिक क्षेत्रों में कार्यरत भौतिकविदों का ध्यान आकर्षित किया है। असल मे यह एक अनुसंधानिक अन्तः विषय के रूप मे उभर कर सामने आया है जिसका उपयोग क्वांटम पदार्थों से लेकर ब्रह्माण्ड विज्ञान को समझने के लिए किया जा रहा है। मालदासेना द्वारा १९९७ में एडीएस/सीएफटी के रूप में इसके प्रतिपादन के बाद ज़ल्द ही इसका उपयोग निम्नऊर्जा भौतिकी के लिए बिना किसी स्ट्रिंग सिद्धांत के किया जाने लगा है। यद्यपि गेज एवं गुरुत्व के मध्य यह द्वैतता केवल एक अवधारणा मात्र है, इसका उपयोग विभिन्न भैतिक समस्यायों जैसे कि क्वांटम रंगगतिकी, द्रढयुग्मित क्वांटम पदार्थ एवं प्रारंभिक ब्रह्माण्ड विज्ञान आदि को समझने हेतु किया जा रहा है। मूलरूप से गेज एवं गुरुत्व के मध्य द्वैतता (d+1)-आयामों में एक गुरुत्वाकर्षण के सिद्धांत एवं d-आयामों में एक क्वांटम फील्ड सिद्धांत के मध्य यथार्थ संबंध को स्थापित करता है। इसका सबसे लोकप्रिय उदाहरण, जो कि एडीएस/सीएफटी के रूप में जाना जाता है, एक एंटी डी-सिटर दिक्-काल में गुरुत्वाकर्षण के सिद्धांत एवं दिक्-काल कि सीमा में परिभाषित कन्फार्मल फील्ड सिद्धांत के मध्य द्वैतीय प्रकृति को दर्शाता है। फिर भी लगभग सभी व्यावहारिक अनुप्रयोगों में गेज एवं गुरुत्व के मध्य द्वैतता को वृहत प्रसंग में देखा जाता है जिसमें दिक्-काल कि सीमा में परिभाषित सीएफटी की संरचना में विभिन्न विकृतियों को दिक्-काल की सीमा से दूर गुरुत्वाकर्षण के सिद्धांत में विकृतियों के रूप में प्रारूपित किया जाता है।

इस शोधप्रबंध में हमने गेज एवं गुरुत्व के मध्य द्वैतता का प्रयोग दृढयुग्मित क्वांटम पदार्थों के कुछ भौतिक अवस्थाओं को समझने के लिए किया है। वर्ष २००८ में हर्टनॉल एवं उनके सहयोगिओं ने उच्च तापमान वाले महाचलकों को समझने के लिए प्रथम होलोग्राफिक नमूना प्रस्तुत किया था। उसके बाद से इस नमूने को विविध परिघटनात्मक प्रसंगों में

अन्वेषित किया गया है। हमने भी इस द्वैतता का उपयोग उच्च तापमान वाले परतदार महाचलकों, अपरंपरागत महतरलों में उत्पन्न भंवरों एवं डिराक तरल क्षेत्र में ग्राफीन के तापवैद्युत परिवहन गुडांकों को समझने हेतु होलोग्राफिक प्रतिरूपों के रूप में किया है। मुख्यारूप से हमने पूर्णतः परिघटनात्मक दृश्टि से बॉर्न-इन्फ़ेल्ड वैद्युत्गतिकी एवं घूर्णित होलोग्राफिक प्रतिरूपों पे पर अपना ध्यान केंद्रित किया है। हमने विश्लेषणात्मक विधि से होलोग्राफिक महाचलक प्रतिरूपों के लिए संघनन संकारक मान एवं क्रांतिक तापमान प्राप्त किये हैं तथा होलोग्राफिक महतरलों में नए भंवरों की खोज की है। इसके बाद हमने इन होलोग्राफिक तरलों में लिफशिज़ प्रवर्धन की उपस्थिति में क्षयकारी प्रभावों पर चर्चा की है एवं कुछ चित्ताकर्षित परिणाम प्राप्त किये हैं। अंततः हमने एक होलोग्राफिक लैटिस प्रतिरूप का भी अध्ययन किया है जिसमें हमने सभी तापवैद्युत परिवहन गुणांकों में बॉर्न-इन्फ़ेल्ड संशोधन प्राप्त किये हैं तथा इन परिणामों का उपयोग एक द्विगेज प्रवाह प्रतिरूप पर चर्चा हेतु किया है।

List of Publications

This thesis is based on the following publications.

(1) **A. Srivastav**, S. Gangopadhyay and A. Saha, *Born-Infeld corrections to holographic transport coefficients with spatially modulated chemical potential*, Eur. Phys. J. C 83, 458 (2023).

(2) **A. Srivastav** and S. Gangopadhyay, *Vortices in a rotating holographic superfluid with Lifshitz scaling*, Phys. Rev. D 107, 086005 (2023).

(3) **A. Srivastav** and S. Gangopadhyay, *Novel vortices and the role of a complex chemical potential in a rotating holographic superfluid*, Phys. Rev. D 104, 126004 (2021).

(4) **A. Srivastav** D. Ghorai and S. Gangopadhyay, *p-wave holographic superconductors with massive vector condensate in Born– Infeld electrodynamics*, Eur. Phys. J. C 80, 219 (2020).

(5) **A. Srivastav** and S. Gangopadhyay, *Analytic investigation of rotating holographic superconductors*, Eur. Phys. J. C 79, 340 (2019).

Contents

List of Figures

List of Tables

CHAPTER 1

Introduction to Applied Gauge/Gravity Duality

1.1 Introduction

Over the last two decades, applied gauge/gravity duality has allowed us to have a peek into the realm of physics where conventional wisdom had little to no access. Empirical findings involving strongly interacting condensed matter systems such as strange metals, high-temperature superconductors etc. have been evading explanation in terms of standard perturbative techniques employed to understand weakly interacting systems [1]. Applied gauge/gravity duality provides an ad-hoc explanation to these phenomena in terms of their gravity duals [2]. Basically, the gauge/gravity duality asserts an exact mathematical correspondence between a classical gravity theory and a quantum field theory at the boundary of the spacetime where gravity theory is defined. Although only a few concrete examples of this duality are firmly known, there are a plenty of toy models which indicate the applicability of the gauge/gravity duality in a broader perspective [3]. In fact, most celebrated example to this duality was crystallised in the form of AdS/CFT correspondence by Juan Maldacena in 1997 in [4] within the superstring framework. In this precise equivalence, Maldacena showed a correspondence between $\mathcal{N} = 4$ super Yang-Mills theory in $D = (3 + 1)$ dimensions and type IIB string theory on super anti de-Sitter spacetime $AdS_5 \times S^5$. The foundations of the gauge/gravity duality were finally laid down in [5, 6] with the observation that in large $\mathcal{N}$ limit, classical actions for various fields coupled to Einstein gravity on anti de-Sitter spacetime provide generating functions for correlators of a strongly coupled conformal field theory on the asymptotic boundary of the spacetime. We shall talk about it in more detail in later sections.

For condensed matter systems, perturbative methods for many body physics have been extremely successful. Fermi liquid theory, based on such perturbative methods, is able to explain almost all the known form of materials, even when they have strong inter-particle interactions [7]. However, success of Fermi liquid theory is limited by the presence of quasiparticles in the system [8]. It turns

out that there are indeed some strongly interacting systems in which quasiparticles are not well defined. Fermi liquid theory and its various modifications fell short in explaining such materials. Applied gauge/gravity duality, by construction, maps such a strongly interacting condensed matter system without quasiparticles into a solvable classical gravity model in one higher dimension [9]. Further details on this shall be discussed in later sections.

In the present thesis, we have explored some of the applications of the gauge/gravity duality to understand properties of physical systems like strongly coupled superconductors, superfluids and strange metals. In the subsequent sections, we shall very briefly review some of the essentials of applied gauge/gravity duality and try to motivate the need of phenomenological approach in building these holographic duals.

1.2 Quantum Matter

The electronic theory of quantum matter began in 1928 when Sommerfeld proposed a theory of metals based on independent-electrons obeying Fermi-Dirac statistics. In simple metals, conduction electrons experience mutual Coulomb interactions much weaker in comparison to their kinetic energy and hence, one may perturbatively incorporate it in the independent-electron paradigm [10]. However, the material becomes strongly correlated when the Coulomb interaction is comparable to or larger than the kinetic energy of the moving electrons. The famous Fermi liquid theory, developed by L. D. Landau, can account for interactions beyond the independent-electron paradigm, which implies the existence of a Fermi surface. Fermi surface in momentum space separates the occupied and the empty states. The key ingredient of Landau's Fermi liquid theory are quasiparticles [11]. Quasiparticle are basically long-lived excitations generated near the Fermi surface. According to Fermi liquid theory, a number of characteristics of metals can be explained in terms of interacting quasiparticles in the Fermi system. It should be noted that interaction among quasiparticles could be strong and it would not be possible to ignore these interactions. It turns out that the concept of Fermi surface is very robust and is precisely defined for a Fermi liquid [12]. The existence of a Fermi surface in a material has following consequences,

1) Entropy and specific heat of a metal vanish as temperature approaches absolute zero.

2) Resistivity of a metal, in the presence of impurities, has quadratic temperature dependence:

$$\rho(T) = \rho_0 + AT^2$$

where ρ_0 is the residual resistivity and the coefficient A depends on quasiparticle interactions.

An important result for Fermi liquids is the Luttinger relation, which says that the volume enclosed by the Fermi surface does not change by switching on the interactions. At the heart of Fermi liquid

theory is the adiabatic hypothesis which asserts that the ground state of free fermion gas can evolve smoothly to the unknown ground state of the interacting-fermion gas [7]. In other words, the idea of adiabatic continuity asserts that while the energy levels and the details of the eigenstate wavefunctions evolve subtly, the good quantum numbers of the initial (unperturbed) problem (e.g. the number of nodes in the wavefunction) are still the appropriate description when the perturbations are applied [8]. Another profound characteristic of the Fermi liquid is the Wiedemann-Franz law, a heuristic discussion of which we shall present now.

1.2.1 The Wiedemann-Franz Law

In the most rudimentary model, metals could be seen as free electron gas as in independent-electron paradigm of Sommerfeld. Naturally in that scenario, electrical conductivity would be infinite. However, real metals are not simply free electron gas. There exist an array of ions and an equal number of electrons which can move around a bit amongst these ions. To account for the presence of these ions one may assume a uniform background of positive charge, like a jelly, in which electrons can move freely. This unrealistic oversimplified model is known as jellium model [13]. We need this background positive charge jelly to keep the overall system electrically neutral. Now this positive charge jelly would be subjected to fluctuations of density due to thermal vibrations and a local condensation of jelly will look like a local positive charge which will scatter the electrons. Apart from it, impurities, dislocations and vacant sites etc are also responsible for the scattering of the conduction electrons in a metal. Notice that background ions do not scatter electrons rather they alter the dynamical properties of these electrons (quasiparticle paradigm). To incorporate all such scattering effects one may introduce a relaxation time, τ, so that an electron[1] is free only for τ seconds (on average) before it gets scattered. This relaxation time paradigm was first introduced by Drude and the so called Drude model of metals made very robust predictions about conductivity of metals. Now let us derive the Wiedemann-Franz law within the relaxation time paradigm [10].

Upon the application of electric field, $\mathcal{E}$, the electron would feel a force equal to $e\mathcal{E}$ which would accelerate it. The drift velocity, in the direction of the applied field, acquired in τ seconds would be,

$$\mathbf{u} \sim \frac{e\mathcal{E}\tau}{m} \,. \tag{1.1}$$

Here m is the mass of the electron. For n electrons per unit volume, this drift motion of electrons would be equivalent to an electric current density,

$$\mathbf{J} \sim ne\mathbf{u} \,. \tag{1.2}$$

[1] dressed electron or quasiparticle due to background lattice. For simplicity we shall still use the word electron throughout the text.

Hence, electrical conductivity of this electron system is given by,

$$\sigma = \frac{\mathbf{J}}{\mathcal{E}} \sim \frac{ne^2\tau}{m} \,. \tag{1.3}$$

This simple formula requires a theory for the relaxation time to compare it with the experiments. Now let us see what happens to such an electron system if one applies temperature gradient, ∇T, instead of electric field. An electron at temperature T has energy $\frac{3}{2}k_BT$, while an electron at temperature $T + \delta T$ would have excess energy $\frac{3}{2}k_B\delta T$. Because of the temperature gradient, this excess energy would change along the wire as if there were a potential field along it. It is as if each electron feels a force of magnitude $\frac{3}{2}k_B\nabla T$. This thermodynamic force on electrons would give rise to drift motion of the electrons controlled by various scattering mechanisms as in the previous case of the applied electric field. The average drift velocity of electrons, using the same arguments as before, turns out to be,

$$\mathbf{u} \sim \frac{3k_B\nabla T\tau}{2m} \,. \tag{1.4}$$

As $\frac{3}{2}k_BT$ amount of heat is carried by each electron, the heat current for the electron system would be,

$$\mathbf{Q} \sim n\Big(\frac{3}{2}k_BT\Big)\mathbf{u} \,. \tag{1.5}$$

Hence, the thermal conductivity would be,

$$\kappa = \frac{\mathbf{Q}}{\nabla T} \sim \Big(\frac{3}{2}\Big)^2 \frac{nk_B^2T\tau}{m} \,. \tag{1.6}$$

The importance of these formulae is that one may eliminate the relaxation time τ from it and discover the following general relation,

$$\frac{\kappa}{\sigma T} \sim \Big(\frac{3}{2}\Big)^2 \frac{k_B^2}{e^2} \,. \tag{1.7}$$

This relation is known as Wiedemann-Franz law, discovered empirically in 1853. A full derivation involving statistical quantum mechanics only introduces a numerical factor of $\frac{\pi^2}{3}$ instead of $\big(\frac{3}{2}\big)^2$. This relation is very robust and survives in the Fermi liquid paradigm as well.

Since 1980s a new class of quantum materials are discovered. These materials are inexplicable within the Fermi liquid paradigm and require new insights [14]. Before discussing properties of these new quantum materials, we shall take a short detour to the phenomenon of superconductivity.

1.2.2 Superconductivity

At the beginning of 20th century, Kamerlingh Onnes discovered a strange phenomenon affecting the properties of mercury at very low temperature. He called it suprageleider. It then translated from Dutch into English to be known as supraconductivity, but sooner it mutated into superconductivity [15, 16]. When an electric current passes through a wire it heats up the wire. This effect is known as Joule heating. Surprisingly, there is no Joule heating in superconductors. A superconductor can carry current with no electrical resistance and hence a superconducting coil can carry current round and round for ever without any external source of energy. However, the material needs to be cooled to a very low temperature for this phenomenon to occur. Moreover, the phenomenon of superconductivity remained inexplicable, at least in K. Onnes' lifetime.

A number of empirical facts about superconductivity had been discovered by the early 1930s. The resistance of the materials showing superconductivity would decrease to zero when cooled down below a critical temperature. This zero resistance state at low temperature, however, is amenable to magnetic field. In fact, experiments showed that the critical magnetic field which would destroy superconductivity was rather small. Another important mile-stone in superconductivity research was the discovery of the Meissner-Ochsenfeld effect. In 1933, Walther Meissner and Robert Ochsenfeld managed to show that the magnetic field was not trapped in (as in perfect conductors) the superconductor but appeared to be expelled from it.

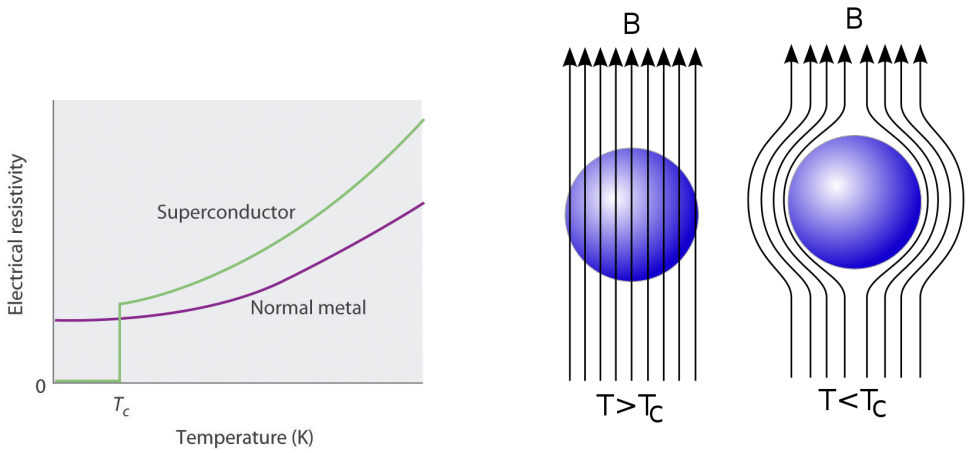

FIGURE 1.1 Two important properties of superconductors

Many of these properties were explained by the Landau-Ginzberg phenomenology [17] and the Bardeen-Cooper-Schrieffer theory (BCS theory) [18], and it was assumed that the theoretical understanding of this surprising phenomenon is almost completed. However, the story of superconductivity was more than what meets the eyes. In 1986, two IBM scientists J. Georg Bednorz and K. Alex Müller had discovered superconductor with critical temperature around 30K [19]. This

discovery was a big blow to the existing theories of superconductivity. All these theories had their roots clinging into weakly coupled quantum field theory. However, these new materials, discovered by Bednorz and Müller, were strongly coupled systems and hence no known field theoretic tricks were able to explain them. Prototype of these high-temperature superconductors (HTSCs) are the Cuprates, which shall be the topic of the subsequent subsection.

1.2.2.1 The Cuprates

The discovery of superconductivity in the copper oxide materials at temperatures higher than expected from the BCS theory is one of the major scientific event of the 20th century. These copper oxide materials are known as Cuprates, and these HTSCs are unusually different from conventional superconductors [20]. The Cuprates are consisted of one or more crystal planes per unit cell having only copper (Cu) and oxygen (O) atoms in a square lattice. It is widely believed that strongly interacting electrons in these CuO_2 planes are the origin of superconductivity in the Cuprates [21]. These 2-dimensional CuO_2 layers are separated by electronically inert ionic buffer layers, known as charge reservoirs, as shown in the Fig.(1.2).

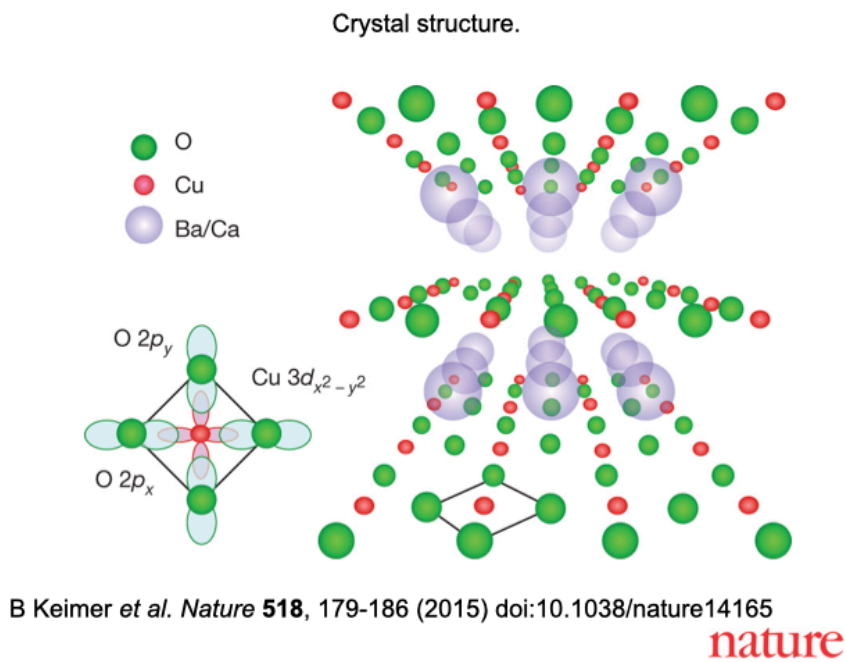

FIGURE 1.2 Crystal Structure of the Cuprates

Since 1986, many HTSCs have been discovered with even higher critical temperature. Fig.(1.3) shows a graph of critical temperature and the year of discovery for different class of HTSCs.

In the absence of doping (electrons or holes), the parent compound for the Cuprates has odd-integer number of electrons per CuO_2 unit cell and it takes a large amount of energy to remove an electron

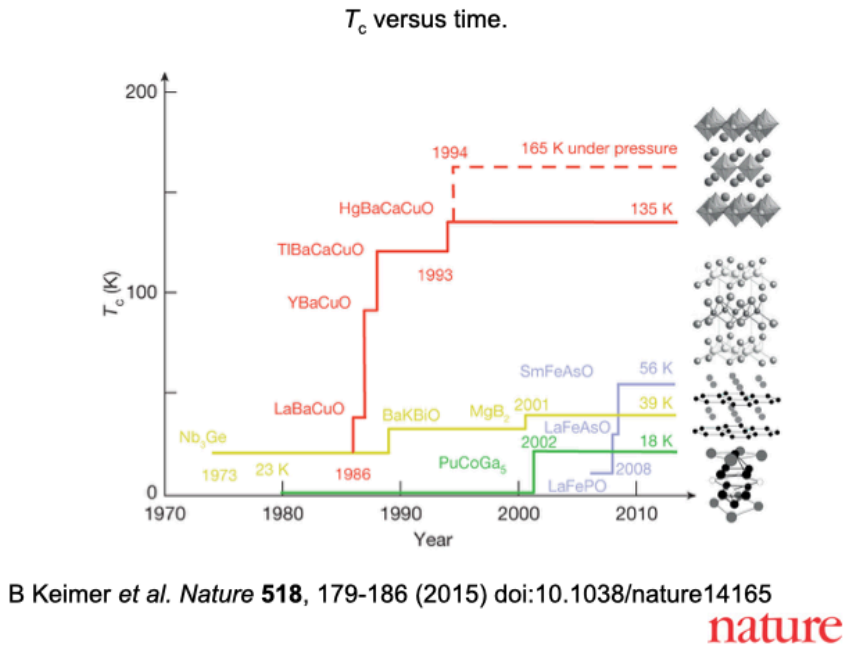

FIGURE 1.3 Year of discovery of various HTSCs and their crystal structures

from one site and add it to another site. This effect produces a sort of traffic jam of electrons and gives rise to the Mott insulating state [14]. However, electrons could be removed (hole doping) and added (electron doping) to the copper oxide planes by changing the chemical composition of the charge reservoirs. As majority of HTSCs fall in the category of hole doped Cuprates [22], we shall discuss the phase diagram of hole-doped system. A typical phase diagram for the hole doped Cuprates [23] is shown in Fig.(1.4). Hole doping decreases antiferromagnetic Mott order and after a critical doping, p_{min}, superconductivity sets in the system. On further increasing the hole doping, superconducting transition temperature starts rising and reaches a maximum at optimal doping, p_{opt}, then it declines on increasing hole doping even further and vanishes at another critical doping, p_{max}. The materials with $p < p_{opt}$ are known as underdoped, $p > p_{opt}$ are overdoped, and $p \sim p_{opt}$ are known as optimally doped.

The phase diagram of the HTSCs is very rich and has so many features that are not explicable with conventional wisdom. Above the superconducting dome sits a metallic phase which is also very different from conventional metals understood within the framework of Fermi liquid theory [67]. This, so called strange metallic phase, is the normal state of many HTSCs near optimal doping which also makes the Cuprates quite different from conventional superconductors.

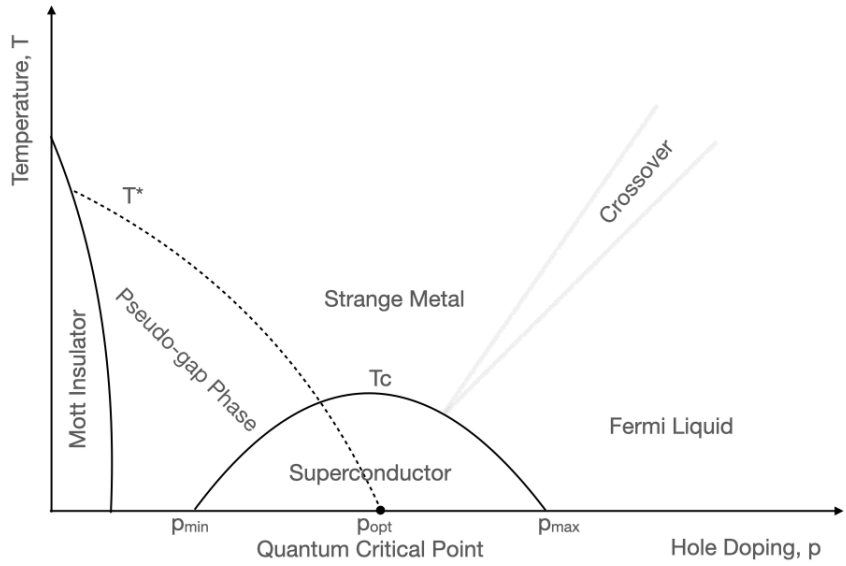

FIGURE 1.4 Graphical representation of a typical hole doped Cuprate HTSC

1.2.2.2 Strange Metals

It was mentioned in the previous subsection that near optimal doping not only the region under the superconducting dome is mysterious but also above the dome lies strange metallic phase which violates Fermi liquid theory. Specifically, well above the critical temperature the conductivity in the Cuprates is much smaller than conventional metals and does not follow conventional temperature and frequency dependence. Marginal Fermi liquid phenomenology does capture some of these strange properties but a general understanding of strange metals is still elusive [14]. Over the years a number of quantum materials have been documented exhibiting similar behaviour which indicates that this is a property of strongly correlated electron systems, and may not be directly related to HTSCs. Among many strange properties of strange metals, violation of Wiedemann-Franz law is very profound and has been observed in various strongly correlated electron systems such as Cuprates, Graphene etc [25–27].

1.2.3 Properties of Non-Fermi Liquid Quantum Matter

Some of the simple consequences of Fermi liquid theory were mentioned in section (1.2). In this section, we shall discuss the general properties of quantum matter which are incompatible with the conventional Fermi liquid paradigm.

1.2.3.1 Linear T resistivity

It is known that electron-phonon(el-ph), electron-impurity (el-imp) and electron-electron (el-el) scatterings contribute strongly to the determination of the resistivity in a metal. However, at low

temperatures, contribution of el-el scattering may dominate over other scattering processes [22]. In standard Fermi liquids, the resistivity due to el-el scattering scales as T^2 as mentioned before. This is an important feature of the Fermi liquid description of the metals and holds true for almost all the known materials at low enough temperatures. It turns out that this quadratic dependence of resistivity on temperature is violated in the Cuprates. The resistivity of the Cuprates rather show a linear T dependency [28–31]. Strange metallic phases in other possible scenarios have also shown such a linear temperature dependency [32, 33], which suggests that this linear T resistivity is a generic feature of a non-Fermi liquid system [8]. Figure (1.5) shows T-linear resistivity for strange metallic compound $La_{2-x}Sr_xCuO_4$.

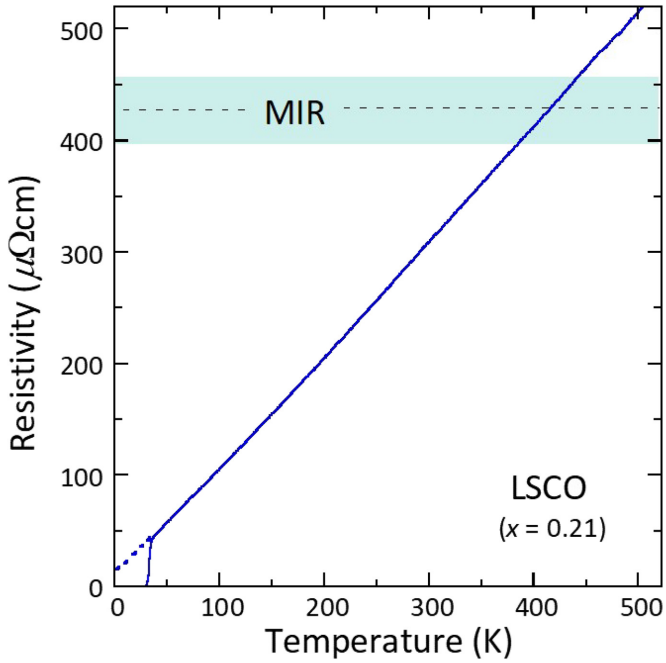

FIGURE 1.5 T-linear resistivity in strange metals (in-plane resistivity of $La_{2x}Sr_xCuO_4$ (x = 0.21) with Mott-Ioffe-Regel (MIR) boundary). (Figure along with modified caption is taken from "Phillips P. W. et al., Stranger than metals. Science 377, eabh4273(2022)")

1.2.3.2 Violations of Wiedemann-Franz Law

Theoretically, the Wiedemann-Franz law is very robust near absolute zero temperatures [34]. It holds in both two and three dimensions, for any strength of interaction and disorder, scattering and magnetic field. This is true not only for simple metals but also for materials with strong electronic correlations such as heavy fermion compounds, or with anisotropic conduction as in quasi-two-dimensional and quasi-one-dimensional systems. All these examples strongly suggest that the ground state of a large number of materials is a Fermi liquid [25]. In case of superconducting phase transition at low temperatures, Wiedemann-Franz law is trivially violated because in the superconducting state, the charge is not transported by fermions but by Cooper pairs, which carry no entropy.

Strange metallic phase above the superconducting dome, shown in Fig.(1.4), indeed shows a strong violation of the Wiedemann-Franz law demonstrating the fact that the ground state of copper oxides may be a non-Fermi liquid state with no quasiparticle description. Another violation of this law was recently observed in the case of ultra-clean Graphene sheet near the charge neutrality point, which is also expected to be the non-Fermi liquid regime [26, 27].

1.2.3.3 Quantum Criticality

For the past few decades, a new kind of phase transition has become a subject of fascination in the research into condensed matter physics. This phase transition is driven by quantum fluctuations, instead of thermal fluctuations, arising due to Heisenberg's uncertainty principle. These quantum fluctuations are known as zero point motion and persist even at absolute zero temperature. The possibility of such a quantum phase transition (QPT) was first discussed by J. Hertz in 1976 [35].

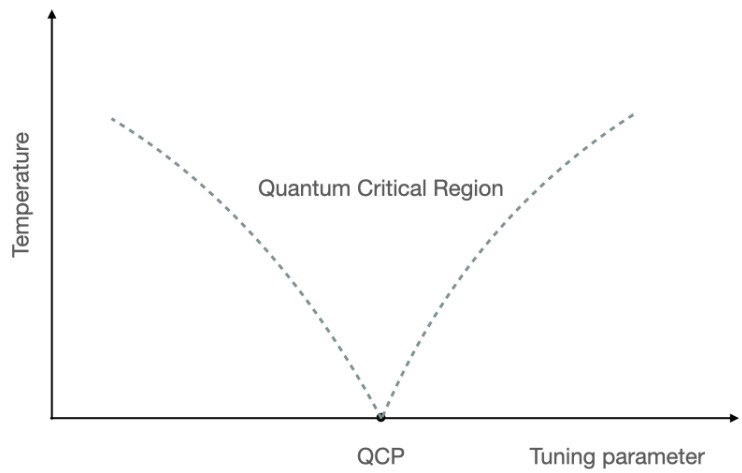

FIGURE 1.6 Schematic diagram of Quantum Critical Region

Recall that the Fermi surface separates the highest energy occupied and lowest energy occupied momentum states for electrons. A simple consequence of the existence of Fermi surface is that thermal energy is absorbed only by electrons near the Fermi surface. It implies that the specific heat of metals is small and it grows linearly with temperature. The coefficient of this linear relation is a rough measure of the effective mass of the highest momentum electron inside the metal and is known as Sommerfeld coefficient. It was observed, in case of quantum phase transitions, that this coefficient is divergent near quantum critical point (QCP). This means that effective mass of electron near QCP approaches infinity on the Fermi surface. Another intriguing property was also noticed near QCP regarding resistivity of metals. Unlike normal metals, resistivity arising due to el-el scattering was found to be linear or quasi-linear near QCP. Based on this, it is strongly believed that the unusual high-T_c superconductivity in the Cuprates is governed by such a quantum criticality [22, 23, 35, 67]. This hypothesis is paradoxically tough to verify as any attempt to

remove the surrounding order would destroy the quantum criticality.

Although QPT occurs strictly at absolute zero temperature and it is not possible to cool down matter to QCP at absolute zero, effects of QCP are prominent even before reaching this point as shown in Fig.(1.6 and 1.7). One should also notice the rough similarity between schematic phase diagram of the Cuprates shown in Fig.(1.4) and schematic diagram for the quantum critical region in Fig.(1.6).

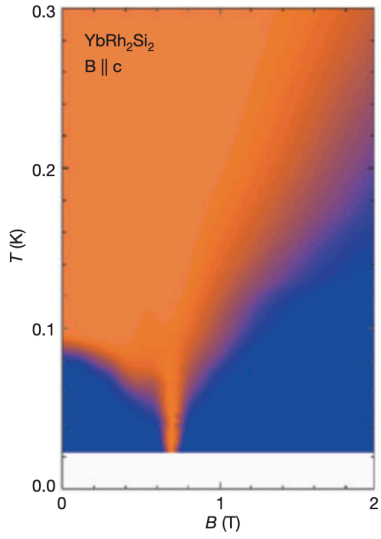

FIGURE 1.7 'Singularity in the phase diagram' illustrated by data taken from the material $YbRh_2Si_2$ where an applied magnetic field tunes the material to a quantum critical point. Blue regions indicate normal metallic behaviour. Orange regions indicate anomalous metallic behaviour with linear resistivity. The singular quantum critical point at absolute zero produces a wide region of unusual metallic behaviour at finite temperatures. (Figure along with caption is taken from "Coleman, P., Schofield, A. Quantum criticality. Nature 433, 226–229 (2005)")

1.3 The Gauge/Gravity Duality

A surprising new direction to understand quantum critical matter emerged by the beginning of 21st century. It is popularly known as the gauge/gravity duality or the holographic duality, which we shall discuss briefly in this section. The gauge/gravity duality relates a quantum field theory (QFT) in d-dimensions to a gravity theory on a $d+1$ dimensional spacetime with a d dimensional asymptotic boundary on which (QFT) is defined [36]. The simplest known example of this duality is the AdS/CFT correspondence [4], which involves a conformal field theory and an anti de-Sitter spacetime. The gauge/gravity duality is still a mathematical conjecture, but a lot of studies indicate that it is true. For the past two decades, this duality has been used to shed light into quantum chromodynamics (QCD), quantum information theory, cosmology and strongly coupled condensed matter systems [1, 2, 37–41]. Our interest in this thesis is on the application of this duality to

understand some physical systems in condensed matter. More specifically, we shall be utilising this duality to understand some universal properties of unconventional superconductors and superfluids.

1.3.1 The Anti de-Sitter Spacetime

The Anti de-Sitter spacetime is the simplest maximally symmetric solution to the Einstein's equations in the presence of a negative cosmological constant. The metric in Anti de-Sitter (AdS) spacetime in $d+1$ dimensions may be written as,

$$ds^2 = L_{AdS}^2\left[-(1+r^2)dt^2 + \frac{dr^2}{(1+r^2)} + r^2 d\Omega_{d-1}^2\right] \tag{1.8}$$

where $d\Omega_{d-1}^2$ is the metric of a unit sphere S^{d-1} and the radius of curvature is L_{AdS}. The Anti de-Sitter spacetime is equipped with bizarre properties [36, 42]. For example, a massive particle can never escape to infinity and the massless particles are able to go infinity and come back in finite time. This is shown in Fig.(1.8).

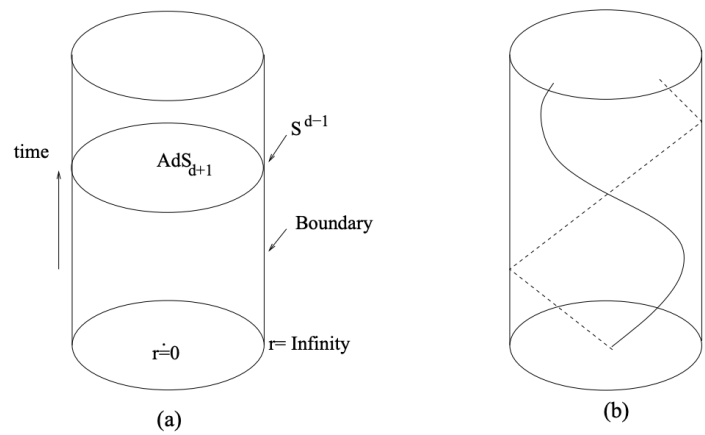

FIGURE 1.8 (a) Penrose diagram of Anti de-Sitter spacetime. (b) Solid line represents massive geodesic and dashed line represents massless geodesic. (Figure is taken from "J. Maldacena. The gauge/gravity duality. arXiv:1106.6073v2 [hep-th]")

The full symmetry group of AdS_{d+1} is SO(2,d), which is the conformal group in d-dimensions. Thus, the local QFT at the asymptotic boundary is a conformal field theory and hence, the name AdS/CFT correspondence.

1.3.2 The GKPW Relation

Soon after the discovery of AdS/CFT correspondence by Maldacena [4] in 1997, general prescription for the gauge/gravity duality was set by seminal works of Steven S. Gubser, Igor R. Klebanov, Alaxander M. Polyakov [5] and Edward Witten [6] (independently). Named after its discoverers,

this GKPW prescription is said to be the backbone of the holographic duality. The GKPW prescription asserts following equality between partition functions for the bulk gravity theory and the boundary quantum field theory [36],

$$\mathcal{Z}_{Gravity}[\Phi \to \phi_0|_{\partial AdS}] = \mathcal{Z}_{QFT}[\phi_0] \tag{1.9}$$

where for simplicity, we have used symbol Φ as shorthand for all kinds of possible fields in the bulk theory and ϕ_0 represents its asymptotic boundary value. This equivalence between partition functions is a strong computational tool [43] as we shall see now.

In a QFT, usually quantity of computational interest is the generating functional which has following schematic form,

$$\mathcal{Z}_{QFT}[\phi_0] = \int DA \exp\left(i\left[S_{QFT} + \int \phi_0 \mathcal{O}(A)\right]\right). \tag{1.10}$$

Here A denotes all the fundamental fields in the QFT which we need to integrate over in the path integral. The action of the theory is given by S_{QFT}, which is a functional of the fields A. $\mathcal{O}(A)$ is an operator of the theory built from the fields A and it must be gauge invariant. In the generating function above, ϕ_0 sources the operator $\mathcal{O}(A)$ and it is non-dynamical. In the context of high-energy physics, correlation functions of the operator $\mathcal{O}$ can be computed by functional differentiation of $\mathcal{Z}_{QFT}[\phi_0]$ with respect to ϕ_0, and subsequently setting $\phi_0 = 0$. The key idea of the gauge/gravity duality is to promote the source ϕ_0 from being a non-dynamical fixed function to a fully dynamical field, in the higher dimensional bulk gravity theory, that will be governed by its own equations of motion. So we have some bulk field $\Phi(x, r)$ controlled only by insisting on its boundary value. It implies that we must require $\Phi(x, r) \to \phi_0(x)$ as we approach the AdS boundary, $r \to 0$. Now according to GKPW prescription, given in eq.(1.9), all the correlation functions for the QFT can also be obtained by functional differentiation of $\mathcal{Z}_{Gravity}[\Phi \to \phi_0|_{\partial AdS}]$ with respect to ϕ_0, and setting source terms to zero at the end. However, it is practically possible only when gravity is classical, in which case we can take saddle point approximation for the bulk partition function: $\mathcal{Z}_{Gravity}[\Phi \to \phi_0|_{\partial AdS}] \simeq e^{iS_{bulk}|_{\Phi\to\phi_0|_{\partial AdS}}}$.

At this point, we would like to emphasise that the GKPW relation allows a two way correspondence which means that it is possible to describe either side of the duality in terms of the variables of the other side.

1.3.2.1 Strong-Weak Duality

The mathematical equivalence of the partition functions, in eq.(1.9), holds true indiscriminately. However, practical computations are not always possible on both sides of the duality. For

example, we have already discussed in the section (1.2) that when electron systems are strongly correlated, it is not always possible to have a meaningful description of it in terms of perturbative QFT. On the other hand when gravity is strong, a quantum theory of gravity is required which is still a long sought puzzle. Various quantum gravity proposals have their own conceptual as well as computational difficulties. So a natural question arises that when is this gauge/gravity duality useful for practical applications? Some heuristic arguments lead to the answer that the gauge/gravity duality is an example of a strong-weak duality which means while considering strong coupling limit of one side of the duality, the other side must be a tractable weakly coupled theory. Let us go through these heuristic arguments now.

The gauge/gravity duality connects the entropy of the black hole in the bulk spacetime with the ordinary thermal entropy of a QFT on the asymptotic AdS boundary. This allows one to compute the thermal properties of QFTs having gravitational duals. It can be argued that the number of fields in the boundary QFT scales like the inverse Newton's constant in the bulk gravity theory. This implies that in order to have a weakly coupled bulk gravity theory, where quantum gravity corrections can be neglected, field theory must have a large number of fields. This requirement of the large number of fields on the boundary theory is related to the fact that the boundary QFT should be a strongly coupled theory. For the detailed description of this reasoning see [36].

1.3.3 Salient Features of The Gauge/Gravity Duality

With the GKPW prescription, some of the important features of the gauge/gravity duality can be listed. This list is often referred to as the holographic dictionary and it is still far from being complete. However, certain entries in this dictionary have been identified and checked in various settings.

1.3.3.1 UV/IR Connection

Ultra-Violet/Infra-Red (UV/IR) connection is one of the important entries in the holographic dictionary [44, 45]. It relates energy scale in the boundary QFT to the radial distances in the bulk direction of the gravity theory. Roughly, physical processes on the boundary QFT at an energy scale $\mathcal{E}$ can be related to the bulk processes on the hypersurface localised at $r \sim \mathcal{E}$. This means that UV (IR) physics in the QFT side is dual to the bulk physics at large (small) values of bulk coordinate r and hence near to (away from) the asymptotic boundary. A pictorial representation of this UV/IR connection is shown in Fig.(1.9) below.

This UV/IR connection, in terms of the hypersurfaces at different radial locations in the bulk theory, is often referred to as the holographic renormalisation or the geometrisation of the renormalisation group flow [47]. Detailed discussion of this topic is theoretically demanding and beyond the scope

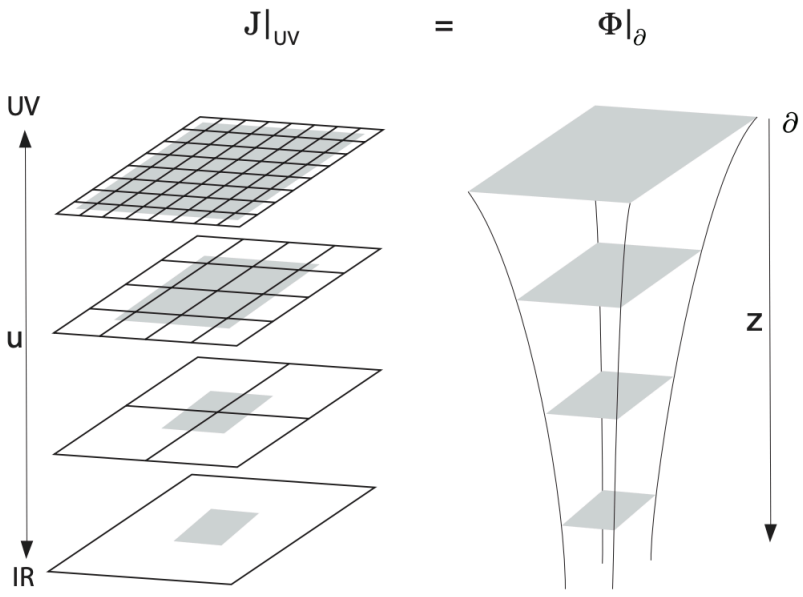

FIGURE 1.9 The Kadanoff-Wilson renormalization of a lattice systems on the boundary QFT (shown on the left) are related to the layers of the higher dimensional space (shown on the right) according to the gauge/gravity duality. Here, u denotes emergent energy scale and Z denotes bulk coordinate. (Figure is taken from "Alfonso V. Ramallo. Introduction to the AdS/CFT correspondence. arXiv:1310.4319v3 [hep-th]" [46])

of the present thesis.

1.3.3.2 Local/Global Symmetry Translation

A simple consequence of the GKPW prescription is that the global spacetime symmetries on the boundary QFT dualises in the bulk gravity theory as local spacetime (isometries) symmetries [36]. Similarly, global internal symmetries on the boundary field theory translate into the bulk gravity theory as local gauge symmetries. This symmetry translation plays a very important for the application of the gauge/gravity duality because to built the gravity duals of boundary systems, since no other general prescription is known so far, often symmetries are the only guide.

1.3.3.3 Field/Operator Map

Another essential entry, for constructing practical models utilising the gauge/gravity duality, in the holographic dictionary is the Field/Operator map. According to this map, boundary values of the fields in the gravity side sources the operator values on the boundary QFT [36]. For example, a scalar field in the bulk gravity theory is dual to a scalar operator, and a vector field is dual to a current operator. A global current operator on the boundary QFT is conserved if the vector field

in the bulk theory is gauged under the corresponding local symmetry. A general discussion of this map is already presented in the section (1.3.2).

1.3.3.4 The Holographic Dictionary

Based on the above discussions, an incomplete holographic dictionary with only relevant entries for the present thesis, is presented in the following table. More detailed dictionary could be found in many other references, e.g. in [1, 2, 40, 41].

Bulk Gravity Theory	**Boundary QFT**
$\mathcal{Z}_{Gravity}$	$\mathcal{Z}_{QFT}$
Scalar Field ϕ	Scalar Operator
Boundary Value of the Fields	Source of the Operators
Boundary Value of the Radial Momentum of the Fields	Vacuum Expectation Value of the Operators
Mass of the Fields	Conformal Dimension of the Operators
Internal Properties of the Fields (Spin, Charge)	Internal Properties of the Operators (Spin, Charge)
Metric Field	Energy-Momentum Tensor
Maxwell Field	Global Internal Symmetry Current
Ratio of Normalisable to Non-normalisable Solution Evaluated at the Boundary	Two-point Correlation Function
Evolution in the Bulk Direction	Renormalisation Group Flow
Hawking Temperature	Finite Temperature
Boundary Value of A_t	Chemical Potential
Black Hole Instabilities	Phase Transitions

TABLE 1.1 The Holographic Dictionary

1.4 Applications of the Gauge/Gravity Duality

Now we are equipped enough to discuss the applications of the gauge/gravity duality. It has been applied to understand diverse problems ranging from elementary particle physics to cosmology. In fact, right after the discovery of the AdS/CFT correspondence, most studied applications were in quantum chromodynamics (QCD) [48]. In 2006, S. Ryu and T. Takayanagi proposed a conjecture within gauge/gravity duality that asserts a quantitative relation between the entanglement entropy of a conformal field theory (CFT) and the geometry of an associated Anti-de Sitter (AdS) spacetime [49]. This additional conjecture opened an interesting possibility for the application of this duality in quantum information theory. A lot of significant work has been done in this direction over the last two decades now. Some proposals in the early universe cosmology

are also available in the literature [41, 50], however these are very limited. Debut of the the gauge/gravity duality in condensed matter systems happened in 2008 when a model for the HTSC was built [51]. Since then, this duality has explored a plethora of strongly correlated condensed matter systems such as unconventional superfluids, strange metals, Mott insulators and Graphene etc. It should be emphasised that many of these systems do not fall under the category where AdS/CFT correspondence is strictly applicable. However, the gauge/gravity duality should be seen in a larger context where deformations in the bulk AdS structure are also dual to deformations from the conformal fixed point of the boundary QFT [1].

There are two approaches to use this duality. In the first approach, which is known as the 'top-down' approach [52], one starts with the underlying string theory model and then consistently constrain it to obtain low energy physics. This approach has been pursued in holographic QCD [53, 54] as well as holographic quantum matter models. However, it is a bit conceptually and computationally difficult to identify right string theory model for low energy systems. On the other hand another approach also exist, which is phenomenological in nature, where rather than writing the full string theory model one can start with building classical gravity models inspired by the symmetries and other physical requirements of the boundary QFT system. This phenomenological approach is known as the 'bottom-up' approach [55] and has been pursued in majority of applications of this duality. In this thesis, also, we have worked with bottom-up holographic models in condensed matter physics. In the next few subsections, we shall briefly mention a few popular applications of this duality.

1.4.1 Quantum Chromodynamics

Quantum chromodynamics (QCD) describes strong interactions in the Standard Model (SM) of particle physics. Even though strong interactions are among basic ingredients of the SM, yet making precise predictions for observables involving strong interactions is extremely difficult. This is so because unlike quantum electrodynamics (QED), QCD does not contain any small dimensionless quantity for perturbative analysis of low-energy observables. Holographic QCD is an attempt to model the bound states of the strong interactions, known as hadrons. Known also as the AdS/QCD, holographic QCD is one of the earliest applications of the gauge/gravity duality. Various holographic QCD models built using top-down and bottom-up approaches made predictions about various aspects of QCD [56]. These holographic models have made some pretty accurate predictions (within 10-25$\%$ for observables below around 1.5GeV) that are insensitive to model details [57].

1.4.2 Cosmology

The application of the gauge/gravity duality in cosmology was envisioned at the very beginning of the 21st century [58–60]. For early universe cosmology, a qualitative new model corresponding to a strongly coupled non-geometric phase of gravity was proposed around 2010 [61]. In this case, the dual picture is of a 3-d Euclidean quantum field theory (EQFT) located at future infinity. In the holographic cosmology, the partition function of the dual EQFT is identified with the wave function of the universe and the cosmic time evolution is mapped to inverse RG flow. However, such a dual description for cosmology is known only for the very early universe, that is the period during inflation, and it provides the initial condition for the subsequent cosmic evolution via Einstein equations. It is interesting to note that predictions of holographic cosmology are consistent with the observations from WMAP [62, 63] and Planck [64, 65] and thus, provide a viable alternative to the Standard Model of cosmology [66].

1.4.3 Condensed Matter Systems

We have discussed in section (1.2) that since the discovery of HTSCs, we have a plethora of strongly correlated systems that escape conventional explanations. In fact, phase diagram for the Cuprates, shown in Fig.(1.4), is least understood in standard Fermi liquid formalism. It is strongly believed now that the mysterious properties in the Cuprate phase diagram arise due to the presence of quantum critical point at optimal doping at zero temperature. The gauge/gravity duality has emerged as an ideal tool to understand these systems [67]. Building on the idea of violation of no-hair theorem for black holes in AdS spacetime by Gubser [68], Hartnoll and colleagues proposed first working model of HTSC utilising this duality [51]. Models of HTSCs based on this duality are now known as holographic superconductors and these models have been analysed in various phenomenological settings [69]. It must be noted though that holographic superconductors and other similar models for quantum matter, built using the gauge/gravity duality, do not constitute microscopic theory. For comparison, consider the case of conventional superconductivity. We know that BCS theory is a microscopic theory that provides us with the underlying mechanism for Cooper pair formation. On the other hand, Landau-Ginzberg free energy analysis is a phenomenological theory that does not account for such microscopics. In a similar way, the applied gauge/gravity duality can be considered as a phenomenological framework to understand these unconventional systems and does not provide any microscopic explanation for these phenomenon [1, 38]. At this point, we would like to emphasise that the original duality conjecture does not prohibit a microscopic understanding of the dual QFT systems. However, one still needs a working theory of quantum gravity for this purpose. Before ending this basic introduction, let us discuss two relevant deformations in the original AdS/CFT correspondence [70, 71].

1.4.3.1 Finite Temperature

As discussed before, the full conformal structure in a condensed matter systems is expected only at the zero temperature quantum critical point. However, our interest is to understand these systems at finite temperature that fall under the quantum critical region. Introduction of such a temperature scale is difficult in conventional QFT methods but in gravity duals, one just need to deform AdS spacetime in the bulk to incorporate a black hole while keeping the asymptotic AdS structure intact. Then according to the holographic dictionary, the Hawking temperature of the black hole act as finite temperature of the boundary field theory systems.

1.4.3.2 Finite Density

Introducing finite density is a bit subtle in the applied gauge/gravity duality. Consider a field theory with a global $U(1)$ current, then a non-zero chemical potential can be introduced as the source of this current. According to the holographic dictionary, we need a vector field dual to this current in the bulk theory and since this current is conserved, vector field must be gauged under $U(1)$ bulk symmetry. In that case, the chemical potential could be considered as the leading order coefficient for the electrostatic potential at the asymptotic boundary. Further, for a consistent gravity theory in the bulk, this electrostatic potential must be sourced from the black hole. This implies that in order to consider finite density boundary systems, we need to consider charged black holes in the bulk gravity dual.

In short, in order to apply the gauge/gravity duality in the boundary systems at finite temperature with finite density, the bulk gravity theory must have a charged black hole geometry with asymptotic Anti de-Sitter structure.

1.5 Organisation of Thesis

We have organised this thesis in the following manner.

1) **Chapter 02:** In this chapter, we have discussed two models of holographic superconductors. In the first model, known as rotating holographic superconductor, we have considered a rotating black hole metric parametrised by a rotation parameter and have analytically investigated its role in the condensation operator and the critical temperature. For this purpose, we have used two analytical techniques known as the matching method and a variational Stürm-Liouville eigenvalue approach. We found that high values of the rotation parameter is favourable for superconductivity in this holographic model. Next, we have analytically investigated a model for p-wave holographic superconductor in the presence of Born-Infeld electrodynamics. In this case, we have concluded that the Born-Infeld electrodynamics is

not supportive to the phenomenon superconductivity in such a holographic modelling.

2) **Chapter 03:** This chapter deals with the analysis of a rotating holographic superfluid. Unlike in the previous chapter, here we have not considered a rotating bulk geometry. Rather, we have introduced rotation into the system via boundary values of the gauge fields. First, we have discovered novel vortex solutions in this holographic superfluid and then we have also discussed their dissipation in the presence of an imaginary chemical potential. We have further extended this investigation to understand behaviour of such a rotating holographic superfluid in the presence of Lifshitz scaling. It is found, in this endeavour, that their is a contrasting behaviour between both the systems.

3) **Chapter 04:** In this chapter, we have considered an inhomogeneous holographic lattice model and obtained the Born-Infeld corrections to all the thermoelectric transport coefficients. We have further studied a two gauge current model in the presence of such a lattice.

4) **Chapter 05:** We have presented thesis summary and a few possible future directions in this last chapter.

CHAPTER 2

Holographic Superconductors

2.1 Introduction

Holographic superconductors were among the first few models that have been studied extensively over the last fifteen years since the advent of the applied gauge/gravity duality in condensed matter physics. These models mimic some of the key properties of the high temperature superconductors (HTSCs) and hence, serve as important toy models to understand these materials. An important class of HTSCs is the layered superconductors such as Cuprates [19,21] and iron pnictides [72,73], in which superconductivity is confined in $(2+1)-$dimensional planes. In the present thesis, we have considered holographic dual to these HTSCs and therefore, worked with $(3+1)$-dimensional gravity theory in the bulk spacetime. A lot of phenomenological investigations, both analytical and numerical, have been done in order to understand these gravity duals and their associated properties [74–81]. For a recent review on various holographic superconductor models, see [69]. In this thesis, we have focused on two important phenomenological parameters and explored their role in certain holographic superconductor models.

We shall discuss these models in the subsequent sections. For now let us first explain an intuitive picture on the working of the holographic superconductors. In typical scenarios on the gravity side, it has been shown that there exist ways through which, at finite temperature, an abelian gauge symmetry could be spontaneously broken for black holes leading to the phenomenon of superconductivity [68]. This symmetry breaking occurs via formation of a superconducting condensate just outside of the black hole horizon. For this to happen, we need a charged matter field which provides superconducting condensate, an interaction that would prevent this condensate to be sucked inside the black hole horizon, and something that keeps it from escaping to infinity [82]. Now in order to imagine a minimalist holographic superconductor, we consider a charged black hole in an asymptomatic anti de-Sitter spacetime with a charged matter field (whose quanta provide a superconducting condensate) around it. Because of no-hair theorem [83], this condensate should not be stable and either should be sucked inside the horizon due to gravitational attraction of the black hole or thrown out towards the AdS boundary due

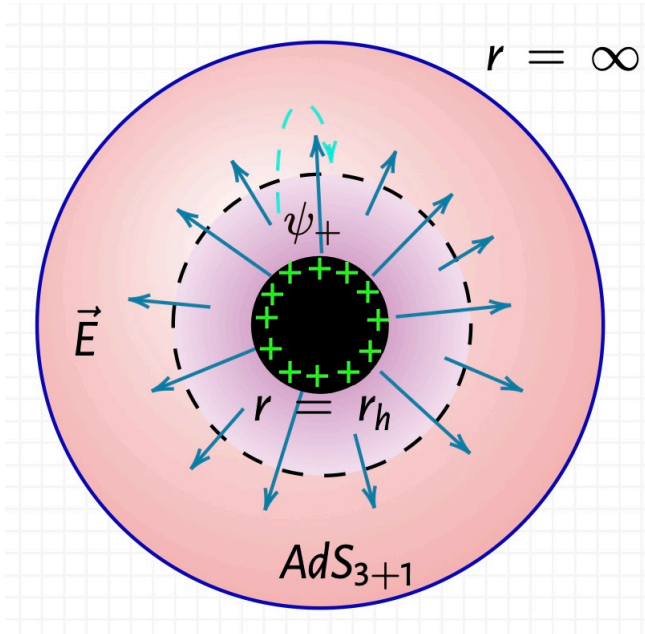

FIGURE 2.1 A pictorial representation of the working mechanism of a typical holographic superconductor model.

to electrostatic repulsion. However, as mentioned in section (1.3.1) that no massive particle can ever reach the AdS-boundary and hence there happen to be a possibility for the condensate to form just outside the black hole horizon. An analogy with the two-fluid model of conventional superconductivity could also be established here if we consider the charged black hole horizon to mimic the normal fluid component and the superconducting condensate to mimic the superconducting component. For the detailed analogy with subtle physical description, we shall recommend [82]. A pictorial representation of this intuitive description is shown in Fig.(2.1).

This chapter is based on the following two papers.

1) *Analytic investigation of rotating holographic superconductors*, **A. Srivastav** and S. Gangopadhyay, Eur.Phys.J.C 79 (2019) 4, 340.

2) *p-wave holographic superconductors with massive vector condensate in Born-Infeld electrodynamics*, **A. Srivastav**, D. Ghorai and S. Gangopadhyay, Eur.Phys.J.C 80 (2020) 3, 219.

In the subsequent section, we have discussed the rotating holographic superconductor in detail.

2.2 Rotating Holographic Superconductor

We know from no-hair theorem that black holes are very simple objects in general relativity. This theorem implies that to characterise a black hole, we need only a few parameters such as mass (M), angular momentum (J), and charge (Q). Hence these parameters provide rich phenomenology from

the bulk (gravity side) perspective. The role of black hole rotation is least studied in holographic superconductor modelling [84, 85] and therefore, we have analytically investigated the role of rotation parameter in a s-wave holographic superconductor [86]. The gravity duals to HTSCs with rotating black holes are called rotating holographic superconductors. In this model, we have obtained the value of the condensation operator as well as the expression for critical temperature using two approximation techniques known as matching method [87] and the Stürm-Liouville eigenvalue approach [81]. We have observed in this investigation that for a certain range of rotation parameter, these rotating holographic superconductors seem more favourable over non-rotating counterparts. Let us now discuss detailed analysis of this model in the subsequent sections.

2.2.1 Building the Gravity Dual

The simplest holographic superconductor model [51] can be built using following Lagrangian density consisting of a complex scalar field, Ψ, minimally coupled to a $U(1)$ gauge field, A_μ,

$$\mathcal{L} = -\frac{1}{4}F^{\mu\nu}F_{\mu\nu} - |D\Psi|^2 - m^2|\Psi|^2 \tag{2.1}$$

where the Faraday tensor and the covariant derivatives are given as,

$$F_{\mu\nu} \equiv \partial_{[\mu}A_{\nu]} \ , \ D \equiv (\partial - iA) \ .$$

We study this model in a rotating black hole geometry with an asymptotic AdS structure in $(3+1)$-dimension. Such a bulk geometry may be given by the following metric [85, 88],

$$ds^2 = -f(r)(\Xi dt - a d\varphi)^2 + r^2(a dt - \Xi d\varphi)^2 + \frac{dr^2}{f(r)} + r^2 d\theta^2 \ . \tag{2.2}$$

The blackening factor is given by $f(r) = \left(r^2 - \frac{r_0^3}{r}\right)$ and $\Xi = (1 + a^2)$. The event horizon of the black hole is at r_0 and the rotation parameter is a, which may take values in the closed interval $[0, 1]$. Here $a = 0$ corresponds to the non-rotating black hole limit. For mathematical convenience, we may set AdS radius, L, to be unity and the cosmological constant is $\Lambda = -3$. Hawking temperature for the above black hole geometry is given by the following expression [85],

$$T = \frac{3r_0}{4\pi\varrho} \tag{2.3}$$

where the rotation parameter, a, enters in the above relation via ϱ which is given as,

$$\varrho = \frac{\Xi}{\Xi^2 - a^2} \ . \tag{2.4}$$

2.2.2 Equations of Motion

Based on symmetry considerations of the metric coefficients in eq.(2.2), we make the following ansatz for the gauge field and the matter field,

$$\Psi = \psi(r) \tag{2.5}$$

$$A_\mu = \delta^t_\mu \Phi(r) + \delta^\varphi_\mu \Omega(r)\ . \tag{2.6}$$

Notice that here we have to consider gauge field $\Omega(r)$ associated to ϕ direction because of the non-diagonal $g_{t\phi}$ term in the metric given in eq.(2.2). Varying the Lagrangian $\mathcal{L}$ in eq.(2.1), we obtain the following coupled equations of motion for the matter field $\psi(r)$ and the gauge fields $\Phi(r)$ and $\Omega(r)$,

$$\psi'' + \left(\frac{f'}{f} + \frac{2}{r}\right)\psi' + \left[\left(\frac{(1+a^2)\Phi + a\Omega}{f(1+a^2+a^4)}\right)^2 - \frac{1}{f}\left(\frac{a\Phi + (1+a^2)\Omega}{r(1+a^2+a^4)}\right)^2 - \frac{m^2}{f}\right]\psi = 0 \tag{2.7}$$

$$\Phi'' + \left(\frac{2(1+a^2)^2}{r(1+a^2+a^4)} - \frac{a^2 f'}{f(1+a^2+a^4)}\right)\Phi' + \left(\frac{2a(1+a^2)}{r(1+a^2+a^4)} - \frac{a(1+a^2)f'}{f(1+a^2+a^4)}\right)\Omega' - \frac{2\psi^2}{f}\Phi = 0 \tag{2.8}$$

$$\Omega'' - \left(\frac{2a^2}{r(1+a^2+a^4)} - \frac{(1+a^2)^2 f'}{f(1+a^2+a^4)}\right)\Omega' - \left(\frac{2a(1+a^2)}{r(1+a^2+a^4)} - \frac{a(1+a^2)f'}{f(1+a^2+a^4)}\right)\Phi' - \frac{2\psi^2}{f}\Omega = 0 \tag{2.9}$$

where derivative with respect to r is denoted with $'$. With the change of the AdS coordinate given by $z = \dfrac{r_0}{r}$, the field eq.(s)(2.7, 2.8, 2.9) take the following form,

$$z\psi'' - \left(\frac{2+z^3}{1-z^3}\right)\psi' + \left(\frac{z((1+a^2)\Phi + a\Omega)^2}{(1+a^2+a^4)^2 r_0^2 (1-z^3)^2} + \frac{z(a\Phi + (1+a^2)\Omega)^2}{(1+a^2+a^4)^2 r_0^2 (z^3-1)} - \frac{m^2}{z(1-z^3)}\right)\psi = 0 \tag{2.10}$$

$$\Phi'' + \frac{3a^2 z^2}{(1+a^2+a^4)(1-z^3)}\Phi' - \frac{2\psi^2}{z^2(1-z^3)}\Phi + \frac{3a(1+a^2)z^2}{(1+a^2+a^4)(1-z^3)}\Omega' = 0 \tag{2.11}$$

$$\Omega'' - \frac{3(1+a^2)^2 z^2}{(1+a^2+a^4)(1-z^3)}\Omega' - \frac{2\psi^2}{z^2(1-z^3)}\Omega - \frac{3a(1+a^2)z^2}{(1+a^2+a^4)(1-z^3)}\Phi' = 0 \tag{2.12}$$

where now $'$ is used to denote derivative with respect to the new coordinate z. Notice that in this new AdS coordinate, horizon of the black hole is at $z = 1$ and the AdS boundary is at $z = 0$.

2.2.3 The Matching Method

We shall now use the matching method [87] to find the critical temperature and the condensation operator values for this rotating holographic superconductor model. In this approach, we first write down the approximate solutions of the field equations for $\psi(r), \Phi(r)$ and $\Omega(r)$ near the black hole horizon and around the asymptotic AdS boundary and after that we match these solutions at some mid-point between the black hole horizon and the AdS boundary to determine the unknown coefficients appearing in the solutions. We also note that due to the finiteness of A_μ at the horizon, the

boundary conditions on the gauge fields A_μ imply $\Phi(1) = 0$ and $\Omega(1) = 0$. We shall carry out the analysis for $m^2 = -2$, which is within the Breitenlohner-Freedman (BF) mass bound[1] [89, 90].

2.2.3.1 Near Horizon Analysis

We start with Taylor expanding the fields $\psi(z), \Phi(z)$ and $\Omega(z)$ near the black hole horizon at $z = 1$ as,

$$\psi(z) = \psi(1) - \psi'(1)(1-z) + \frac{1}{2}\psi''(1)(1-z)^2 + ... \tag{2.13}$$

$$\begin{aligned}\Phi(z) &= \Phi(1) - \Phi'(1)(1-z) + \frac{1}{2}\Phi''(1)(1-z)^2 + ... \\ &\approx -\Phi'(1)(1-z) + \frac{1}{2}\Phi''(1)(1-z)^2\end{aligned} \tag{2.14}$$

$$\begin{aligned}\Omega(z) &= \Omega(1) - \Omega'(1)(1-z) + \frac{1}{2}\Omega''(1)(1-z)^2 + ... \\ &\approx -\Omega'(1)(1-z) + \frac{1}{2}\Omega''(1)(1-z)^2 \, .\end{aligned} \tag{2.15}$$

While writing down these expressions, we have utilised the boundary conditions $\Phi(1) = 0$ and $\Omega(1) = 0$. We also obtain from eq.(2.10) in the $z \to 1$ limit,

$$\psi'(1) = \frac{2}{3}\psi(1) \, . \tag{2.16}$$

Eq.(2.11) in the limit $z \to 1$ provides us with the following constraint,

$$a\Phi'(1) + (1+a^2)\Omega'(1) = 0 \, . \tag{2.17}$$

Eq.(s)(2.10, 2.11, 2.12) in the limit $z \to 1$ also put the following constraints on the second derivatives as well,

$$\psi''(1) = -\left[\frac{4}{9} + \frac{((1+a^2)\Phi'(1) + a\Omega'(1))^2}{18r_0^2(1+a^2+a^4)^2}\right]\psi(1) \tag{2.18}$$

$$\Phi''(1) = -\frac{2}{3}\psi^2(1)\Phi'(1) \tag{2.19}$$

$$\Omega''(1) = -\frac{2}{3}\psi^2(1)\Omega'(1) \qquad . \tag{2.20}$$

The near horizon Taylor series expansions of the fields $\psi(z), \Phi(z)$ and $\Omega(z)$ are now given as,

$$\psi(z) \approx \alpha\left[\frac{1}{3} + \frac{2}{3}z - \left(\frac{2}{9} + \frac{((1+a^2)\beta + a\gamma)^2}{36r_0^2(1+a^2+a^4)^2}\right)(1-z)^2\right] \tag{2.21}$$

$$\Phi(z) \approx \beta(1-z) + \frac{1}{3}\alpha^2\beta(1-z)^2 \tag{2.22}$$

[1]BF bound provides a lower bound for the mass of a bulk field in AdS spacetime above which even a negative mass does not necessarily lead to any instability.

$$\Omega(z) \approx \gamma(1-z) + \frac{1}{3}\alpha^2\gamma(1-z)^2 \ . \tag{2.23}$$

We have set $\alpha \equiv \psi(1)$, $\beta \equiv -\Phi'(1)$ and $\gamma \equiv -\Omega'(1)$ in the above expressions.

2.2.3.2 AdS Boundary Analysis

Near the asymptotic AdS boundary $z \to 0$, the field $\psi(z)$ takes the following form,

$$\psi(z) \approx \frac{\langle \mathcal{O}_\Delta \rangle}{\sqrt{2} r_0^\Delta} z^\Delta \tag{2.24}$$

where Δ represents conformal dimension of the condensation operator $\mathcal{O}$ in the boundary field theory. The vacuum expectation value $\langle \mathcal{O}_\Delta \rangle$ provides the superconducting order parameter in this gravity dual. We have mentioned earlier that we shall be working with $m^2 = -2$, which determines the conformal dimensions to be $\Delta = 1, 2$ [43].
Fields $\Phi(z)$ and $\Omega(z)$ also admit similar expansions near the asymptotic AdS boundary,

$$\Phi(z) \approx \mu - \frac{\rho}{r_0} z \tag{2.25}$$

$$\Omega(z) \approx \nu - \frac{\zeta}{r_0} z \ . \tag{2.26}$$

In the gauge/gravity duality, μ and ρ are interpreted as the chemical potential and the charge density of the boundary system.

2.2.3.3 Critical Temperature

Connecting these approximate solutions at some mid point between both the spacetime boundaries, we might be able to fix some free parameters determining the critical temperature and the condensation operator values. In order to achieve this, we start with comparing the first derivatives of eq.(s)(2.22, 2.25) at some point $z = z_m$,

$$\frac{\rho}{r_0} = \beta + \frac{2}{3}\alpha^2\beta(1 - z_m) \ . \tag{2.27}$$

We may solve this equation for α near $T \sim T_c$ and obtain the following,

$$\alpha = \sqrt{\frac{3}{(1-z_m)}}\sqrt{1 - \frac{T}{T_c}} \ . \tag{2.28}$$

Here we have used eq.(2.3) for T and T_c, which is the critical temperature given by the following expression,

$$T_c = \frac{3}{4\pi\varrho}\sqrt{\frac{\rho}{\tilde{\beta}}} \ , \ \tilde{\beta} = \frac{\beta}{r_0} \ . \tag{2.29}$$

2.2.3.4 Condensation Operator Values

We notice that with the choice of $m^2 = -2$, there are two conformal scaling dimensions, with which condensation operator value scales at the AdS boundary, available in this model. These are $\Delta = (1, 2)$. We shall analyse both of these one by one in the following discussion. We shall start with analysing the case with the conformal dimension $\Delta = 1$.

For $\Delta = 1$, from eq.(2.24) $\psi(z)$ and $\psi'(z)$ can be written as,

$$\psi(z) \approx \frac{\langle \mathcal{O}_1 \rangle}{\sqrt{2} r_0} z \tag{2.30}$$

$$\psi'(z) \approx \frac{\langle \mathcal{O}_1 \rangle}{\sqrt{2} r_0} \, . \tag{2.31}$$

Now we shall match eq.(2.21) with eq.(2.30) and the first derivative of eq.(2.21) with eq.(2.31) at the matching point $z = z_m$, which shall result in the following,

$$\frac{\langle \mathcal{O}_1 \rangle}{\sqrt{2} r_0} z_m = \alpha \left[\frac{1}{3} + \frac{2}{3} z_m - \left(\frac{2}{9} + \frac{((1+a^2)\beta + a\gamma)^2}{36 r_0^2 (1+a^2+a^4)^2} \right) (1 - z_m)^2 \right] \tag{2.32}$$

$$\frac{\langle \mathcal{O}_1 \rangle}{\sqrt{2} r_0} = \alpha \left[\frac{2}{3} + \left(\frac{4}{9} + \frac{((1+a^2)\beta + a\gamma)^2}{18 r_0^2 (1+a^2+a^4)^2} \right) (1 - z_m) \right] . \tag{2.33}$$

Ratio of eq.(s)(2.32) and (2.33) along with using eq.(2.17) to substitute for $\gamma \equiv -\Omega'(1)$ imply the following results,

$$\tilde{\beta} = 2 \sqrt{\frac{(1 + 2 z_m^2)}{(1 - z_m^2)}} (1 + a^2) \, . \tag{2.34}$$

Now substituting for $\tilde{\beta}$ from eq.(2.34) in eq.(2.29) yields the critical temperature for the rotating holographic superconductor with the conformal dimensions $\Delta = 1$,

$$T_c = \frac{3}{4\sqrt{2}\pi} \sqrt[4]{\left(\frac{1 - z_m^2}{1 + 2 z_m^2} \right)} \eta \sqrt{\rho} \tag{2.35}$$

where $\eta = \dfrac{1}{\varrho \sqrt{1 + a^2}} = \dfrac{\Xi^2 - a^2}{\Xi^{3/2}}$.

Derivative of $\eta(a)$ with respect to a shows that η hits a minimum at $a \approx 0.5165$,

$$\frac{d\eta}{da} = \frac{(1+a^2)^{\frac{3}{2}} (2a + 4a^3) - \frac{3}{2} (1 + a^2 + a^4)(1 + a^2)^{\frac{1}{2}}}{(1 + a^2)^3} \, .$$

Hence we find that the critical temperature also attains a minimum at $a \approx 0.5165$.

Now using eqs.(2.17, 2.28, 2.34) in eq.(2.33) near $T \sim T_c$, we determine the condensation operator value to be given by the following expression,

$$\frac{\langle \mathcal{O}_1 \rangle}{T_c} = \frac{8\pi\varrho}{9}\sqrt{\frac{6}{f(a)(1-z_m)}}\left(\frac{2+z_m}{1+z_m}\right)\sqrt{1-\frac{T}{T_c}}\,. \tag{2.36}$$

From eqs.(2.35, 2.36), we notice that the value of the critical temperature and the condensation operator depends on the rotation parameter of the black hole geometry in this gravity dual. We also observe that the critical temperature has a minimum for the value of the rotation parameter $a_{min} \approx 0.5165$. This in turn implies that there is a range of a in the closed interval $[0, a_{min}]$, where the critical temperature decreases and hence superconductivity is not favoured upto this value of rotation parameter. On the other hand, for the rotation parameter $a > a_{min}$, the critical temperature increases indicating a situation favouring superconductivity. We also observe that the value of the condensation operator decreases with an increase in the rotation parameter of the black hole. These observations are presented in fig.(2.2), where the matching method results have also been compared with the SL results.

We shall now focus on the second case, where the conformal dimension is given by $\Delta = 2$. In this case, from eq.(2.24) we may write $\psi(z)$ and $\psi'(z)$ as,

$$\psi(z) \approx \frac{\langle \mathcal{O}_2 \rangle}{\sqrt{2}r_0^2} z^2 \tag{2.37}$$

$$\psi'(z) \approx \frac{\sqrt{2}\langle \mathcal{O}_2 \rangle}{r_0^2} z\,. \tag{2.38}$$

Just like in the previous case, we shall now match eq.(2.21) with eq.(2.37) and derivative of eq.(2.21) with eq.(2.38) at the matching point $z = z_m$ and shall arrive at,

$$\frac{\langle \mathcal{O}_2 \rangle}{\sqrt{2}r_0^2} z_m^2 = \alpha\left[\frac{1}{3} + \frac{2}{3}z_m - \left(\frac{2}{9} + \frac{((1+a^2)\beta + a\gamma)^2}{36r_0^2(1+a^2+a^4)^2}\right)(1-z_m)^2\right] \tag{2.39}$$

$$\frac{\sqrt{2}\langle \mathcal{O}_2 \rangle}{r_0^2} z_m = \alpha\left[\frac{2}{3} + \left(\frac{4}{9} + \frac{((1+a^2)\beta + a\gamma)^2}{18r_0^2(1+a^2+a^4)^2}\right)(1-z_m)\right]\,. \tag{2.40}$$

Again taking the ratio of eq.(2.39) and eq.(2.40) and using eq.(2.17) to substitute for γ, we get

$$\tilde{\beta} = 2\sqrt{\frac{(1+5z_m)}{(1-z_m)}}(1+a^2)\,. \tag{2.41}$$

Once again $\tilde{\beta}$ could be substituted from eq.(2.41) in eq.(2.29), which shall result in the following

expression for the critical temperature,

$$T_c = \frac{3}{4\sqrt{2}\pi}\sqrt[4]{\left(\frac{1-z_m}{1+5z_m}\right)}\eta\sqrt{\rho}\,. \tag{2.42}$$

where η depends on the rotation parameter and is defined above.

Utilising eq.(s)(2.17, 2.28, 2.41) in eq.(2.40) near $T \sim T_c$, we shall obtain the expression for the condensation value,

$$\frac{\sqrt{\langle\mathcal{O}_2\rangle}}{T_c} = \frac{4\pi\varrho}{3}\sqrt[4]{\frac{2(2+z_m)^2}{3f(a)(1-z_m)}}\sqrt[4]{1-\frac{T}{T_c}}\,. \tag{2.43}$$

This once again exhibits the effect of the rotation parameter of the black hole geometry. The dependence of T_c and the condensation operator on the rotation parameter has been displayed in fig.(2.2).

In the following table, we have presented the results for the critical temperature T_c for different choices of the matching points z_m for the two possible values of the condensation operators. It can be seen that the results are in agreement with the SL results given in [85].

Matching point, z_m	T_c from matching method	
	$\Delta = 1$	$\Delta = 2$
0.1	$0.1675\eta\sqrt{\rho}$	$0.1486\eta\sqrt{\rho}$
0.3	$0.1582\eta\sqrt{\rho}$	$0.1228\eta\sqrt{\rho}$
0.5	$0.1419\eta\sqrt{\rho}$	$0.1038\eta\sqrt{\rho}$
0.7	$0.1203\eta\sqrt{\rho}$	$0.0858\eta\sqrt{\rho}$

TABLE 2.1 Critical temperature at different matching points for $\Delta = 1, 2$.

2.2.4 The Stürm-Liouville Eigenvalue Approach

In this subsection, we shall solve EOMs given by eq.(s)(2.10, 2.11, 2.12) using a variational approach, also known as the Stürm-Liouville eigenvalue method and compare our results with those obtained from the matching method discussed in the previous subsection. We first recall that the scalar field $\psi(z)$, should vanish at the critical temperature T_c. This is so because $\psi(z)$ represents superconducting order parameter which is zero at the critical temperature and starts gaining profile through a second order phase transition just below T_c. Hence, at $T = T_c$ eq.(s)(2.11, 2.12) simplify

as,

$$\Phi'' + \frac{3a^2z^2}{(1+a^2+a^4)(1-z^3)}\Phi' + \frac{3a(1+a^2)z^2}{(1+a^2+a^4)(1-z^3)}\Omega' = 0 \tag{2.44}$$

$$\Omega'' - \frac{3(1+a^2)^2z^2}{(1+a^2+a^4)(1-z^3)}\Omega' - \frac{3a(1+a^2)z^2}{(1+a^2+a^4)(1-z^3)}\Phi' = 0\ . \tag{2.45}$$

Eq.(s)(2.44, 2.45) are still coupled differential equations for $\Phi(z)$ and $\Omega(z)$. However, we may decouple these eq.(s) in the following way,

$$\Phi''' + \frac{2}{z}\left(\frac{2z^3+1}{z^3-1}\right)\Phi'' = 0 \tag{2.46}$$

$$\Omega''' + \frac{2}{z}\left(\frac{2z^3+1}{z^3-1}\right)\Omega'' = 0\ . \tag{2.47}$$

These decoupled eq.(s)(2.46, 2.47) yield the following exact solutions for $\Phi(z)$ and $\Omega(z)$ [85].

$$\Phi(z) = \mu - \frac{\rho}{r_{0c}}z + C_1\left[\sqrt{12}\arctan\left(\frac{1+2z}{\sqrt{3}}\right) + \ln\left(\frac{1+z+z^2}{(1-z)^2}\right)\right] \tag{2.48}$$

$$\Omega(z) = \nu - \frac{\zeta}{r_{0c}}z + C_2\left[\sqrt{12}\arctan\left(\frac{1+2z}{\sqrt{3}}\right) + \ln\left(\frac{1+z+z^2}{(1-z)^2}\right)\right]\ . \tag{2.49}$$

Here μ, ρ, ν and ζ have the usual interpretations in the boundary field theory in the gauge/gravity duality. Now in view of the boundary conditions at the horizon $\Phi(1) = 0$ and $\Omega(1) = 0$, we write

$$\Phi = \lambda r_{0c}(1-z) \tag{2.50}$$

$$\Omega = \bar{\lambda} r_{0c}(1-z)\ . \tag{2.51}$$

Where $\lambda = \dfrac{\rho}{r_{0c}^2}$ and r_{0c} is the horizon radius at the critical temperature. $\bar{\lambda}$ is related to λ through following relation

$$a\lambda + (1+a^2)\bar{\lambda} = 0\ . \tag{2.52}$$

This relation readily follows from using eq.(s)(2.17, 2.50, 2.51).

Now considering the following boundary scaling form of the field $\psi(z)$,

$$\psi(z) = \frac{\langle \mathcal{O}_\Delta \rangle}{\sqrt{2}r_0^\Delta} z^\Delta F(z) \tag{2.53}$$

such that the boundary conditions are still satisfied with $F(0) = 1$ and $F'(0) = 0$. With this form

of the field $\psi(z)$, eq.(2.10) becomes

$$-F'' + \frac{1}{z}\left(\frac{2+z^3}{1-z^3} - 2\Delta\right)F' + \frac{\Delta^2 z}{(1-z^3)}F = \frac{\tilde{\lambda}^2}{(1+z+z^2)^2}F \tag{2.54}$$

where $\tilde{\lambda} = \dfrac{\lambda}{(1+a^2)}$.

2.2.4.1 Analysis for Conformal Dimension $\Delta = 1$

In this case, eq.(2.54) takes the following form,

$$-F'' + \frac{3z^2}{(1-z^3)}F' + \frac{z}{(1-z^3)}F = \frac{\tilde{\lambda}^2}{(1+z+z^2)^2}F \ . \tag{2.55}$$

This equation may be rearranged into the Stürm-Liouville eigenvalue equation in the following manner,

$$\frac{d(p(z)F')}{dz} + q(z)F + \tilde{\lambda}^2 r(z)F = 0 \ . \tag{2.56}$$

Here $p(z) = (1-z^3),\ q(z) = -z$ and $r(z) = \left(\dfrac{1-z}{1+z+z^2}\right)$. According to the standard Stürm-Liouville eigenvalue approach, the eigenvalue $\tilde{\lambda}^2$ which minimizes the above expression may be obtained by the following integral,

$$\tilde{\lambda}^2 = \frac{\int_0^1 dz\Big(p(z)F'^2 - q(z)F^2\Big)}{\int_0^1 dz r(z)F^2} = \frac{\int_0^1 dz\Big((1-z^3)F'^2 + zF^2\Big)}{\int_0^1 dz \dfrac{(1-z)}{(1+z+z^2)}F^2} \ . \tag{2.57}$$

In order to proceed further, we consider a trial function for $F(z)$ with a parameter $\tilde{\alpha}$ such that it satisfy the required boundary conditions viz. $F_{\tilde{\alpha}}(0) = 1$ and $F'_{\tilde{\alpha}}(0) = 0$,

$$F_{\tilde{\alpha}}(z) = (1 - \tilde{\alpha}z^2) \tag{2.58}$$

With this trial function, eq.(2.57) takes the following form,

$$\tilde{\lambda}^2_{\tilde{\alpha}} = \frac{\int_0^1 dz\Big(4\tilde{\alpha}^2 z^2(1-z^3) + z(1-\tilde{\alpha}z^2)^2\Big)}{\int_0^1 dz \dfrac{(1-z)}{(1+z+z^2)}(1-\tilde{\alpha}z^2)^2}$$

$$\tilde{\lambda}^2_{\tilde{\alpha}} = \frac{6 - 6\tilde{\alpha} + 10\tilde{\alpha}^2}{2\sqrt{3}\pi - 6ln3 + 4(\sqrt{3}\pi + 3ln3 - 9)\tilde{\alpha} + (12ln3 - 13)\tilde{\alpha}^2} \ . \tag{2.59}$$

In this expression, one may notice that $\tilde{\lambda}^2_{\tilde{\alpha}}$ attains a minimum with respect to $\tilde{\alpha}$ at $\tilde{\alpha} \approx 0.2389$. This in turn determine the eigenvalue as,

$$\tilde{\lambda}^2_{0.2389} \approx 1.268 \ .$$

Using eq.(2.3), the critical temperature could be given by the following relation,

$$\begin{aligned} T_c = \frac{3r_{0c}}{4\pi\varrho} &= \frac{3}{4\pi\varrho}\sqrt{\frac{\rho}{\lambda}} \\ &= \frac{3}{4\pi\varrho}\sqrt{\frac{\rho}{\tilde{\lambda}}}\frac{1}{\sqrt{1+a^2}} \\ &= \frac{3}{4\pi}\eta\sqrt{\frac{\rho}{\tilde{\lambda}}} \ . \end{aligned} \tag{2.60}$$

Again $\eta = \dfrac{1}{\varrho\sqrt{1+a^2}}$.

Replacing $\tilde{\lambda}$ in eq.(2.60) with the estimated value of $\tilde{\lambda}_{0.2389}$ obtained through the Stürm-Liouville analysis shown above, we finally get the critical temperature,

$$T_c = 0.225\eta\sqrt{\rho} \ . \tag{2.61}$$

We shall now focus on finding the value of condensation operator using this analysis. For this purpose, we first write down the following approximate expressions for the fields $\psi(z)$, $\Phi(z)$ and $\Omega(z)$ near the critical temperature T_c,

$$\psi(z) = \frac{\langle\mathcal{O}_1\rangle}{\sqrt{2}r_0} z F(z) \tag{2.62}$$

$$\frac{\Phi(z)}{r_0} \approx \lambda(1-z) + \frac{\langle\mathcal{O}_1\rangle^2}{r_0^2}\chi(z) \tag{2.63}$$

$$\frac{\Omega(z)}{r_0} \approx \bar{\lambda}(1-z) + \frac{\langle\mathcal{O}_1\rangle^2}{r_0^2}\varsigma(z) \tag{2.64}$$

where $\chi(z)$ and $\varsigma(z)$ are fluctuation fields.

Now using eq.(s)(2.62, 2.63, 2.64) in eq.(s)(2.11, 2.12), we get the following field eq.(s) for the fluctuation fields $\chi(z)$ and $\varsigma(z)$ to be

$$\chi'' + \frac{3az^2\Lambda'}{(1+a^2+a^4)(1-z^3)} = \frac{\lambda(1-z)F^2}{(1-z^3)} \tag{2.65}$$

$$\varsigma'' + \frac{3(1+a^2)z^2\Lambda'}{(1+a^2+a^4)(z^3-1)} = \frac{\bar{\lambda}(1-z)F^2}{(1-z^3)} \tag{2.66}$$

where $\Lambda(z)$ is given by

$$\Lambda(z) = a\chi(z) + (1+a^2)\varsigma(z) \, .$$

Now multiplying eq.(2.65) by a and eq.(2.66) by $(1+a^2)$ and adding them up together with the condition (2.52), we arrive at the following equation that is entirely given in terms of $\Lambda(z)$

$$\Lambda'' + \frac{3z^2}{(z^3-1)}\Lambda' = 0 \, . \tag{2.67}$$

With the boundary conditions discussed earlier, we can solve eq.(2.67) to obtain

$$\Lambda'(z) = 0 \, . \tag{2.68}$$

With this condition eq.(2.65) reduces to

$$\chi'' = \frac{\lambda(1-z)}{(1-z^3)}F^2 \, . \tag{2.69}$$

Integrating eq.(2.69) with respect to z between 0 and 1, we get the following result

$$\chi'(1) - \chi'(0) = \lambda \int_0^1 dz \frac{1-z}{1-z^3}F^2 \, . \tag{2.70}$$

We now expand the fluctuation field $\chi(z)$ about $z = 0$ in the following manner,

$$\chi(z) = \chi(0) + \chi'(0)z + ... \, . \tag{2.71}$$

Using the above expansion of $\chi(z)$ in eq.(2.63) and equating it to the asymptotic solution for $\Phi(z)$ given in eq.(2.25), we get

$$\frac{\mu}{r_0} - \frac{\rho}{r_0^2}z = \lambda(1-z) + \frac{\langle \mathcal{O}_1 \rangle^2}{r_0^2}(\chi(0) + \chi'(0)z + ...) \, . \tag{2.72}$$

Comparing the coefficients of z on both sides of the above equation gives

$$\frac{\rho}{r_0^2} = \lambda - \frac{\langle \mathcal{O}_1 \rangle^2}{r_0^2}\chi'(0) \, . \tag{2.73}$$

Now replacing $\chi'(z)$ from eq.(2.70) in eq.(2.73), we obtain

$$\frac{\rho}{r_0^2} = \lambda\left(1 + \frac{\langle \mathcal{O}_1 \rangle^2}{r_0^2}\mathcal{A}\right) - \frac{\langle \mathcal{O}_1 \rangle^2}{r_0^2}\chi'(1) \tag{2.74}$$

where $\mathcal{A} = \int_0^1 dz \frac{1-z}{1-z^3} F^2$. To proceed further we need the value of $\chi'(1)$ in the above equation.

To obtain this, we need to recall that we have earlier found the exact solutions for the fields $\Phi(z)$ and $\Omega(z)$ at $T = T_c$ in eq.(s)(2.50, 2.51). We can assume that near T_c, the field $\Phi(z)$ takes the following form

$$\Phi = \lambda r_0 (1-z) + \frac{\langle \mathcal{O}_1 \rangle^2}{r_0} \bigg(\chi(1) + (z-1)\chi'(1) + ... \bigg) \, . \tag{2.75}$$

We now equate the coefficient of $(1-z)$ in above equation with that of the solution for the field $\Phi(z)$ at T_c given by eq.(2.50)

$$\lambda r_{0c} = \lambda r_0 - \frac{\langle \mathcal{O}_1 \rangle^2}{r_0} \chi'(1) \, . \tag{2.76}$$

Rearranging the above equation, we have

$$\chi'(1) = \frac{\lambda r_0}{\langle \mathcal{O}_1 \rangle^2} (r_0 - r_{0c}) \, . \tag{2.77}$$

Using the above relation in eq.(2.74), we obtain

$$\frac{\rho}{r_0^2} = \lambda \bigg(\frac{r_{0c}}{r_0} + \frac{\langle \mathcal{O}_1 \rangle^2}{r_0^2} \mathcal{A} \bigg) \, . \tag{2.78}$$

Replacing r_0, ρ and λ using eq.(s)(2.3, 2.60) finally leads to the following result for the condensation operator value,

$$\langle \mathcal{O}_1 \rangle = \gamma T_c \sqrt{\bigg(1 - \frac{T}{T_c} \bigg)} \tag{2.79}$$

$$\gamma = \frac{4\pi}{3} \bigg(\frac{1+a^2}{1+a^2+a^4} \bigg) \sqrt{\frac{1}{\mathcal{A}}} \, .$$

Once again we notice that the rotation parameter a affects the condensate in a non-trivial way.

2.2.4.2 Analysis for Conformal Dimension $\Delta = 2$

We shall now consider the analysis for other conformal dimensions given by $\Delta = 2$. In this case, eq.(2.54) reduces to the following form,

$$-F'' + \frac{1}{z} \bigg(\frac{5z^3 - 2}{1-z^3} \bigg) F' + \frac{4z}{(1-z^3)} F = \frac{\tilde{\lambda}^2}{(1+z+z^2)^2} F \tag{2.80}$$

which we may, like previously, recast into the Stürm-Liouville eigenvalue form,

$$\frac{d(1-z^3)F'z^2}{dz} - 4z^3F + \frac{\tilde{\lambda}^2 z^2(1-z)}{(1+z+z^2)}F = 0\ . \tag{2.81}$$

Here the eigenvalue $\tilde{\lambda}^2$ reads

$$\tilde{\lambda}^2 = \frac{\int_0^1 dz\Big(z^2(1-z^3)F'^2 + 4z^3F^2\Big)}{\int_0^1 dz\frac{z^2(1-z)}{(1+z+z^2)}F^2}\ . \tag{2.82}$$

Once again we take $F_{\tilde{\alpha}}(z) = (1-\tilde{\alpha}z^2)$ as a trial function to estimate the eigenvalue. With this trial function, we may now write eq.(2.82) as,

$$\begin{aligned}\tilde{\lambda}^2_{\tilde{\alpha}} &= \frac{\int_0^1 dz\Big(4\tilde{\alpha}^2(z^4-z^7) + 4z^3(1-\tilde{\alpha}z^2)^2\Big)}{\int_0^1 dz\frac{z^2(1-z)}{(1+z+z^2)}(1-\tilde{\alpha}z^2)^2} \\ &= \frac{60-80\tilde{\alpha}+48\tilde{\alpha}^2}{2.62765-(1.8335)\tilde{\alpha}+(0.45561)\tilde{\alpha}^2}\ .\end{aligned} \tag{2.83}$$

We found that eq.(2.83) attains its minima for $\tilde{\alpha} \approx 0.60159$. This gives

$$\tilde{\lambda}^2_{0.60159} \approx 17.309\ .$$

The critical temperature, hence, is given by the following relation,

$$\begin{aligned}T_c = \frac{3r_{0c}}{4\pi\varrho} &= \frac{3}{4\pi\varrho}\sqrt{\frac{\rho}{\lambda}} \\ &= \frac{3}{4\pi\varrho}\sqrt{\frac{\rho}{\tilde{\lambda}}}\frac{1}{\sqrt{1+a^2}} \\ &= \frac{3}{4\pi}\eta\sqrt{\frac{\rho}{\tilde{\lambda}}} \\ &= 0.117\eta\sqrt{\rho}\end{aligned} \tag{2.84}$$

where we have used the minimised value of $\tilde{\lambda}^2$, given by $\tilde{\lambda}^2_{0.60159}$, to determine this critical temperature.

As in the previous case, we may now consider the following forms for the fields $\psi(z), \Phi(z)$ and

$\Omega(z)$,

$$\psi(z) = \frac{\langle \mathcal{O}_2 \rangle}{\sqrt{2} r_0^2} z^2 F(z) \tag{2.85}$$

$$\frac{\Phi(z)}{r_0} \approx \lambda(1-z) + \frac{\langle \mathcal{O}_2 \rangle^2}{r_0^4} \chi(z) \tag{2.86}$$

$$\frac{\Omega(z)}{r_0} \approx \bar{\lambda}(1-z) + \frac{\langle \mathcal{O}_2 \rangle^4}{r_0^4} \varsigma(z) \ . \tag{2.87}$$

Using eq.(s)(2.85, 2.86, 2.87) in eq.(s)(2.11, 2.12), we get the following equations in terms of the fluctuation fields,

$$\chi'' + \frac{3az^2\Lambda'}{(1+a^2+a^4)(1-z^3)} = \frac{\lambda(1-z)z^2F^2}{(1-z^3)} \tag{2.88}$$

$$\varsigma'' + \frac{3(1+a^2)z^2\Lambda'}{(1+a^2+a^4)(z^3-1)} = \frac{\bar{\lambda}(1-z)z^2F^2}{(1-z^3)} \tag{2.89}$$

where $\Lambda(z) = a\chi(z) + (1+a^2)\varsigma(z)$.

Multiplying eq.(2.88) by a and eq.(2.89) by $(1+a^2)$ and adding them up together with the boundary condition given in eq.(2.52), we arrive at the following equation

$$\Lambda'' + \frac{3z^2}{(z^3-1)}\Lambda' = 0 \ . \tag{2.90}$$

Solving this equation would yield the following result,

$$\Lambda'(z) = 0. \tag{2.91}$$

now using eq.(2.91) in eq.(2.88) gives the following equation,

$$\chi'' = \frac{\lambda(1-z)}{(1-z^3)} z^2 F(z)^2 \ . \tag{2.92}$$

We may now Integrate this equation with respect to z between 0 and 1 and arrive at following result,

$$\chi'(1) - \chi'(0) = \lambda \int_0^1 dz \frac{1-z}{1-z^3} z^2 F(z)^2 \ . \tag{2.93}$$

Notice that we may expand the fluctuation field $\chi(z)$ about $z = 0$ in the following manner,

$$\chi(z) = \chi(0) + \chi'(0)z + ... \tag{2.94}$$

and using above expansion in eq.(2.86) and equating it to the asymptotic solution for $\Phi(z)$ given

in eq.(2.25), we get

$$\frac{\mu}{r_0} - \frac{\rho}{r_0^2} z = \lambda(1-z) + \frac{\langle \mathcal{O}_2 \rangle^2}{r_0^4} (\chi(0) + \chi'(0) z + ...) \ . \tag{2.95}$$

Comparing the coefficients of z on both sides of eq.(2.95), we get

$$\frac{\rho}{r_0^2} = \lambda - \frac{\langle \mathcal{O}_2 \rangle^2}{r_0^4} \chi'(0) \ . \tag{2.96}$$

In this expression, we may now replace $\chi'(0)$ from eq.(2.93) and obtain the following result,

$$\frac{\rho}{r_0^2} = \lambda \left(1 + \frac{\langle \mathcal{O}_2 \rangle^2}{r_0^4} \mathcal{B} \right) - \frac{\langle \mathcal{O}_2 \rangle^2}{r_0^4} \chi'(1) \tag{2.97}$$

where $\mathcal{B} = \int_0^1 dz \frac{1-z}{1-z^3} z^2 F(z)^2$.

Once again we may use the exact solutions for the fields at $T = T_c$ given by eq.(s)(2.50, 2.51) and $\psi(z) = 0$ to estimate $\chi'(1)$. Also, near T_c we may write the following expression for the field $\Phi(z)$

$$\Phi = \lambda r_0 (1-z) + \frac{\langle \mathcal{O}_2 \rangle^2}{r_0^3} \left(\chi(1) + (z-1)\chi'(1) + ... \right) \ . \tag{2.98}$$

Equating the coefficients of $(1-z)$ in this equation with that of the solution at $T = T_c$ given in eq.(2.50), we get

$$\lambda r_{0c} = \lambda r_0 - \frac{\langle \mathcal{O}_2 \rangle^2}{r_0^3} \chi'(1) \ . \tag{2.99}$$

Rearranging eq.(2.99), we find

$$\chi'(1) = \frac{\lambda r_0^3}{\langle \mathcal{O}_2 \rangle^2} (r_0 - r_{0c}) \ . \tag{2.100}$$

Now we use the above relation for $\chi'(1)$ in eq.(2.99) to obtain,

$$\frac{\rho}{r_0^2} = \lambda \left(\frac{r_{0c}}{r_0} + \frac{\langle \mathcal{O}_2 \rangle^2}{r_0^4} \mathcal{B} \right) \ . \tag{2.101}$$

Rewriting ρ, r_0 and r_{0c} in terms of T and T_c, we arrive at the following expression for the condensation operator value,

$$\sqrt{\langle \mathcal{O}_2 \rangle} = \gamma T_c \sqrt[4]{\left(1 - \frac{T}{T_c} \right)} \tag{2.102}$$

where $\gamma = \frac{4\pi}{3}\left(\frac{1+a^2}{1+a^2+a^4}\right)\sqrt[4]{\frac{1}{\mathcal{B}}}$.

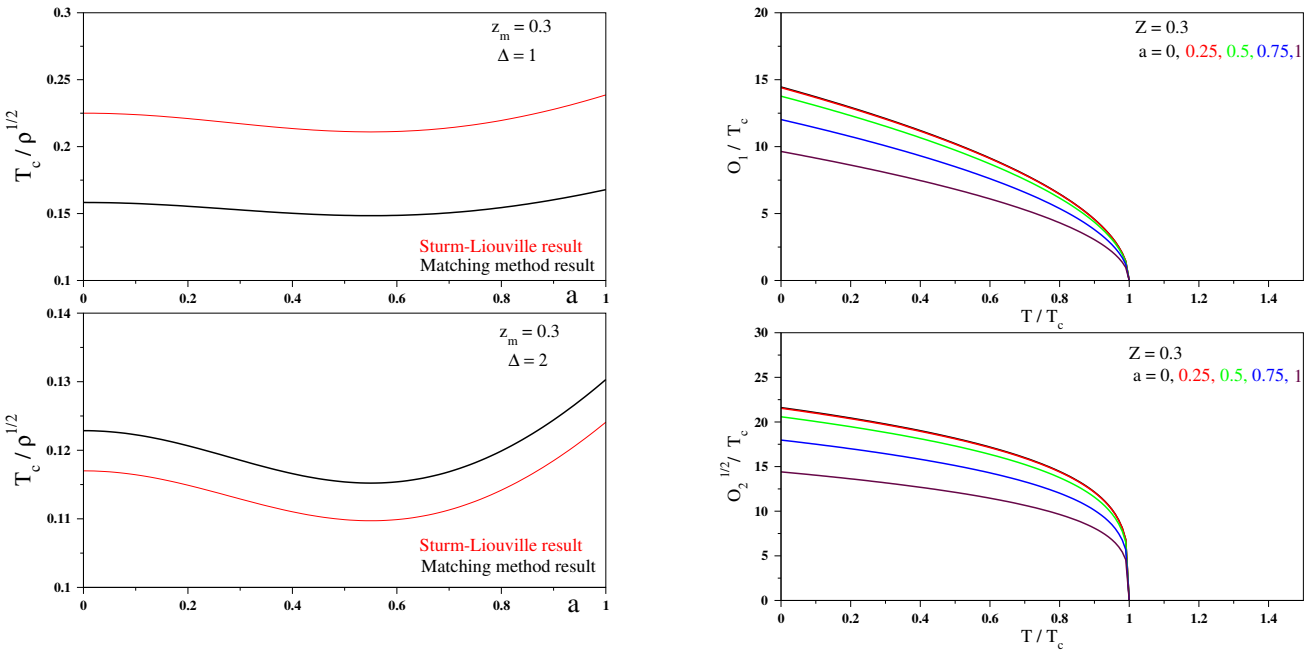

FIGURE 2.2 Analytical results using matching method and Stürm-Liouville analysis

2.2.5 Discussion on Results

We have considered a rotating holographic superconductor and obtained the expression for the vacuum expectation value (vev) of the superconducting condensation operator for the boundary system using two analytic techniques viz. the matching method and the Stürm-Liouville eigenvalue analysis. We have also obtained the critical temperature for this holographic model using both the methods. These results are graphically shown in Fig.(2.2). It is clear from these results that condensation operator values does exhibit a second order superconducting phase transition. It can be seen from the graphs on the right hand side of the Fig.(2.2) that an increase in the rotation parameter makes the condensation harder, however, exact value the vev of the condensation operator is not of much relevance. For these models, possibility of condensate formation is enough to make qualitative observations regarding the phenomenon of superconductivity. On the other hand, possibility of having higher critical temperature is more important to compare two different holographic superconductor models. With this line of reasoning, we have interpreted the left hand side of graphs in Fig.(2.2), which clearly show that there is indeed a possibility of having higher critical temperature in models with high values of rotation parameter in comparison to the original non-rotating model, whose results are recovered in our analysis if we set the rotation parameter $a = 0$. Apart from it, we would like to point out that in the matching method results, there is no clear way of choosing the matching point. So we have tabulated critical temperature for different choices of matching point in table (2.1). From this table, we may

observe that choice of matching point near horizon is more favourable for higher values of critical temperature and hence for the subsequent analysis we have fixed the matching point at $z = 0.3$.

Now we shall move on to discuss another model of holographic superconductor, which has been shown to exhibit p-wave type gap in the holographic literature.

2.3 p-wave Holographic Superconductor

In the previous section, we have analysed a s-wave holographic superconductor, which is supposed to be a gravity dual of a HTSCs having s-wave gap in its ground state. Basically, superconductors (both conventional and unconventional) can be categorised by the symmetries of the Cooper pairs in its ground state. In principle, there could be many types of symmetries available; for example (s, p, d, ...)-wave. However, in case of HTSCs (especially Cuprates) it is experimentally known that these materials show a d-wave type gap structure in under-doped and optimally doped regions [20, 21, 91–94]. Although for some over-doped HTSCs, existence of s-wave gap has also been reported [22, 95]. p-wave type HTSCs are categorised as exotic materials and so far remain a tool for scientific curiosity [96]. Still it is interesting to study gravity duals of p-wave HTSCs purely from phenomenological point of view. Earlier a model of p-wave holographic superconductor was built using non-abelian gauge fields [82] and has been studied extensively over the years. Recently, a more simple holographic model with a massive vector field was constructed for this purpose and it was shown that this model does mimic a p-wave gap in its ground state [97]. In the present thesis, we have incorporated effects of non-linear gauge field viz. Born-Infeld electrodynamics to this holographic dual of the p-wave HTSCs [98].

As we have mentioned in the introduction of this chapter that we are looking for a certain spontaneous symmetry breaking in these gravity duals. This is nothing but the famous $U(1)$ symmetry that gives rise to the phenomenon of superconductivity [99]. Formation of the superconducting condensate fulfils this requirement. To have a p-wave type ground state, we need an additional breaking of $SO(2)$ symmetry in the formed condensate. Earlier a gravity dual built out of Einstein-Yang-Mills theory in AdS_4 was shown to exhibit such a p-wave gap in its ground state [82]. Key idea in that model was to treat $U(1)$ subgroup of the $SU(2)$ gauge field as the gauge group of electromagnetism and allow off-diagonal gauge bosons charged under this $U(1)$ to form superconducting condensate outside the black hole horizon. Recently, a different model consisting of Einstien-Maxwell-complex vector field in AdS_4 spacetime was used as a p-wave holographic superconductor [97]. This model is mathematically more simpler than previous one to deal with analytically. Also it allows us to study the effects of non-linear electrodynamics in such a p-wave holographic superconductors, which was not the case in the old model. Hence, in this thesis, we have studied the effects of non-linearity introduced in the gauge sector of this gravity dual via.

the presence of a Born-Infeld parameter. It turns out that Born-Infeld electrodynamics suppresses formation of condensate at higher temperatures and hence, is not a phenomenologically suitable parameter in such p-wave HTSC mimickers. In the following sections, we shall discuss mathematical details of this model which lead us to such an interesting conclusion.

2.3.1 The Holographic Model

Simple holographic models for superconductors with p-wave gap are based on Einstein-Yang-Mills theory with a negative cosmological constant. The action for this model is given by,

$$\mathcal{S} = \frac{1}{2\mathcal{G}^2}\int d^4x\left(\mathcal{R} - \frac{1}{4}(F^a_{\mu\nu})^2 + \frac{6}{L^2}\right) \tag{2.103}$$

where $F^a_{\mu\nu}$ is the field strength tensor of an $SU(2)$ gauge field. This model has been studied in various phenomenological settings and on top of various bulk geometries having asymptotic AdS structure. [69]

However, recently a new gravity dual for such a p-wave superconductor has been proposed. This gravity dual is given by Einstein-Maxwell action along with a minimally coupled massive vector field. The action for this model is given as,

$$\mathcal{S} = \frac{1}{16\pi G}\int d^4x\sqrt{-g}\left(\mathcal{R} - 2\Lambda + \mathcal{L}\right). \tag{2.104}$$

Here the Lagrangian density for matter sector is given by the following equation.

$$\mathcal{L} = \frac{1}{b}\left(1 - \sqrt{1 + \frac{b}{2}F^{\mu\nu}F_{\mu\nu}}\right) - \frac{1}{2}\rho^\dagger_{\mu\nu}\rho^{\mu\nu} - m^2\rho^\dagger_\mu\rho^\mu\,. \tag{2.105}$$

The Faraday tensor and the covariant derivatives have standard form, which are given by $F_{\mu\nu} \equiv \partial_{[\mu}A_{\nu]}$ and $D_\mu \equiv (\partial_\mu - iA_\mu)$ respectively. In addition to it, $\rho_{\mu\nu}$ is defined below,

$$\rho_{\mu\nu} \equiv D_\mu\rho_\nu - D_\nu\rho_\mu.$$

The gauge sector of the Lagrangian density, $\mathcal{L}$, consists of Born-Infeld electrodynamics with b being the Born-Infeld parameter such that $b \to 0$ recovers the Maxwell electrodynamics.

We shall study this model on top of the planar Schwarzschild black hole geometry in AdS_{3+1} spacetime, which is given by,

$$ds^2 = -f(r)dt^2 + r^2(dx^2 + dy^2) + \frac{dr^2}{f(r)} \tag{2.106}$$

where the blackening factor is given as,

$$f(r) = \left(r^2 - \frac{r_0^3}{r}\right) .$$

Here, the event horizon of the black hole is at r_0, and the AdS radius has been set to unity. The Hawking temperature for this black hole geometry is given by,

$$T = \frac{3r_0}{4\pi} . \tag{2.107}$$

We shall be analysing this model in the probe approximation, as in the previous model, where we assume that the background geometry is not back-reacted by the matter present in the spacetime.

2.3.2 Equations of Motion

Varying the action, $\mathcal{S}$, given in eq.(2.104), following equations of motion for the matter field, $\rho(r)$, and the gauge field, $\Phi(r)$, can be obtained,

$$\rho'' + \frac{f'}{f}\rho' + \left(\frac{\Phi^2}{f^2} - \frac{m^2}{f}\right)\rho = 0 \tag{2.108}$$

$$\Phi'' + \frac{2}{r}\Phi'(1 - b\Phi'^2) - \frac{2\Phi\rho^2}{r^2 f}(1 - b\Phi'^2)^{3/2} = 0 \tag{2.109}$$

where the derivative with respect to r is denoted by prime $(')$. However, we shall be working in a changed coordinate for AdS direction given by $z = \frac{r_0}{r}$, such that the horizon of the black hole is at $z = 1$ while the AdS boundary is at $z = 0$. In this new coordinate, the field eq.(s)(2.108, 2.109) take the following form

$$\rho'' - \frac{3z^2}{(1 - z^3)}\rho' + \frac{1}{z^2(1 - z^3)}\left(\frac{z^2\Phi^2}{r_0^2(1 - z^3)} - m^2\right)\rho = 0 \tag{2.110}$$

$$\Phi'' + \frac{2bz^3}{r_0^2}\Phi'^3 - \frac{2\Phi\rho^2}{r_0^2(1 - z^3)}\left(1 - \frac{bz^4}{r_0^2}\Phi'^2\right)^{3/2} = 0 \tag{2.111}$$

where prime now denotes derivative with respect to the coordinate z.

According to the gauge/gravity duality, $\Phi(z)$ and $\rho(z)$ near the AdS boundary are known to have the following scaling form,

$$\Phi(z) = \mu - \frac{\tilde{\rho}}{r_0}z \tag{2.112}$$

$$\rho(z) \simeq \frac{\rho_+}{r_0^{\Delta_+}}z^{\Delta_+} + \frac{\rho_-}{r_0^{\Delta_-}}z^{\Delta_-} \tag{2.113}$$

where μ is interpreted as the chemical potential and $\tilde{\rho}$ as the charge density of the dual conformal field theory system. $\Delta_{\pm}$ are roots of the following equation,

$$\Delta = \frac{1}{2}(1 \pm \sqrt{1+4m^2}) \, . \tag{2.114}$$

Δ is known as the conformal dimension of the dual operator and it depends on m^2 through the above relation[2]. Eq.(2.113) requires that Δ must be real and positive. This condition on Δ further restricts the choice of m^2 in the bulk theory as well. To fulfil the above mentioned condition for Δ, m^2 needs to satisfy the following lower bound,

$$m^2 \geq -\frac{1}{4} \, . \tag{2.115}$$

Eq.(2.115) is famously known as the Breitenlohner-Freedman (BF) bound [89, 90], which implies that even a negative mass vector field is stable in AdS spacetime as long as eq.(2.115) is satisfied.

2.3.3 The Stürm-Liouville Eigenvalue Analysis

In order to solve this model analytically, we have again pursued the Stürm-Liouville Eigenvalue approach. We start with recalling that the matter field $\rho(z)$ vanishes at the critical temperature T_c. Hence, at $T = T_c$, eq.(2.111) simplifies to the following form

$$\Phi'' + \frac{2bz^3}{r_0^2}\Phi'^3 = 0 \, . \tag{2.116}$$

The analytic solution of eq.(2.116) up to first order in terms of the Born-Infeld parameter b is given by [77],

$$\Phi(z) = \lambda r_0 (1-z)\left[1 - \frac{b(\lambda^2|_{b=0})}{10}\zeta(z)\right] \tag{2.117}$$

where $\zeta(z) = (1+z+z^2+z^3+z^4)$ and $\lambda = \dfrac{\tilde{\rho}}{r_{0c}^2}$. r_{0c} is the black hole horizon radius at the critical temperature. From eq.(2.107), we find the critical temperature to be

$$T_c = \frac{3}{4\pi}\sqrt{\frac{\tilde{\rho}}{\lambda}} \, . \tag{2.118}$$

Using eq.(2.117) in eq.(2.110), we get the following field equation for ρ,

$$\rho'' - \frac{3z^2}{(1-z^3)}\rho' + \frac{\lambda^2}{(1+z+z^2)^2}\left(1 - \frac{b(\lambda^2|_{b=0})}{5}\zeta(z)\right)\rho - \frac{m^2}{z^2(1-z^3)}\rho = 0 \, . \tag{2.119}$$

[2]This relation can be obtained using eq.(2.113) in eq.(2.110).

2.3.3.1 The Critical Temperature

In order to proceed further for the explicit expression for the critical temperature, we shall consider the following non-trivial profile of the field $\rho(z)$,

$$\rho(z) = \frac{\langle \mathcal{O}_\Delta \rangle}{\sqrt{2} r_0^\Delta} z^\Delta F(z) \tag{2.120}$$

with the boundary conditions $F(0) = 1$ and $F'(0) = 0$. These boundary conditions on $F(z)$ are consistent with the behaviour of $\rho(z)$, near the AdS boundary, given by eq.(2.113). We shall now substitute the form of the field $\rho(z)$ from eq.(2.120) in eq.(2.119) to obtain,

$$(z^{2\Delta}(1-z^3)F')' - (3\Delta z^{2\Delta+1} + m^2 z^{2\Delta-2} - \Delta(\Delta-1)z^{2\Delta-2}(1-z^3))F + \frac{\lambda^2 z^{2\Delta}(1-z)}{(1+z+z^2)}\left(1 - \frac{b(\lambda^2|_{b=0})}{5}\zeta(z)\right)F = 0\,.$$

We may cast this equation in the standard form of the Stürm-Liouville eigenvalue equation,

$$\frac{d(p(z)F')}{dz} - q(z)F + \lambda^2 r(z)F = 0\,. \tag{2.121}$$

Here the functions $p(z)$, $q(z)$ and $r(z)$ are given below,

$$\begin{aligned} p(z) &= z^{2\Delta}(1-z^3) \\ q(z) &= 3\Delta z^{2\Delta+1} + m^2 z^{2\Delta-2} - \Delta(\Delta-1)z^{2\Delta-2}(1-z^3) \\ r(z) &= \frac{z^{2\Delta}(1-z)}{(1+z+z^2)}\left(1 - \frac{b(\lambda^2|_{b=0})}{5}\zeta(z)\right). \end{aligned} \tag{2.122}$$

We can now determine the eigenvalue λ in eq.(2.121) using the following equation,

$$\lambda^2 = \frac{\int_0^1 dz\left(p(z)F'^2 + q(z)F^2\right)}{\int_0^1 dz r(z)F^2}\,. \tag{2.123}$$

In order to determine λ, we may choose a trial function for $F(z)$ with some parameter α as $F_\alpha(z) = (1-\alpha z^2)$. The eigenvalue λ is, then, determined by minimising eq.(2.123) with respect to α. The value of $\lambda_{\alpha_{min.}}$ can then be used in eq.(2.118) to determine the critical temperature of the p-wave holographic superconductor from the following equation,

$$T_c = \frac{3}{4\pi}\sqrt{\frac{\tilde{\rho}}{\lambda_{\alpha_{min.}}}}\,. \tag{2.124}$$

To proceed further, we now select some particular conformal dimension via eq.(2.114). We shall focus on the following choices of m^2 and its corresponding conformal dimensions $\Delta = (\Delta_+,\ \Delta_-)$.

$$m^2 = 0 \ \ \rightarrow \ \ \Delta = (1,\ 0) \tag{2.125}$$

$$m^2 = -\frac{3}{16} \ \ \rightarrow \ \ \Delta = \left(\frac{3}{4},\ \frac{1}{4}\right). \tag{2.126}$$

We know that near the AdS boundary $\rho(z)$ is given by eq.(2.113). To have spontaneous symmetry breaking, we now set the source term $\rho_- = 0$ for the above choices. Therefore the boundary behaviour of $\rho(z)$ is now given by following equation,

$$\rho(z) \simeq \frac{\rho_+}{r_0^{\Delta_+}} z^{\Delta_+}\ . \tag{2.127}$$

For notational simplicity, we shall drop the subscripts $(+)$ from now on.

Case(I): $m^2 = 0,\ \Delta = 1$

In this case, the SL coefficient functions in eq.(2.122) are given by the following form,

$$\begin{aligned} p(z) &= z^2(1-z^3) \\ q(z) &= 3z^3 \\ r(z) &= \frac{z^2(1-z)}{(1+z+z^2)}\left(1 - \frac{b(\lambda^2|_{b=0})}{5}\zeta(z)\right). \end{aligned} \tag{2.128}$$

Here also, using the trial function $F_\alpha(z) = (1-\alpha z^2)$ in eq.(2.123) with SL coefficients given in eq.(2.128), the eigenvalue λ may be obtained from the following,

$$\lambda_\alpha^2 = \frac{\int_0^1 dz\Big(4\alpha^2 z^4(1-z^3) + 3z^3(1-\alpha z^2)^2\Big)}{\int_0^1 dz \frac{z^2(1-z)}{(1+z+z^2)}\left(1 - \frac{b(\lambda^2|_{b=0})}{5}\zeta(z)\right)(1-\alpha z^2)^2}\ . \tag{2.129}$$

We obtain, on solving this equation,

$$\lambda_\alpha^2 = \frac{60\left(\alpha - \frac{3}{4} - \frac{27\alpha^2}{40}\right)}{\left[(30\ln 3 - 10\sqrt{3}\pi + 21)\alpha^2 + (120\ln 3 - 130)\alpha + (30\ln 3 + 10\sqrt{3}\pi - 90) + \frac{b(\lambda^2|_{b=0})}{5}\right.} \\ \left.\left((30\ln 3 + 10\sqrt{3}\pi - 85.91)\alpha^2 + (-60\ln 3 + 20\sqrt{3}\pi - 48.14)\alpha + (72 - 60\ln 3)\right)\right] \tag{2.130}$$

In case of $b = 0$, that is when Born-Infeld parameter vanishes, the eigenvalue expression (2.130) reduces to the following form,

$$\lambda^2_\alpha|_{b=0} = \frac{60\left(\alpha - \frac{3}{4} - \frac{27\alpha^2}{40}\right)}{(30\ln 3 - 10\sqrt{3}\pi + 21)\alpha^2 + (120\ln 3 - 130)\alpha + (30\ln 3 + 10\sqrt{3}\pi - 90)} \,. \quad (2.131)$$

This expression attains a minima at $\alpha \approx 0.50775$. The minimum value of $\lambda^2_\alpha|_{b=0}$ is then found to be

$$\lambda^2_{\alpha_{min.}}|_{b=0} \approx 13.7674 \,. \quad (2.132)$$

The critical temperature may now be determined using eq.(2.124) and is given by the following equation,

$$T_c = \frac{3}{4\pi}\sqrt{\frac{\tilde{\rho}}{\lambda_{\alpha_{min.}}|_{b=0}}} \approx 0.1239\sqrt{\tilde{\rho}} \,. \quad (2.133)$$

At this point, we would like to emphasise that the critical temperature obtained in this gravity dual of p-wave superconductors, when the BI parameter vanishes, is matching exactly with the obtained value of the critical temperature in the holographic p-wave superconductor model constructed out of the Einstein-Yang-Mills theory [82].

It should be noted that in eq.(2.129) we shall now use $\lambda^2_{\alpha_{min.}}|_{b=0}$ in place of $\lambda^2|_{b=0}$ for successive computations of the eigenvalues with different values of the BI parameter b. In that case, we may write eq.(2.130) as below

$$\lambda^2_\alpha = \frac{60\left(\alpha - \frac{3}{4} - \frac{27\alpha^2}{40}\right)}{\left[(30\ln 3 - 10\sqrt{3}\pi + 21)\alpha^2 + (120\ln 3 - 130)\alpha + (30\ln 3 + 10\sqrt{3}\pi - 90) + \frac{b(13.7674)}{5}\right.} \quad (2.134)$$
$$\left.\left((30\ln 3 + 10\sqrt{3}\pi - 85.91)\alpha^2 + (-60\ln 3 + 20\sqrt{3}\pi - 48.14)\alpha + (72 - 60\ln 3)\right)\right]$$

where we have made the substitution $\lambda^2|_{b=0} = 13.7674$.

Taking small value for BI parameter b in eq.(2.134), we shall minimize it with respect to α to find out the corresponding eigenvalue $\lambda^2_{\alpha_{min.}}|_{b\neq 0}$. We may then determine the critical temperature using eq.(2.124). These critical temperatures, T_c, for some values of the BI parameter, b, are given in Table (2.2).

Case(II): $m^2 = -3/16,\ \Delta = 3/4$

Here as well, we shall follow the same procedure as in **Case(I)**. We shall start with finding out the critical temperature when there is no BI correction and then provide the critical temperature for some small values of the BI parameter b. In order to achieve that, we first write the functions $p(z)$, $q(z)$ and $r(z)$ deduced from eq.(2.122) for this case. These functions are given as,

$$\begin{aligned} p(z) &= z^{3/2}(1-z^3) \\ q(z) &= \frac{33}{16}z^{5/2} \\ r(z) &= \frac{z^{3/2}(1-z)}{(1+z+z^2)}\left(1-\frac{b(\lambda^2|_{b=0})}{5}\zeta(z)\right). \end{aligned} \tag{2.135}$$

Now we shall again use the same trial function $F_\alpha(z)$ along with the above functions to find eigenvalue given by,

$$\lambda^2_\alpha = \frac{\int\limits_0^1 dz\Big(4\alpha^2 z^{7/2}(1-z^3)+\frac{33}{16}z^{5/2}(1-\alpha z^2)^2\Big)}{\int\limits_0^1 dz\frac{z^{3/2}(1-z)}{(1+z+z^2)}\left(1-\frac{b(\lambda^2|_{b=0})}{5}\zeta(z)\right)(1-\alpha z^2)^2}\,. \tag{2.136}$$

Solving for the integrals in the above expression we find,

$$\lambda^2_\alpha = \frac{\frac{3465}{5040}\Big(3780\alpha-2970-3178\alpha^2\Big)}{\mathcal{D}}\,. \tag{2.137}$$

Here $\mathcal{D}$ is given by,

$$\begin{aligned} \mathcal{D} = \Bigg[&(-3465\ln 3+3776)\alpha^2+(-3465\ln 3+3465\sqrt{3}\pi-14916)\alpha+(1732.5\ln 3+1732.5\sqrt{3}\pi-1150)+\frac{b(\lambda^2|_{b=0})}{5} \\ &\Big((1732.5\ln 3+1732.5\sqrt{3}\pi-11234.1667)\alpha^2+(6930\ln 3-7974.1538)\alpha+(1732.5\ln 3-1732.5\sqrt{3}\pi+7994)\Big)\Bigg]\,. \end{aligned}$$

To find out the critical temperature in this case, we again consider some small values for the BI parameter, b, in the above expression for the eigenvalue and then we go on to minimize it with respect to α. Once we obtain the corresponding minimum value $\lambda^2_{\alpha_{min.}}$, we shall use eq.(2.124) to determine the critical temperature T_c.

In Table (2.2), we have provided tabular summary for the critical temperatue with the Born-Infeld correction for both the cases we have discussed above. It should be noted that the presence of the BI parameter is weakening the critical temperature for both the cases.

Born-Infeld parameter, b	The critical temperature, T_c	
	$m^2 = 0,\ \Delta = 1$	$m^2 = -3/16,\ \Delta = 3/4$
0.0	$0.1239\sqrt{\tilde{\rho}}$	$0.1425\sqrt{\tilde{\rho}}$
0.01	$0.1221\sqrt{\tilde{\rho}}$	$0.1414\sqrt{\tilde{\rho}}$
0.02	$0.1201\sqrt{\tilde{\rho}}$	$0.1402\sqrt{\tilde{\rho}}$
0.03	$0.1182\sqrt{\tilde{\rho}}$	$0.1390\sqrt{\tilde{\rho}}$

TABLE 2.2 Critical temperature with the Born-Infeld correction

2.3.3.2 Condensation Operator Values

Next we shall focus on the condensation operator value. We notice that near the critical temperature, $\rho(z)$ is given by eq.(2.120). We also know the solution for the field $\Phi(z)$ at T_c (eq.(2.117)). We now assume that near the critical temperature, $\Phi(z)$ would differ slightly from eq.(2.117). Hence, we add a small fluctuation field $\chi(z)$ in the solution given in eq.(2.117) considering appropriate boundary conditions. So we have,

$$\Phi(z) = \lambda r_0(1-z)\left[1 - \frac{b(\lambda^2|_{b=0})}{10}\zeta(z)\right] + \frac{\langle\mathcal{O}_\Delta\rangle^2}{r_0^{2\Delta-1}}\chi(z) \tag{2.138}$$

where the boundary conditions are $\chi(1) = 0$ and $\chi'(1) = 0$.

Near the critical temperature, in order to determine the specific form of the field $\Phi(z)$, we substitute eq.(2.138) in eq.(2.111) keeping terms only of $\mathcal{O}(b)$ and $\mathcal{O}(\langle\mathcal{O}_\Delta\rangle^2)$. Equation for the fluctuation field $\chi(z)$, therefore, reads

$$\chi'' + 6b\lambda^2 z^3\chi' = \frac{\lambda z^{2\Delta}F^2}{r_0^2(1+z+z^2)}\left[1 - \frac{b}{2}\left(\frac{(\lambda|_{b=0})^2}{5}\zeta(z) + 3\lambda^2 z^4\right)\right]. \tag{2.139}$$

Due to smallness of the BI parameter b, we shall approximate λ^2 in eq.(2.139) with $(\lambda|_{b=0})^2$ wherever it appears with b. In that approximation, eq.(2.139) reduces to the following equation,

$$\chi'' + 6b(\lambda|_{b=0})^2 z^3\chi' = \frac{\lambda z^{2\Delta}F^2}{r_0^2(1+z+z^2)}\left[1 - \frac{b}{2}(\lambda|_{b=0})^2\left(\frac{\zeta(z)}{5} + 3z^4\right)\right]. \tag{2.140}$$

In order to figure out the solution of the above equation, we shall multiply eq.(2.140) with $e^{\left(\frac{3b}{2}(\lambda|_{b=0})^2 z^4\right)}$ and rearrange it in the following form,

$$\left(e^{\left(\frac{3b}{2}(\lambda|_{b=0})^2 z^4\right)}\chi'\right)' = \frac{\lambda z^{2\Delta}F^2}{r_0^2(1+z+z^2)}\left[1 - \frac{b}{2}(\lambda|_{b=0})^2\left(\frac{\zeta(z)}{5} + 3z^4\right)\right]e^{\left(\frac{3b}{2}(\lambda|_{b=0})^2 z^4\right)} \tag{2.141}$$

Upon integration, eq.(2.141), between $z = 0$ and $z = 1$ with the given boundary conditions on $\chi(z)$ and $\chi'(z)$, we shall find the following condition on the fluctuation field near the AdS boundary,

$$\chi'(0) = -\frac{\lambda}{r_0^2}\mathcal{A}_\Delta \tag{2.142}$$

where

$$\mathcal{A}_\Delta = \int_0^1 dz \frac{z^{2\Delta}F^2}{(1+z+z^2)}\left[1 - \frac{b}{2}(\lambda|_{b=0})^2\left(\frac{\zeta(z)}{5} + 3z^4\right)\right]\exp\left(\frac{3b}{2}(\lambda|_{b=0})^2 z^4\right) . \tag{2.143}$$

We shall now Taylor expand the field $\chi(z)$ near the AdS boundary,

$$\chi(z) = \chi(0) + z\chi'(0) + ... \tag{2.144}$$

and compare the coefficients of z of eq.(s)(2.138, 2.112), considering the above expansion of the field $\chi(z)$, which yields,

$$-\frac{\tilde{\rho}}{r_0} = -\lambda r_0 + \frac{\langle\mathcal{O}_\Delta\rangle^2}{r_0^{2\Delta-1}}\chi'(0) . \tag{2.145}$$

Now we shall substitute for $\chi'(0)$ using eq.(2.142) in the above equation, which would produce following result,

$$\frac{\tilde{\rho}}{r_0^2} = \lambda\left(1 + \frac{\langle\mathcal{O}_\Delta\rangle^2}{r_0^{2\Delta+2}}\mathcal{A}_\Delta\right) . \tag{2.146}$$

At the end, we shall now replace r_0 in terms of the Hawking temperature T from eq.(2.107) and λ in terms of the critical temperature T_c using the relation $\lambda = \frac{\tilde{\rho}}{r_{0c}^2}$. The condensation operator is then obtained to have the following form,

$$\frac{\langle\mathcal{O}_\Delta\rangle}{T_c^{(\Delta+1)}} = \sqrt{\frac{2}{\mathcal{A}_\Delta}}\left(\frac{4\pi}{3}\right)^{(\Delta+1)}\sqrt{\left(1 - \frac{T}{T_c}\right)} . \tag{2.147}$$

Δ, in the above result, can take any positive value that is consistent with eq.(s)(2.114, 2.115). It is also apparent that the condensation operator shows the second order phase transition with the critical exponent $1/2$.

In the previous section, we have considered two cases by choosing m^2 and the corresponding the conformal dimension Δ. The condensation operator values for those cases is given below.

Case (I): $m^2 = 0,\ \Delta = 1$

For this choice, eq.(2.147) reduces to,

$$\frac{\langle \mathcal{O}_1 \rangle}{T_c^2} = \sqrt{\frac{2}{\mathcal{A}_1}} \left(\frac{4\pi}{3}\right)^2 \sqrt{\left(1 - \frac{T}{T_c}\right)} \tag{2.148}$$

where

$$\mathcal{A}_1 = \int_0^1 dz \frac{z^2 F^2}{(1+z+z^2)} \left[1 - \frac{b}{2}(\lambda|_{b=0})^2 \left(\frac{\zeta(z)}{5} + 3z^4\right)\right] \exp\left(\frac{3b}{2}(\lambda|_{b=0})^2 z^4\right). \tag{2.149}$$

We shall now find the value of $\frac{\langle \mathcal{O}_1 \rangle}{T_c^2}$ near $T \to 0$ such that eq.(2.150) gives

$$\frac{\langle \mathcal{O}_1 \rangle}{T_c^2} \simeq \sqrt{\frac{2}{\mathcal{A}_1}} \left(\frac{4\pi}{3}\right)^2 \approx \frac{24.8137}{\sqrt{\mathcal{A}_1}} \tag{2.150}$$

Cosidering the trial function $F_\alpha = (1 - \alpha z^2)$ with the value of α that minimizes the eigenvalue $\lambda^2_{\alpha_{min.}}$ in $\mathcal{A}_1$ given by eq.(2.149), we shall obtain,

$$\mathcal{A}_1 = \int_0^1 dz \frac{z^2(1-\alpha z^2)^2}{(1+z+z^2)} \left[1 - \frac{b}{2}(\lambda|_{b=0})^2 \left(\frac{\zeta(z)}{5} + 3z^4\right)\right] \exp\left(\frac{3b}{2}(\lambda|_{b=0})^2 z^4\right). \tag{2.151}$$

Starting with the case when $b = 0$, eq.(2.151) becomes

$$\mathcal{A}_1 = \int_0^1 dz \frac{z^2(1 - 0.50775 z^2)^2}{(1+z+z^2)}\,. \tag{2.152}$$

In the eq.(2.152), we have utilised the value $\alpha \approx 0.50775$ obtained in the previous section. It was found there that for this value of α, the eigenvalue attains its minimum value and $\lambda^2_{\alpha_{min.}}|_{b=0} \approx 13.7674$, when there is no BI correction. Using eq.(2.152) in eq.(2.150), we found the value of $\frac{\langle \mathcal{O}_1 \rangle}{T_c^2}$ is approximately 87.2482.

Here also, we have considered the BI correction to the condensation operator values which are listed in Table (2.3) for some small values of the BI parameter b.

Case (II): $m^2 = -3/16,\ \Delta = 3/4$

We shall now present the value of the condensation operator for the choice $m^2 = -\frac{3}{16}$ and $\Delta = \frac{3}{4}$.

From eq.(2.147), we get the following form of the condensation operator value in this case,

$$\frac{\langle \mathcal{O}_{3/4} \rangle}{T_c^{7/4}} = \sqrt{\frac{2}{\mathcal{A}_{3/4}}} \left(\frac{4\pi}{3}\right)^{7/4} \sqrt{\left(1 - \frac{T}{T_c}\right)} \tag{2.153}$$

where

$$\mathcal{A}_{3/4} = \int_0^1 dz \frac{z^{3/2} F^2}{(1+z+z^2)} \left[1 - \frac{b}{2}(\lambda|_{b=0})^2 \left(\frac{\zeta(z)}{5} + 3z^4\right)\right] \exp\left(\frac{3b}{2}(\lambda|_{b=0})^2 z^4\right). \tag{2.154}$$

As in the previous case, we find that near $T \to 0$ the value of $\frac{\langle \mathcal{O}_{3/4} \rangle}{T_c^{7/4}}$ is given by,

$$\frac{\langle \mathcal{O}_{3/4} \rangle}{T_c^{7/4}} \simeq \sqrt{\frac{2}{\mathcal{A}_{3/4}}} \left(\frac{4\pi}{3}\right)^{7/4} \approx \frac{17.3448}{\sqrt{\mathcal{A}_{3/4}}}. \tag{2.155}$$

We now use the trial function $F_\alpha = (1 - \alpha z^2)$ with the value of α that minimizes the eigenvalue $\lambda^2_{\alpha_{min.}}$ in $\mathcal{A}_{3/4}$ given by eq.(2.149) to get,

$$\mathcal{A}_{3/4} = \int_0^1 dz \frac{z^{3/2}(1-\alpha z^2)^2}{(1+z+z^2)} \left[1 - \frac{b}{2}(\lambda|_{b=0})^2 \left(\frac{\zeta(z)}{5} + 3z^4\right)\right] \exp\left(\frac{3b}{2}(\lambda|_{b=0})^2 z^4\right). \tag{2.156}$$

We have obtained the BI corrections to the condensation operator value in this case as well which are listed in Table (2.3) for some small values of the BI parameter b.

In the table (2.3), we display the value of condensation operator near $T = 0$ for the cases ($m^2 = 0, \Delta = 1$) and ($m^2 = -3/16, \Delta = 3/4$). We have noted earlier in table (2.2) that the critical temperature T_c matches exactly for both the holographic p-wave superconductor models for the case ($m^2 = 0, \Delta = 1$) when the BI parameter b is zero. However, the value of the condensation operator given in table (2.3) shows a departure by a factor of $\sqrt{2}$ from the value of condensation operator obtained in the Einstein-Yang-Mills p-wave holographic superconductor [82]. It is also worth noting that the BI correction is increasing the values of the condensation operator in both the cases we have discussed.

2.3.4 Discussion on Results

We have shown through this analytical study of the holographic p-wave superconductor that an increase in the Born-Infeld parameter improves the value of the superconducting condensate. This is the case observed, as shown in table (2.3), with two different choices of the mass of the charged vector field (and hence corresponds to two different scaling dimension of the boundary superconductor near the critical temperature.). However, as argued before in the case of rotating holographic super-

Born-Infeld parameter (b)	The condensation operator value, $\langle \mathcal{O}_\Delta \rangle / T_c^{\Delta+1}$	
	$m^2 = 0,\ \Delta = 1$	$m^2 = -3/16,\ \Delta = 3/4$
0.0	87.2482	49.509
0.01	89.4636	50.1235
0.02	92.5642	50.8645
0.03	96.9787	51.7611

TABLE 2.3 Condensation operator value for different values of BI parameter

conductor model that mere formation of superconducting condensate is enough from holographic point of view and increase or decrease of the exact value of the condensation operator does not add anything qualitative. On the other hand, table (2.2) indicates that for both the choices of scaling dimensions (for different masses) critical temperature in this model decreases with an increase in the value of the Born-Infeld parameter. Hence, we may conclude from this observation that Born-Infeld corrections to the gauge field are not favourable for superconductivity in these gravity duals of unconventional superconductors having p-wave gap. It should also be noted that if we set Born-Infeld parameter to zero, our results match with the Einstein-Yang-Mills model upto some numerical factor (mentioned in previous sections.).

2.4 Conclusions and Remarks

In this chapter, we have primarily presented two simple phenomenological applications of the gauge/gravity duality to understand (unconventional) HTSCs via their gravity duals. We have first explored a holographic model for s-wave HTSCs incorporating a rotating black hole in the description of the bulk geometry. The inclusion of rotation in the gravity dual, in such phenomenology, is well motivated on the gravity side due to no-hair theorem. Also in the gauge/gravity duality, it is widely believed that rotation of the black hole behaves as the application of the magnetic field in the holographic model [84]. However, holographic model with Kerr metric is very complicated and is not suitable to handle analytically. So we have considered an ad-hoc black hole geometry with the rotation parameter given in [88]. For this simple rotating geometry, we have been able to analytically obtain the expressions for the critical temperature and the condensation operator values. We have observed in this phenomenological endeavour that rotating holographic superconductor model supports superconductivity better than its non-rotating counterpart for high values of the rotation parameter. We would also like to point out that our analytical results are in agreement with the numerical results obtained in [85] for this model.

In another application of the gauge/gravity duality, we have been able to incorporate the Born-Infeld corrections in the gauge sector of the gravity dual for a p-wave holographic model of the

HTSCs. The key motivation for considering such a non-linear correction in the gauge field comes from the low energy limit of the string theory [100, 101]. It is also worth mentioning here that recently it was shown that holographic models with non-linear corrections in the gauge sector recover properties of Mott physics, driven by strong el-el interactions [102]. Phenomenology of holographic superconductors with non-linear gauge corrections thus hold special importance. We know that Born-Infeld electrodynamics is special over other non-linear electrodynamics as this theory not only eradicate self-energy problem of the Maxwell electrodynamics but also preserves electric-magnetic duality as well as does not show birefringence [103]. These properties of Born-Infeld electrodynamics motivates special attention for the investigations of the holographic superconductors in its presence. With this clear motivation, we have analytically investigated a p-wave holographic superconductor model built out of Einstein-Born-Infeld-complex vector field theory in the bulk AdS_4 geometry. We have observed that presence of non-linear correction (in terms of Born-Infeld parameter) is not favourable for these HTSC mimickers. One should note that turning off these corrections restore the results for the Einstein-Maxwell-complex vector field model presented in [97].

There are many open directions in which one may advance in the applications of the gauge/gravity duality in such unconventional superconductors. For example, obtaining analytic expression for conductivity in p-wave holographic superconductors is difficult, although it has been numerically explored. Next it should be interesting to show more exotic properties associated with these models such as existence of vortices and vortex lattices in the presence of magnetic field which has also been explored to some extent. One particular extension that should be worth exploring is the incorporation of holographic lattice in these superconductor models. Also holographic models having more realistic d-wave gap form an interesting and important class of problems within the applications of the gauge/gravity duality.

CHAPTER 3

Vortices in Holographic Superfluids

3.1 Introduction

In the previous chapter, we have discussed two models of holographic superconductors, which mimic the properties of the high temperature superconductors [86, 98]. Another closely related phenomenon is the unconventional superfluidity, which is also less understood in standard settings due to the presence of strong inter-particle interactions. Applied gauge/gravity duality has shed some light in this problem as well [75]. In fact, the models that we have discussed in the previous chapter are essentially models of superfluids and do not quite explain superconductors in strict sense [104]. It is so because according to the gauge/gravity duality, global symmetries of the boundary field theories are dualised as local (gauge) symmetries in the bulk theory [36]. Hence, the broken $U(1)$ symmetry in these gravity dual correspond to broken global $U(1)$ symmetry for the boundary system, which give rise to phenomenon of superfluidity[1]. In order to mimic the phenomenon of superconductivity in the boundary field theory, we need dynamical gauge field at the boundary theory as well (that is local $U(1)$ gauge field). It has been shown in the past that such a bona-fide holographic model of superconductivity is possible and could be realised using mixed boundary conditions [105–107]. However, this ad-hoc terminology for holographic superconductors/superfluids is quite popular in applied holography and has been interchangeably used according to the context of the problem. We have also followed this terminology in the same spirit. So in this chapter we shall be calling these models as holographic superfluids.

Now let us first describe an important property of the superfluids, which has been experimentally observed and is very unique. It has been observed that if one rotates a superfluid in a container then above a critical value of the rotation velocity certain point like objects start to appear that rotate rigidly with the wall of the container and then form a particular lattice pattern, at equilibrium, known as vortex lattice in the literature [108, 109]. If one keeps on increasing the rotation velocity indiscriminately then these vortices start merging into each other after smearing about axes parallel

[1]However, it should also be noted that these holographic superconductors show gapped structure in its energy spectrum, which is a characteristic of superconductors. This is another reason for the confusing terminology used for these gravity duals. I would like to thank Dr. D. Ghorai for pointing this out.

to rotation axis of the container. Much beyond this critical rotation velocity these vortices fill up the whole space of the container and the superfluid nature is lost. Studying such vortices within applied gauge/gravity duality framework constitutes an interesting problem. A lot of work has already been done on various phenomenological settings where existence of such vortices and vortex lattice has been shown [110–116]. Also, vortex dynamics and superfluid turbulence have also been studied numerically in [117] within the holographic settings. However, in this thesis we have approached this problem analytically and were able to discover new single vortex solutions that were not known previously [124]. Also, we have been able to show that these vortex solutions also admit Feynman like linear relation between winding numbers associated with the vortices and the quantised rotation velocity. In this study, we have also discovered contrast behaviour between relativistic and non-relativistic superfluids holographically [125].

In the subsequent section, we have discussed formation of novel vortex solutions in gravity dual of a relativistic superfluid. We have then continued to analyse the behaviour of quantised rotation velocity in the presence of imaginary chemical potential. It was interesting to note that presence of imaginary chemical potential supports formation of higher winding number vortices. Therefore it may be concluded, from our analysis, that increasing imaginary chemical potential introduces more dissipation in relativistic superfluids. We shall further continue to generalise such vortex solutions in the presence of Lifshitz fixed point in the boundary superfluid system. Some surprising results indicate that these superfluids behave very differently from relativistic superfluids.

This chapter is based on following two publications.

1) *Novel vortices and the role of a complex chemical potential in a rotating holographic superfluid*, **A. Srivastav** and S. Gangopadhyay, Phys.Rev.D 104:12, 126004 (2021).

2) *Vortices in a rotating holographic superfluid with Lifshitz scaling*, **A. Srivastav** and S. Gangopadhyay, Phys.Rev.D 107:8, 086005 (2023).

3.2 Rotating Holographic Superfluid

In this section, we have analytically studied a holographic model of relativistic superfluid having conformal fixed point (or having conformal symmetry), which we shall call relativistic conformal holographic superfluid (RCHS). We have already mentioned that out interest lies in the study of vortex solutions in holographic superfluid under rotation. To do that there are two ways:

1) Consider a static holographic superfluid system in a rotating black hole geometry. This model is more intuitive to put it in correspondence with an experimental situation where

static superfluid is in a rotating container. However, this model could be a bit mathematically involved.

2) Second way is to consider a rotating holographic superfluid in a static black hole geometry. This is a bit easy to handle analytically and can be argued to mimic the situation of case (1) if we realise that radial flows are prohibited in the superfluid [115].

In this thesis, we have followed this second route. Analysing this scenario near the equilibrium situation, where vortices are possible, we have obtained single vortex solutions and have explicitly shown that rotation velocity gets quantised. We have then looked at the bulk direction and found that for condensate to remain real, we have to allow imaginary values for the chemical potential. It turns out from the Stürm-Liouville analysis that there is an increasing trend between rotation velocity and the values of imaginary chemical potential. It is well known in holography that vortices allow fluctuations at the boundary to tunnel into black hole horizon, and hence may be considered as source of dissipation in the holographic superfluid system [117]. In light of this realisation, we may interpret from our results that increasing imaginary chemical potential increases the number of vortices and hence, dissipation in RCHS. Next, we shall provide the mathematical details of this model and vortex solutions in the subsequent sections.

3.2.1 The Holographic Model

We start with fixing up the background geometry to be a static black hole in AdS_{3+1} spacetime. Such a geometry could be given by the following metric, written in Eddington-Finkelstein coordinates [118],

$$ds^2 = \frac{l^2}{u^2}[-f(u)dt^2 - 2dtdu + dr^2 + r^2 d\theta^2] \ . \tag{3.1}$$

The blackening factor in this case is given by $f(u) = \left(1 - u^3\right)$. The AdS radius is denoted by l and the AdS coordinate u, the bulk direction, is scaled in such a way that the AdS boundary is at $u = 0$ and $u = 1$ represents the event horizon of the black hole. Coordinates (r, θ) define a flat $2D$ disc at the AdS boundary. For mathematical convenience, we would set the AdS radius to be unity (that is, $l = 1$) and the cosmological constant $\Lambda = -3$. The Hawking temperature associated with this black hole geometry is given by $T = \dfrac{3}{4\pi}$.

A simple model for holographic superfluid could be studied on top of this geometry. The matter sector of such a model is given by following action,

$$\mathcal{S} = \frac{l^2}{2\kappa_4^2 e^2} \int_{\mathcal{M}} d^4x \, \mathcal{L}_m \ . \tag{3.2}$$

The matter Lagrangian density, $\mathcal{L}_m$, is given by following expression,

$$\mathcal{L}_m = -\frac{1}{4}F^{\mu\nu}F_{\mu\nu} - |D\Psi|^2 - m^2|\Psi|^2 \ . \tag{3.3}$$

This Lagrangian density consists of a Maxwell field and a complex scalar field minimally coupled to A_μ. Also, the Faraday tensor and the covariant derivative are defined as usual by $F_{\mu\nu} \equiv \partial_{[\mu}A_{\nu]}$ and $D \equiv (\nabla - ieA)$ respectively. m and e represent mass and charge of the scalar field.

We shall analyse this model in the probe limit, that is neglecting the backreaction of the matter sector in the geometry, achievable by rescaling $A_\mu \to \frac{A_\mu}{e}$ and $\Psi \to \frac{\Psi}{e}$ and taking the limit $e \to \infty$. Mathematically, this limit is equivalent to setting $e = 1$ in the action of our theory.

3.2.2 Equations of Motion

To write the equations of motion for the matter and the gauge fields, we shall vary the action $\mathcal{S}$, given by eq.(3.2), for Ψ and A_μ and get the following equations,

$$(D^2 - m^2)\Psi = 0 \tag{3.4}$$

$$\nabla_\nu F_\mu^{\ \nu} = j_\mu \ . \tag{3.5}$$

The bulk current is defined as,

$$j_\mu := i\{(D_\mu\Psi)^\dagger\Psi - \Psi(D_\mu\Psi)\} \ . \tag{3.6}$$

Owing to our interest in understanding the behaviour of this holographic system near equilibrium, we shall assume that all the fields are stationary. Also we shall be working in the axial gauge, that is where $A_u = 0$. In which case eq.(3.4) reduces to the following equation,

$$\{\mathcal{D}(u) + \mathcal{D}(r) + \frac{1}{r^2}\mathcal{D}(\theta)\}\Psi(u, r, \theta) = 0 \ . \tag{3.7}$$

The segregated derivative operators $\mathcal{D}(u)$, $\mathcal{D}(r)$ and $\mathcal{D}(\theta)$ in the above equation are given by,

$$\begin{aligned}
\mathcal{D}(u) &\equiv u^2\partial_u\Big(\frac{f(u)}{u^2}\partial_u\Big) + iu^2\partial_u\Big(\frac{A_t}{u^2}\Big) + iA_t\partial_u - \frac{m^2}{u^2} \\
\mathcal{D}(r) &\equiv \frac{1}{r}\partial_r(r\partial_r) - \frac{i}{r}\partial_r(rA_r) - iA_r\partial_r - A_r^2 \\
\mathcal{D}(\theta) &\equiv \partial_\theta{}^2 - i(\partial_\theta A_\theta + A_\theta\partial_\theta) - A_\theta{}^2 \ .
\end{aligned} \tag{3.8}$$

3.2.3 The Vortex Solution

Our interest lies in the equilibrium state, where vortices in the rotating superfluid exist, so we define a small deviation parameter, ϵ, from the critical rotation velocity, denoted by Ω_c, in the following relation,

$$\epsilon := \frac{\Omega - \Omega_c}{\Omega_c} \tag{3.9}$$

where Ω is the constant angular velocity of the disc. As argued in [118], one should note that there is a relative velocity between the superfluid and the disc. Hence, a static superfluid in a rotating disc could be represented by a rotating superfluid in a static disc. In this analysis, we shall be working with the latter scenario. In order to study this holographic system very near to Ω_c, we shall series expand all the fields, that is Ψ and A_μ, as well as the bulk current j_μ in order of ϵ in the following manner [119],

$$\Psi(u,r,\theta) = \sqrt{\epsilon}\Big(\Psi_1(u,r,\theta) + \epsilon\Psi_2(u,r,\theta) + ...\Big) \tag{3.10}$$

$$A_\mu(u,r,\theta) = \Big(A^{(0)}_\mu(u,r,\theta) + \epsilon A^{(1)}_\mu(u,r,\theta) + ...\Big) \tag{3.11}$$

$$j_\mu(u,r,\theta) = \epsilon\Big(j^{(0)}_\mu(u,r,\theta) + \epsilon j^{(1)}_\mu(u,r,\theta) + ...\Big)\,. \tag{3.12}$$

3.2.3.1 Zeroth order solutions near AdS boundary

In this model, critical rotation field and the chemical potential can be introduced via zeroth order solutions for gauge fields. In axial gauge ($A_u = 0$), these are given by the following relations,

$$A^{(0)}_t(u) = \mu(1-u), \quad A^{(0)}_r = 0, \quad A^{(0)}_\theta(r) = \Omega r^2\,. \tag{3.13}$$

Notice that the condition $A^{(0)}_r = 0$ imposes restrictions to any superfluid flow in the radial direction while $A^{(0)}_\theta$ allows the superfluid to rotate with constant angular velocity, Ω, about an axis passing through $r = 0$.

With these zeroth order solutions for gauge fields near the AdS boundary, we may rewrite eq.(3.7) for lowest order in ϵ in the following form,

$$\{\mathcal{D}^{(0)}(u) + \mathcal{D}^{(0)}(r) + \frac{1}{r^2}\mathcal{D}^{(0)}(\theta)\}\Psi_1(u,r,\theta) = 0 \tag{3.14}$$

where the zeroth order derivative operators now take the following form,

$$\mathcal{D}^{(0)}(u) \equiv u^2\partial_u\Big(\frac{f(u)}{u^2}\partial_u\Big) + iu^2\partial_u\Big(\frac{A^{(0)}_t}{u^2}\Big) + iA^{(0)}_t\partial_u - \frac{m^2}{u^2}$$

$$\mathcal{D}^{(0)}(r) \equiv \frac{1}{r}\partial_r(r\partial_r) \tag{3.15}$$
$$\mathcal{D}^{(0)}(\theta) \equiv {\partial_\theta}^2 - i(\partial_\theta A_\theta^{(0)} + A_\theta^{(0)}\partial_\theta) - A_\theta^{(0)2} \ .$$

In order to solve eq.(3.14), we may now use the method of variable separation and separate $\Psi_1(u, r, \theta)$ in terms of separated functions of AdS coordinate u and the boundary disc coordinates (r, θ) in the following manner,

$$\Psi_1(u, r, \theta) = \Phi(u)\xi(r, \theta) \ . \tag{3.16}$$

With such a separation of matter field, eq.(3.14) could be decoupled in the following separate eigenvalue equations,

$$\mathcal{D}^{(0)}(u)\Phi(u) = \lambda\Phi(u) \tag{3.17}$$
$$\{\mathcal{D}^{(0)}(r) + \frac{1}{r^2}\mathcal{D}^{(0)}(\theta)\}\xi(r, \theta) = -\lambda\xi(r, \theta) \tag{3.18}$$

where λ is some unknown separation parameter. Note that both eq.(s)(3.17, 3.18) are eigenvalue equations with eigenvalue λ. Next, we shall be determining λ by solving eigenvalue equation for the boundary disc coordinates (r, θ).

3.2.3.2 Vortex solutions on the boundary disc

We now consider a disc of radius R at the AdS boundary. As this boundary disc has $2D$ rotational symmetry, we may take following ansatz to proceed further,

$$\xi(r, \theta) = \eta_p(r)e^{ip\theta} \tag{3.19}$$

where the single valuedness of the solution restricts p to be an integer, that is $p \in \mathcal{Z}$. Also, it should be noted that $\eta_p(r)$ must satisfy following boundary conditions to be well behaved. In this case, we chose to be working with the Neumann boundary conditions at both the disc boundaries, that is at $r = 0$ as well as at $r = R$,

$$\partial_r\eta_p|_{r=0} = 0 = \partial_r\eta_p|_{r=R} \ . \tag{3.20}$$

Now using ansatz given in eq.(3.19) in eq.(3.18), we shall obtain following differential equation,

$${\partial_r}^2\eta_p(r) + \frac{1}{r}\partial_r\eta_p(r) + \left\{\lambda - \left(\frac{p}{r} - \Omega r\right)^2\right\}\eta_p(r) = 0 \ . \tag{3.21}$$

This equation needs to be solved subjected to the boundary conditions given by eq.(3.20). In order to pursue this analysis ahead, we shall take following ansatz for $\eta_p(r)$,

$$\eta_p(r) = F_p(r)e^{-\Omega r^2/2} \ . \tag{3.22}$$

With this ansatz, eq.(3.21) takes the following form,

$$\partial_r{}^2 F_p(r) + \Big(\frac{1}{r} - 2p\Omega\Big)\partial_r F_p(r) + \Big(\tilde{\lambda} - 2\Omega - \frac{p^2}{r^2}\Big)F_p(r) = 0 \ . \tag{3.23}$$

We shall now apply Frobenius series solution method in order to solve eq.(3.23). Hence, considering that $F_p(r)$ is given by following series,

$$F_p(r) = \sum_{n=0}^{\infty} a_n r^{n+k} \quad , \quad (a_0 \neq 0) \tag{3.24}$$

where $k \in \mathcal{Z}$. The derivatives of $F_p(r)$ with respect to r are then given by,

$$\begin{aligned} \partial_r F_p(r) &= \sum_{n=0}^{\infty} a_n (n+k) r^{n+k-1} \ . \\ \partial_r^2 F_p(r) &= \sum_{n=0}^{\infty} a_n (n+k)(n+k-1) r^{n+k-2} \ . \end{aligned} \tag{3.25}$$

Using eqs.(3.24, 3.25 and 3.25) in eq.(3.23), we find the following condition,

$$\sum_{n=0}^{\infty} a_n \{(n+k)^2 - p^2)\} r^{n+k} + \sum_{n=0}^{\infty} a_n \{\lambda + 2\Omega(p-1-n-k)\} r^{n+k+2} = 0 \ . \tag{3.26}$$

This condition implies that coefficient for each order of r should separately satisfy eq.(3.26), that is,

$$\begin{aligned} r^k : a_0(k^2 - p^2) = 0 \ &\Longrightarrow \ k = \pm p \\ r^{k+1} : a_1((k+1)^2 - p^2) = 0 \ &\Longrightarrow \ (k+1) = \pm p \ . \end{aligned}$$

With these conditions, the regularity of the solutions at $r = 0$ implies that we shall consider $k = p$ and consequently, this would yield $a_1 = 0$. Similarly, we get the following recurrence relation if we set the coefficient for $r^{(k+n+2)}$ equal to zero.

$$\frac{a_{n+2}}{a_n} = \frac{(\lambda - 2\Omega(n+1))}{((n+2)^2 + 2p(n+2))} \ . \tag{3.27}$$

In deriving this result, we have already assumed that $k = p$. This recurrence relation connects all the even coefficients with a_0 and all the odd coefficients with a_1. Hence, we shall get a series solution for $F_p(r)$ with even terms only, because $a_1 = 0$.

We must terminate this series at some point, in order to have normalizable solutions, which determines λ in terms of Ω and n, that is,

$$\lambda = 2\Omega(n+1). \tag{3.28}$$

This relation implies that the eigenvalue λ is quantized. With this condition, the above series solution becomes a polynomial of order n. Thus we can write the solution for $\eta_p(r)$ with an additional index depicting the order of the polynomial as,

$$\eta_{p,n}(r) = a_0 e^{-\Omega r^2/2} F_{p,n}(r) \tag{3.29}$$

where

$$F_{p,n}(r) = r^p\Big(1 + \frac{a_2}{a_0}r^2 + \frac{a_4}{a_0}r^4 + ... + \frac{a_n}{a_0}r^n\Big)\,.$$

Let us now discuss the family of solutions with $n = 0$. In this case,

$$F_{p,0}(r) = r^p$$

and hence,

$$\eta_{p,0}(r) = a_0 r^p e^{-\Omega r^2/2} \quad ; \quad (\lambda = 2\Omega) \tag{3.30}$$

This solution is subjected to the Neumann boundary conditions mentioned earlier. This means the following first derivative of eq.(3.30) must vanish at the disc boundaries,

$$\partial_r \eta_{p,0}(r) = a_0 r^{p-1} e^{-\Omega r^2/2}(p - \Omega r^2)\,. \tag{3.31}$$

Now the boundary condition at $r = 0$ gives the following lower bound for p,

$$\partial_r \eta_{p,0}(r)|_{r=0} = 0 \quad \Longrightarrow \quad p > 1. \tag{3.32}$$

Applying the boundary condition at the disc boundary at $r = R$ gives the following linear relation between p and Ω,

$$\partial_r \eta_{p,0}(r)|_{r=R} = 0 \quad \Longrightarrow \quad p = \Omega R^2. \tag{3.33}$$

Since p is an integer, hence the above relation between p and Ω implies a quantization of the angular velocity Ω and also a quantization of the angular momenta in the rotating superfulid. Note that the radius R in the model is fixed. This implies that there is a linear relation between p and Ω. This is a nice result that comes from our analysis.

Let us now consider the solution for $n = 2$, which is given as,

$$\eta_{p,2}(r) = a_0 r^p e^{-\Omega r^2/2}\Big(1 - \frac{2\Omega}{(p+2)}r^2\Big) \;;\; (\lambda = 6\Omega)\;. \tag{3.34}$$

For this solution, we have,

$$\partial_r \eta_{p,2}(r) = a_0 r^{p-1} e^{-\Omega r^2/2}\Big(p - 3\Omega r^2 + \frac{2(\Omega r^2)^2}{p+2}\Big). \tag{3.35}$$

In this case, the boundary condition at $r = 0$ gives us the same lower bound for p,

$$\partial_r \eta_{p,2}(r)|_{r=0} = 0 \quad \Longrightarrow \quad p > 1. \tag{3.36}$$

However, the boundary condition at $r = R$ gives us the following condition,

$$\partial_r \eta_{p,2}(r)|_{r=R} = 0 \implies \Big(p - 3\Omega R^2 + \frac{2(\Omega R^2)^2}{p+2}\Big) = 0. \tag{3.37}$$

From this condition, we get,

$$\Omega R^2 = 3\frac{(p+2)}{4}\Big(1 \pm \sqrt{1 - \frac{8p}{9(p+2)}}\Big). \tag{3.38}$$

For $p >> 2$, the above result again provides a linear relation between p and Ω, that is, $\Omega R^2 \sim p$.

3.2.4 Stürm-Liouville Analysis in the Bulk Direction

We shall now solve equation for the matter field along bulk direction, that is eq.(3.17), using Stürm-Liouville eigenvalue approach. We shall be analysing this equation near the critical chemical potential ($\mu \sim \mu_c$) so that we may take the following ansatz for gauge fields near the AdS boundary[1],

$$A_t^{(0)}(u) = \mu, \quad A_r^{(0)} = 0, \quad A_\theta^{(0)}(r) = \Omega r^2\;. \tag{3.39}$$

For mathematical simplicity, we shall consider the case with $m^2 = -2$ and $\Delta = 1$. With these considerations, eq.(3.17) reduces to the following equation,

$$u^2\partial_u\Big(\frac{1-u^3}{u^2}\partial_u\Phi(u)\Big) + iu^2\partial_u\Big(\frac{\mu}{u^2}\Phi(u)\Big) + i\mu\partial_u\Phi(u) + \frac{2}{u^2}\phi = 2\Omega\Phi(u)\;. \tag{3.40}$$

In this investigation, we have focused on the simplest case of the lowest order vortex solutions with $(n = 0)$ and hence, have associated eigenvalue is given by $\lambda = 2\Omega$. For this case, eq.(3.40)

[1] $A_t^{(0)}(u) = \mu(1-u) \simeq \mu$ for $u \to 0$. Note that $A_t^{(0)}(u)$ vanishes at the black hole horizon $u = 1$.

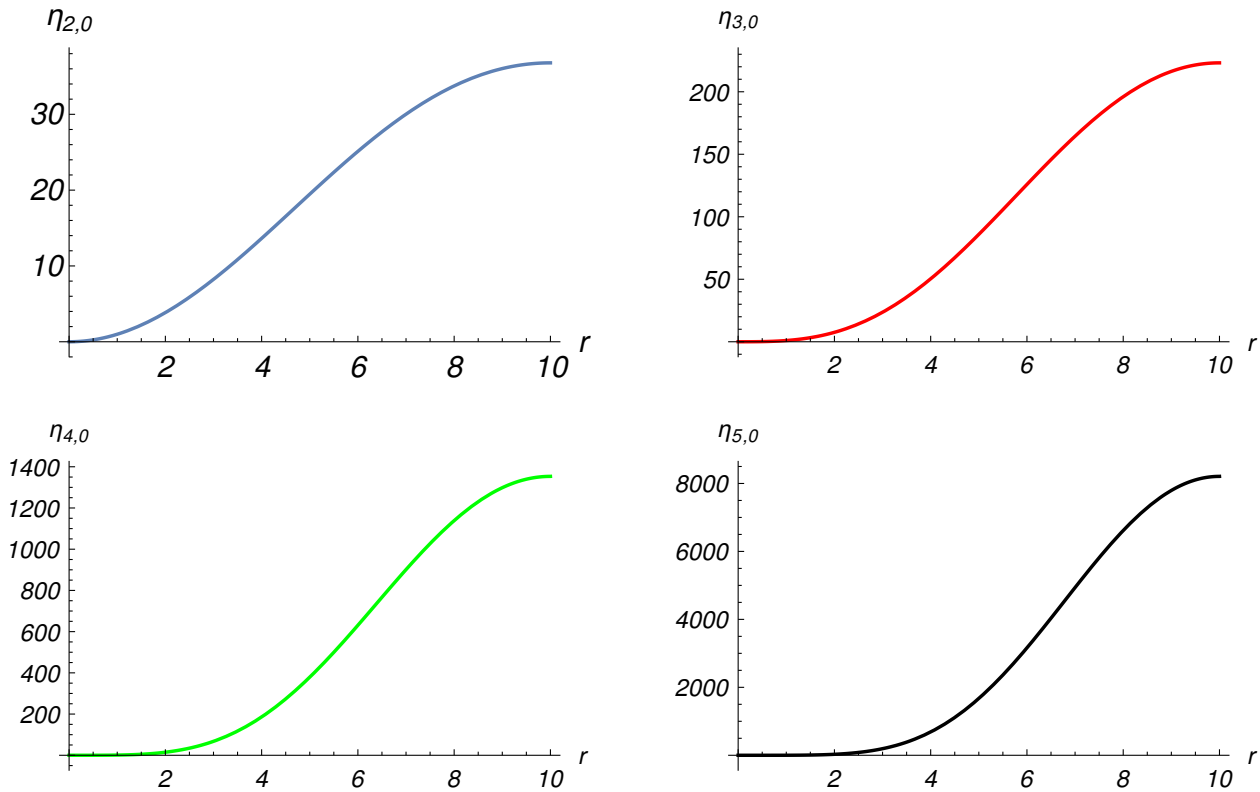

FIGURE 3.1 Un-normalized lowest order ($n = 0$) vortex solutions for different winding numbers. (The value of R is set to be equal to 10).

simplifies to following form,

$$(1-u^3)\partial_u^2\Phi - \left(u^2 + \frac{2}{u} - 2i\mu\right)\partial_u\Phi - \left(2\Omega - \frac{2}{u^2} + \frac{2i\mu}{u}\right)\Phi = 0\,. \tag{3.41}$$

As we know that around asymptotic AdS boundary (that is, $u \to 0$), the matter field, $\Phi(u)$, scales with the conformal dimension $(\Delta = 1)$ in the following manner,

$$\Phi(u) \simeq < \mathcal{O}_1 > u\Lambda(u) \tag{3.42}$$

such that $\Lambda(u)$ satisfies following boundary conditions,

$$\Lambda(0) = 1 \;\;;\;\; \partial_u\Lambda(0) = 0\,. \tag{3.43}$$

Using eq.(3.42) in eq.(3.41), equation for $\Phi(u)$ may be recasted as an equation in terms of $\Lambda(u)$ which is given below,

$$(1-u^3)\Lambda'' - (3u^2 - 2i\mu)\Lambda' - (u + 2\Omega)\Lambda = 0\,. \tag{3.44}$$

In the above equation, $'$ is used to denote derivative with respect to bulk coordinate u. If we now consider $\Lambda(u)$ to be real function, because this is ultimately related to superfluid condensate,

eq.(3.44) then implies that μ must be purely imaginary. For this reason, we have set $Re(\mu) = 0$, and $Im(\mu) = \mu^I$. With this, eq.(3.44) may be written as,

$$(1-u^3)\Lambda'' - (3u^2 + 2\mu^I)\Lambda' - (u + 2\Omega)\Lambda = 0 \ . \tag{3.45}$$

However, for notational simplicity we shall denote μ^I with μ from now on. We now multiply eq.(3.45) with the integrating factor $R(u)$ so that it takes the standard Stürm-Liouville form. This integrating factor, $R(u)$, is given as,

$$R(u) = \Big(\frac{1-u}{\sqrt{1+u+u^2}}\Big)^{\frac{2\mu}{3}} exp\Big(-\frac{2\mu}{\sqrt{3}}\arctan(\frac{1+2u}{\sqrt{3}})\Big) \ .$$

Eq.(3.45) can now be put into the following Stürm-Liouville form,

$$\begin{aligned} (P(u)\Lambda'(u))' + Q(u)\Lambda(u) + \Omega S(u)\Lambda(u) = 0 \qquad & (3.46) \\ P(u) = (1-u^3)R(u) \\ Q(u) = -uR(u) \\ S(u) = 2R(u) \ . \end{aligned}$$

The eigenvalue Ω can be obtained by solving the following integral,

$$\Omega = \frac{\int_0^1 du(P(u)(\Lambda'(u))^2 - Q(u)\Lambda^2(u))}{\int_0^1 du S(u)\Lambda^2(u)} \ . \tag{3.47}$$

In order to advance in these calculations, we shall take a trial function for $\Lambda(u)$ that respects the given boundary conditions, which are $\Lambda(0) = 1, \ \partial_u\Lambda(0) = 0$. The following trial function is a reasonable choice,

$$\Lambda_\alpha(u) = (1 - \alpha u^2) \ .$$

With this trial function, we have to optimise the following equation with respect to α so as to determine the eigenvalue Ω_α,

$$\Omega_\alpha = \frac{\int_0^1 du(P(u)(\Lambda'_\alpha(u))^2 - Q(u)\Lambda^2_\alpha(u))}{\int_0^1 du S(u)\Lambda^2_\alpha(u)} \ . \tag{3.48}$$

To analytically handle integrals in eq.(3.48), we shall further approximate $R(u)$ near the asymptotic AdS boundary, $u \to 0$, in the following manner,

$$R(u) \simeq \Big(1 - \frac{2\mu}{\sqrt{3}}\arctan(\frac{1+2u}{\sqrt{3}})\Big) \ . \tag{3.49}$$

Thus, using eq.(3.49) into eq.(3.48), we get the following equation for Ω_α,

$$\Omega_\alpha = \frac{\int_0^1 du\Big(1 - \frac{2\mu}{\sqrt{3}}\arctan(\frac{1+2u}{\sqrt{3}})\Big)\Big(u + 4\alpha^2u^2 - 2\alpha u^3 - 3\alpha^2u^5\Big)}{\int_0^1 du\Big(1 - \frac{2\mu}{\sqrt{3}}\arctan(\frac{1+2u}{\sqrt{3}})\Big)\Big(1 + \alpha^2u^4 - 2\alpha u^2\Big)} \,. \tag{3.50}$$

We need to extremize Ω_α with respect to α. Now there are two values of α which extremize eq.(3.50). In order to understand the qualitative role of μ, we have plotted these extremized values of Ω_α for a range of μ. These extremized values of Ω_α, corresponding to both values of α, for μ between 4.0 and 4.5 are shown in Fig.(3.2) and Fig.(3.3).

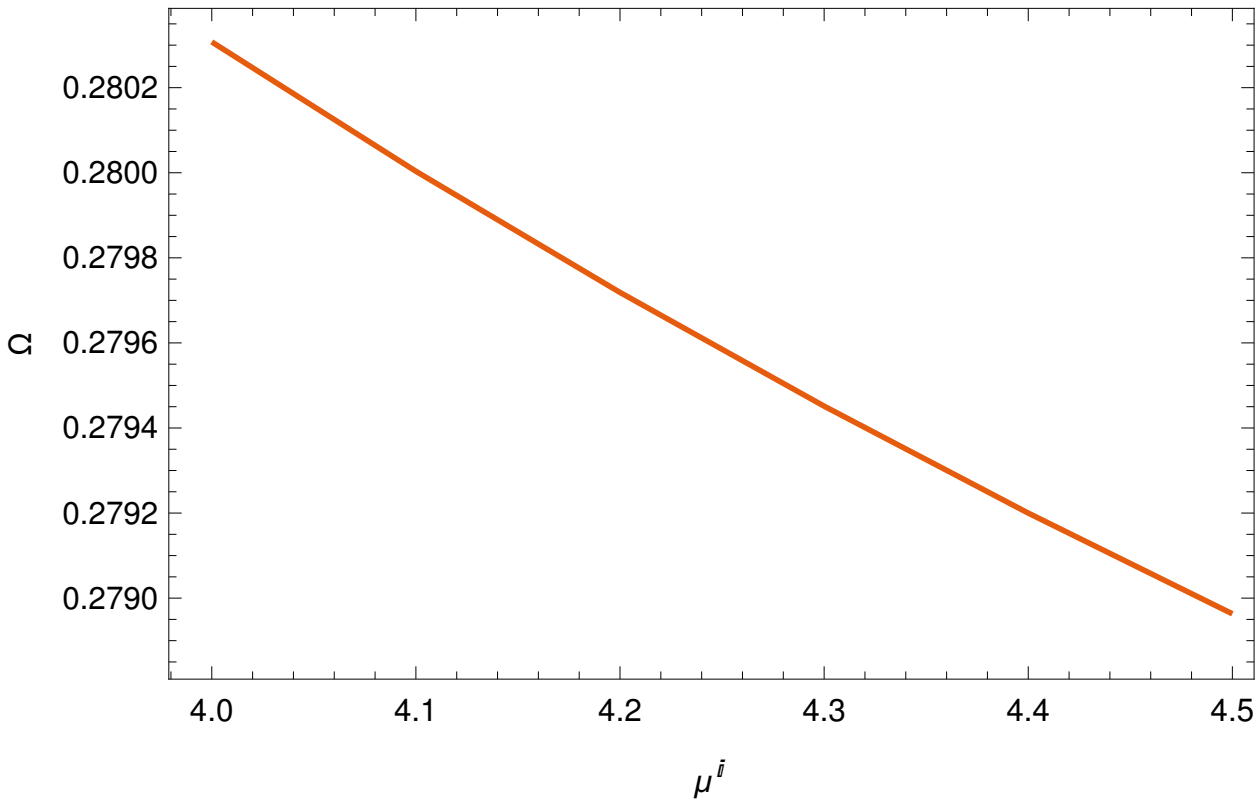

FIGURE 3.2 Ω vs μ for lowest order ($n = 0$) vortex solutions for first values of α that extremize Ω_α in eigenvalue equation (3.50).

There happens to be a remarkable trend in these plots, we notice that in both the cases, extremized values of Ω consistently decrease with an increase in the value of imaginary chemical potential. Some subtle observations are in order here. We have earlier shown in subsection (3.2.3.2) that for these vortices, Ω are quantized with the following relation,

$$\Omega = \frac{p}{R^2}$$

where R is the radius of the disc. We shall interpret this relation in conjuction with Fig.(3.2) and Fig.(3.3). It implies that for a disc with a fixed radius R, there is a decrease in the winding numbers

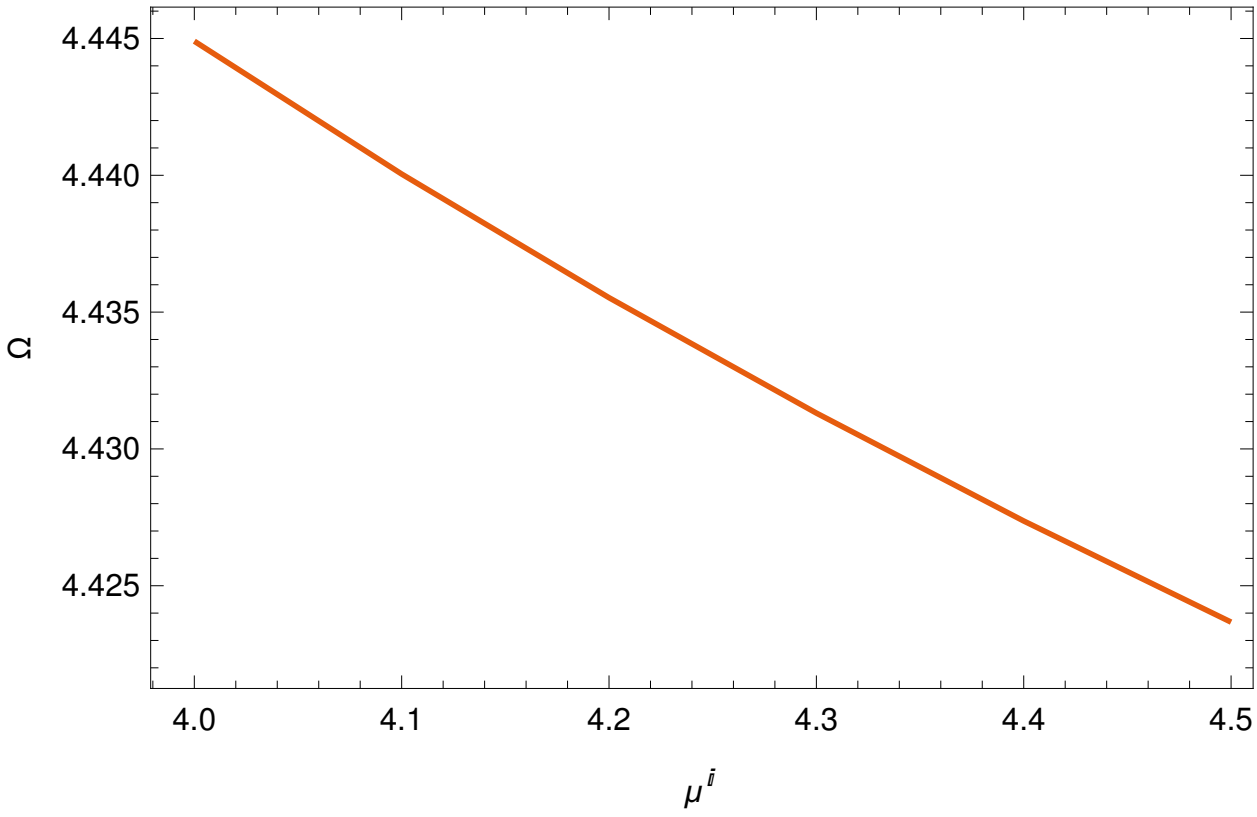

FIGURE 3.3 Ω vs μ for lowest order ($n = 0$) vortex solutions for second values of α that extremize Ω_α in eigenvalue equation (3.50).

of the vortices with the rise of the imaginary chemical potential. This seems to be an interesting observation from holographic point of view. In order to better understand this result, we have further considered the time-dependent terms in the equation of motions given by eq.(3.7). The corresponding time-dependent equation is given as,

$$\{\mathcal{D}(u) + \mathcal{D}(r) + \frac{1}{r^2}\mathcal{D}(\theta) - 2\partial_u\partial_t + \frac{2}{u}\partial_t\}\Psi(t, u, r, \theta) = 0. \tag{3.51}$$

We may now linearise this equation with the following form of $\delta\Psi$ and δA_μ,

$$\delta\Psi = p(u, r)e^{i\omega t+in\theta} \;\; ; \;\; \delta A_\mu = a_t(u, r)e^{i\omega t+in\theta}$$

Along with the boundary conditions given above, this would reduce to the following equations after the separation of variables for $p(u, r) = \Phi(u)\eta_p(r)$,

$$\partial_r{}^2\eta_p(r) + \frac{1}{r}\partial_r\eta_p(r) + \Big\{\lambda - \Big(\frac{p}{r} - \Omega r\Big)^2\Big\}\eta_p(r) = 0\,. \tag{3.52}$$

$$(1 - u^3)\partial_u^2\Phi - \Big(u^2 + \frac{2}{u} - 2i(\mu - \omega)\Big)\partial_u\Phi - \Big(-\frac{2}{u^2} + \frac{2i(\mu - \omega)}{u}\Big)\Phi = \lambda\Phi\,. \tag{3.53}$$

It should be noticed that these equations are similar to the eqs.(3.21, 3.41) that we had obtained for the case of stationary fields. The only difference is that in eq.(3.53), μ is now replaced with $(\mu-\omega)$. Hence, it immediately points towards a connection between imaginary chemical potential and imaginary part of the frequency, ω. As it is well known that imaginary part of the frequency, ω, implies dissipation in the system, hence we may attach a similar meaning to μ. We have observed in Fig.(3.2) and Fig.(3.3) that there is a decrease in the winding number of vortices with a rise in the value of the imaginary chemical potential. On the other hand, in Fig.(3.4), we observe that with increase in ω, Ω increases which means that the winding number of vortices also increases. Now increase in the vortex winding number can be understood as an increase of dissipation in the superfluid system [117]. Hence, the presence of both the imaginary chemical potential,'μ' and the frequency 'ω' of the quasi-normal modes affects the dissipation in the system.

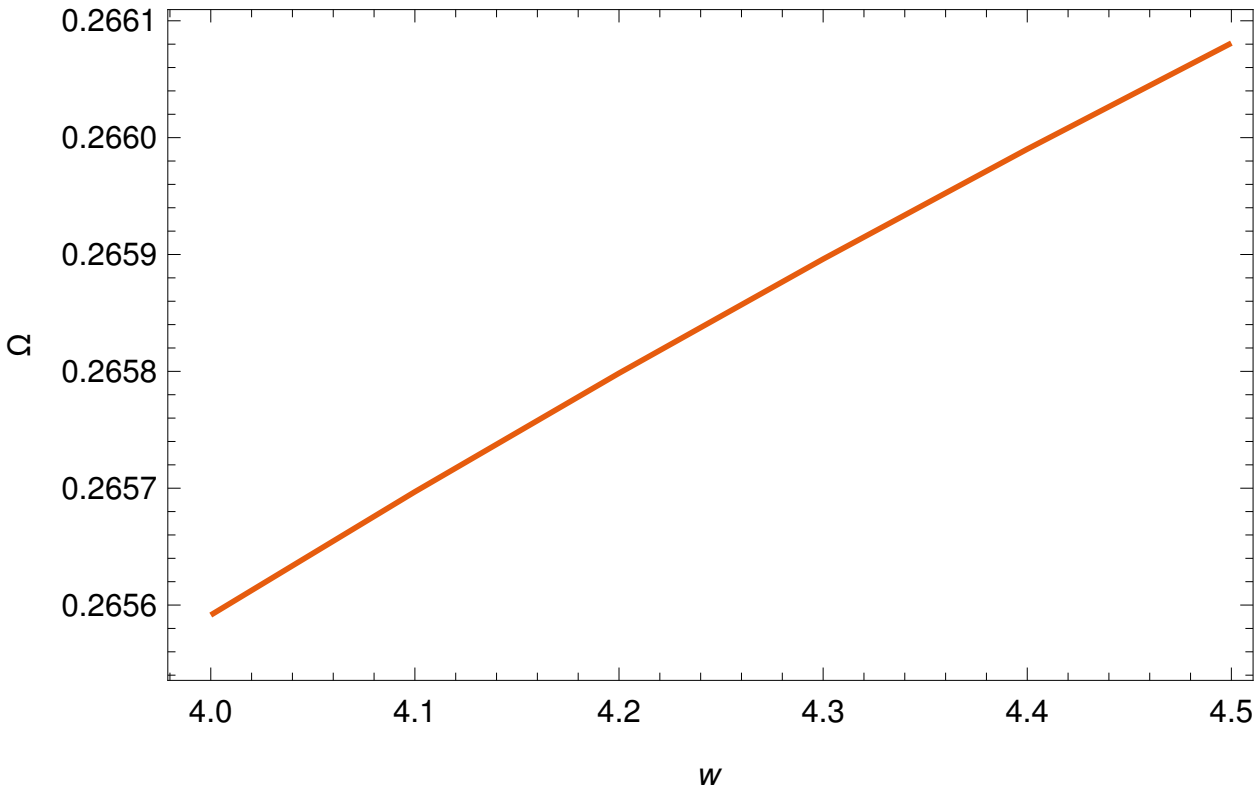

FIGURE 3.4 Ω vs ω for lowest order ($n = 0$) vortex solutions for first values of α that extremize Ω_α in eigenvalue equation obtained by eq.(3.53).

3.2.5 Discussion on Results

Let us summarise the findings of this analytic adventure. We showed that holographic superfluid model, with a boundary disc of radius R, does support vortex solutions above a critical rotation velocity Ω_c. These vortices are given as,

$$\xi(r,\theta) = \eta_{p,n}(r)e^{ip\theta} = a_0 e^{-\Omega r^2/2} F_{p,n}(r) e^{ip\theta} \tag{3.54}$$

where p may take only integer values for single valuedness of the solution and the eigenvalue $\lambda = 2\Omega(n+1)$. Also,

$$F_{p,n}(r) = r^p\Big(1 + \frac{a_2}{a_0}r^2 + \frac{a_4}{a_0}r^4 + ... + \frac{a_n}{a_0}r^n\Big) .$$

We again mention few crucial observations about these vortices.

1) These vortices are rotationally symmetric and follow Neumann boundary conditions given by,

$$\partial_r\eta_p|_{r=0} = 0 = \partial_r\eta_p|_{r=R} . \tag{3.55}$$

In the above equation, R is the boundary disc radius.

2) For $n = 0$, above boundary conditions enforce the quantisation of the angular velocity: $\Omega = \frac{p}{R^2}$ for all the values of $p > 1$.

3) For the next case of $n = 2$, these boundary conditions again impose restriction $p > 1$. A linear relation, however, between Ω and p is obtained only for large values of p.

There exist a linear relation between number of vortices and the rotation velocity, in case of large number of vortices, known as Feynman relation [118]. In our case, Feynman type linear relation is found to hold between winding number and the rotation velocity. This implies a quantisation of the angular momentum associated with these vortices. This linear relation is obtained analytically for lowest order ($n = 0$) vortex solution as an exact condition while for vortex solutions with ($n = 2$) such a linear relation emerges for large values of p. It is well known that high winding number vortex solutions are usually unstable and are likely to break into multiple vortices with low winding numbers. So we may interpret the relation obtained holographically as reminiscence of Feynman relation. Although, to establish it concretely we have to do the free energy analysis, which we have left for future explorations.

Looking at the equation of motion along the bulk direction, now, we have found that there is a requirement for an imaginary chemical potential. If we allow such a chemical potential, then we discover that presence of imaginary chemical potential discourages formation of high winding number vortices (and in turn less vortices with small winding number) and thereby, reduce dissipation into the superfluid system. This is the key finding of this study. Although we need more physical understanding of imaginary chemical potential and its meaning in the superfluid system, it is still interesting to analyse this from purely phenomenological perspective. It should be noted that such appearance of imaginary chemical potential has also been reported in the models of holographic QCD [120] as well as in the study of Bose condensate in a condensed matter

model [121]. Such complex chemical potential has been associated with the dissipative effects in these applications as well.

Next we have extended our analysis for the case of a Lifshitz holographic superfluid model.

3.3 Extension to Lifshitz spacetime

It was shown in earlier studies that the domain of the gauge/gravity duality can be extended to incorporate symmetries other than conformal as well. One particular extension is known as Lifshitz geometry which is expected to be dual to a boundary quantum field theory having Lifshitz fixed point [122]. The Lifshitz geometry admits following scaling symmetries in the bulk spacetime [123],

$$t \to \lambda^z t, \qquad x^i \to \lambda x^i \ . \tag{3.56}$$

Here z is known as dynamical exponent. This Lifshitz geometry does not respect Lorentz symmetry as it treats time and space components in non-equal footing. Hence boundary system is also supposed to be non-relativistic.

In this part of the thesis, our prime interest is to study possible vortex solutions for such a non-relativistic superfluid system with Lifshitz fixed point (rather than conformal fixed point) using applied gauge/gravity duality. We shall call this boundary system a non-relativistic Lifshitz holographic superfluid (NRLHS). It turns out that Lifshitz geometry could be seen as generalisation of $AdS_{(3+1)}$ in terms of the dynamical exponent z such that $z = 1$ restores the standard relativistic case of $AdS_{(3+1)}$ model. This dynamical exponent may take values in the interval $[1, 2]$. However, $z = 2$ is a special case in $(3 + 1)$-dimensions as gauge field diverges logarithmically near the asymptotic boundary. So we have restricted values of z in the interval $[1, 2)$ in this analysis. In the following sections we have now discussed vortex structure for this case in mathematical details.

3.3.1 Setting Up the Gravity Dual

We shall consider the same matter action, as considered in the subsection (3.2.1), for a holographic superfluid,

$$\mathcal{S} = \frac{l^2}{16\pi G e^2} \int_{\mathcal{M}} d^4x \{-\frac{1}{4}F^2 - |D\Psi|^2 - m^2\Psi^2\} \ . \tag{3.57}$$

In the above matter action, various symbols have their usual interpretations such as l represents the radius of curvature of the spacetime geometry, e denotes charge, G is used for the Newton's constant, the mass of the scalar field is taken to be m and $F^2 \equiv F_{\mu\nu}F^{\mu\nu}$. The Faraday tensor

and covariant derivative also have the usual forms given by $F_{\mu\nu} = \partial_{[\mu}A_{\nu]}$ and $D_\mu = \nabla_\mu - ieA_\mu$ respectively. We shall be using the probe approximation in the analysis of this model. In the probe approximation, it is assumed that matter sector does not back-react with the black hole background geometry and so we may fix it and analyse the dynamics of other fields on top of it. Mathematically, probe approximation is achieved by rescaling scalar and gauge fields with the charge e as $A_\mu \to \frac{A_\mu}{e}$ and $\Psi \to \frac{\Psi}{e}$, and then taking limit $e \to \infty$. It is equivalent to setting $e = 1$ in this model.

This simple holographic superfluid model is analysed on top of a $(3+1)$-dimensional Lifshitz black hole geometry with the scaling symmetries given by eq.(3.56). Such a black hole spacetime is realised by the following metric [123],

$$ds^2 = -\frac{f(u)}{u^{2z}}dt^2 + \frac{du^2}{f(u)u^2} + \frac{1}{u^2}(dr^2 + r^2 d\theta^2) \ . \tag{3.58}$$

The blackening factor for this black hole geometry is given by $f(u) = (1 - u^{z+2})$. In our analysis, we have set l and $16\pi G$ to be unity for convenience. Also we have rescaled the bulk direction in such a way that the asymptomatic spacetime boundary is at $u = 0$ and $u = 1$ represents the event horizon of the black hole. The boundary coordinates (r, θ) define a 2-dimensional flat disc. It should be noted from eq.(3.58) that setting $z = 1$ would restore $AdS_{(3+1)}$ black hole spacetime structure.

Let us now write the metric (3.58) in Eddington-Finkelstein (EF) coordinates,

$$ds^2 = -\frac{f(u)}{u^{2z}}dt^2 - \frac{2}{u^{z+1}}dtdu + \frac{1}{u^2}(dr^2 + r^2 d\theta^2) \ . \tag{3.59}$$

Here, the EF-time label is redefined by t for notational simplicity. Equations of motion for the matter and the gauge fields in the present case are given by,

$$(D^2 - m^2)\Psi = 0 \tag{3.60}$$

$$\nabla_\nu F_\mu^{\ \nu} = j_\mu := i\{(D_\mu\Psi)^\dagger\Psi - \Psi(D_\mu\Psi)\} \ . \tag{3.61}$$

Similar to the previous case, here also we shall be assuming no explicit time dependency in the model so that all the fields remain stationary. This assumption is again justified in view of our interest in equilibrium analysis of the rotating superfluid system. In addition to it, we shall be working in the axial gauge, that is, $A_u = 0$. With all these considerations, eq.(3.60) reduces to the following equation,

$$\{\mathcal{D}(u) + \mathcal{D}(r) + \frac{1}{r^2}\mathcal{D}(\theta)\}\Psi(u, r, \theta) = 0 \ . \tag{3.62}$$

The explicit form of the derivative operators are given below,

$$\begin{aligned}
\mathcal{D}(u) &\equiv u^{z+1}\partial_u\Big(\frac{f(u)}{u^2}\partial_u\Big) + iu^{z+1}\partial_u\Big(\frac{A_t}{u^2}\Big) + iu^{z-1}A_t\partial_u - \frac{m^2}{u^2} \\
\mathcal{D}(r) &\equiv \frac{1}{r}\partial_r(r\partial_r) - \frac{i}{r}\partial_r(rA_r) - iA_r\partial_r - A_r^2 \\
\mathcal{D}(\theta) &\equiv {\partial_\theta}^2 - i(\partial_\theta A_\theta + A_\theta\partial_\theta) - {A_\theta}^2 \,.
\end{aligned} \tag{3.63}$$

It is interesting to note here that all the information about dynamical exponent z is solely contained in the derivative operator along bulk direction u only. The other two derivative operators (along boundary coordinates r and θ) remain same as they were in the case of AdS black hole spacetime model studied in the previous section.

3.3.2 The Holographic Vortex

As discussed before, vortices in a superfluid start to appear after a critical value of the rotation velocity and at equilibrium a vortex pattern is formed in the rotating superfluid system. In this work, we are interested in this equilibrium state of the holographic system. In order to do so, we define a deviation parameter, ϵ, from this critical value of rotation, Ω_c, by the following relation,

$$\epsilon := \frac{\Omega - \Omega_c}{\Omega_c} \tag{3.64}$$

where Ω is the constant angular velocity of the rotating disc. As argued in the previous case that the superfluid and the boundary disc have a relative velocity and, hence, a static superfluid in a rotating boundary disc could be replaced by a rotating superfluid in a static disc. In the present case also, we have pursued this second scenario.

Near to the critical rotation velocity, we may series expand all the fields and currents in the following way [119],

$$\Psi(u,r,\theta) = \sqrt{\epsilon}\Big(\Psi_1(u,r,\theta) + \epsilon\Psi_2(u,r,\theta) + ...\Big) \tag{3.65}$$

$$A_\mu(u,r,\theta) = \Big(A_\mu^{(0)}(u,r,\theta) + \epsilon A_\mu^{(1)}(u,r,\theta) + ...\Big) \tag{3.66}$$

$$j_\mu(u,r,\theta) = \epsilon\Big(j_\mu^{(0)}(u,r,\theta) + \epsilon j_\mu^{(1)}(u,r,\theta) + ...\Big)\,. \tag{3.67}$$

3.3.3 Lowest order solutions near spacetime boundary

Working in the axial gauge, one can generate rotation field and the chemical potential in the holographic system using the lowest order solutions for gauge fields as given by the following relations,

$$A_t^{(0)}(u) = \mu(1 - u^{2-z}), \quad (z < 2) \tag{3.68}$$

$$A_r^{(0)} = 0, \quad A_\theta^{(0)}(r) = \Omega r^2 \, . \tag{3.69}$$

Here the radial component of the gauge field, $A_r^{(0)}$, restricts the superfluid flow in the radial direction of the boundary disc and the angular component of the gauge field, $A_\theta^{(0)}$, introduces rotation into the superfluid. We would like to emphasise here that the case with dynamical exponent $z = 2$ is non-trivial due to logarithmic divergence in the $A_t^{(0)}(u)$ near the spacetime boundary. For the present analysis, we have excluded this value as it is extremely difficult to deal with it analytically. Hence, in this thesis we have kept ourselves restricted to the values of the dynamical exponent z in the interval [1,2).

Now we have considered the lowest order solutions for fields near the spacetime boundary and rewrite eq.(3.62) for lowest order in ϵ,

$$\{\mathcal{D}^{(0)}(u) + \mathcal{D}^{(0)}(r) + \frac{1}{r^2}\mathcal{D}^{(0)}(\theta)\}\Psi_1(u, r, \theta) = 0 \, . \tag{3.70}$$

Again the explicit form of various zeroth order derivative operators in the above equation are following,

$$\begin{aligned}
\mathcal{D}^{(0)}(u) &\equiv u^{z+1}\partial_u\Big(\frac{f(u)}{u^2}\partial_u\Big) + iu^{z+1}\partial_u\Big(\frac{A_t^{(0)}}{u^2}\Big) + iu^{z-1}A_t^{(0)}\partial_u - \frac{m^2}{u^2} \\
\mathcal{D}^{(0)}(r) &\equiv \frac{1}{r}\partial_r(r\partial_r) \\
\mathcal{D}^{(0)}(\theta) &\equiv {\partial_\theta}^2 - i(\partial_\theta A_\theta^{(0)} + A_\theta^{(0)}\partial_\theta) - {A_\theta^{(0)}}^2 \, .
\end{aligned} \tag{3.71}$$

Similar to the calculations in the previous case, we shall be using method of variable separation to solve eq.(3.70). We would start with a separation ansatz for $\Psi_1(u, r, \theta)$ in terms of a function of u and (r, θ) separately as shown below,

$$\Psi_1(u, r, \theta) = \Phi(u)\xi(r, \theta) \, . \tag{3.72}$$

Using ansatz given in eq.(3.72) in eq.(3.70), we shall obtain the following separated equations,

$$\mathcal{D}^{(0)}(u)\Phi(u) = \lambda\Phi(u) \tag{3.73}$$

$$\{\mathcal{D}^{(0)}(r) + \frac{1}{r^2}\mathcal{D}^{(0)}(\theta)\}\xi(r, \theta) = -\lambda\xi(r, \theta) \tag{3.74}$$

where λ is an unknown separation constant. We need to solve for these eigenvalue eqs.(3.73, 3.74) with eigenvalue λ. We have pointed out earlier that all the information about dynamical exponent, z, is only in the equation of motion along bulk direction, that is eq.(3.73) while the equation along the boundary disc coordinates (r, θ), that is eq.(3.74), remains same as in the previous case discussed in the section (3.2). This equation needs no separate investigation. Also it implies that even in this

non-relativistic rotating superfluid case, the structure and properties of the vortices associated with the boundary disc coordinates remain same as in the case of relativistic rotating superfluid case. Next, we shall analyse the equation of motion along bulk direction which must capture the effect of the dynamical exponent.

3.3.4 Stürm-Lioüville Eigenvalue Analysis

In this subsection, we shall be solving eq.(3.73) using Stürm-Lioüville eigenvalue approach for the simplest vortex solution ($n = 0$) with the eigenvalue $\lambda = 2\Omega$. Near the critical chemical potential ($\mu \sim \mu_c$), the following ansatz for the lowest order gauge fields may be admissible,

$$A_t^{(0)}(u) = \mu, \quad A_r^{(0)} = 0, \quad A_\theta^{(0)}(r) = \Omega r^2 \ . \tag{3.75}$$

For the calculational simplicity, we shall consider $m^2 = -2z$ and $\Delta = z$. With these considerations, we would get from eq.(3.73),

$$u^{z+1}\partial_u\Big(\frac{1-u^{z+2}}{u^2}\partial_u\Phi(u)\Big) + iu^{z+1}\partial_u\Big(\frac{\mu}{u^2}\Phi(u)\Big) + iu^{z-1}\mu\partial_u\Phi(u) + \frac{2z}{u^2}\phi = 2\Omega\Phi(u) \ . \tag{3.76}$$

This equation could be simplified in the following manner,

$$u^{z-1}(1-u^{z+2})\partial_u^2\Phi - \Big(zu^{2z} + 2u^{z-2} - 2i\mu u^{z-1}\Big)\partial_u\Phi - \Big(2\Omega - \frac{2z}{u^2} + 2i\mu u^{z-2}\Big)\Phi = 0 \ . \tag{3.77}$$

We may write $\Phi(u)$ near the asymptotic AdS boundary ($u \to 0$) in terms of conformal dimension $\Delta = z$,

$$\Phi(u) \simeq < \mathcal{O} > u^z\Lambda(u)$$

so that $\Lambda(u)$ must be subjected to the following boundary conditions,

$$\Lambda(0) = 1 \ ; \ \ \partial_u\Lambda(0) = 0 \ . \tag{3.78}$$

Substituting this asymptotic form of $\Phi(u)$ in eq.(3.77), we would obtain the following equation in terms of $\Lambda(u)$,

$$(1-u^{z+2})\Lambda'' + \Big(\frac{2(z-1)}{u} - 3zu^{z+1} + 2i\mu\Big)\Lambda' + \Big(\frac{z(z-3)}{u^2} + \frac{2i\mu(z-1)}{u} + \frac{2z}{u^{z+1}} - \frac{2\Omega}{u^{z-1}} - z^2u^z\Big)\Lambda = 0 \ . \tag{3.79}$$

Here $'$ is used to denote the derivative with respect to u in the above equation. It is now required in the eq.(3.79) that μ must be purely imaginary for $\Lambda(u)$ to be real. Hence, we must set $Re(\mu) = 0$ and $Im(\mu) = \mu^I$ in above equation. For notational simplicity, we shall be denoting imaginary chemical potential using μ in the subsequent discussion. With this imaginary chemical potential,

eq.(3.79) takes the following form,

$$(1-u^{z+2})\Lambda''+\Big(\frac{2(z-1)}{u}-3zu^{z+1}-2\mu\Big)\Lambda'+\Big(\frac{z(z-3)}{u^2}-\frac{2\mu(z-1)}{u}+\frac{2z}{u^{z+1}}-\frac{2\Omega}{u^{z-1}}-z^2u^z\Big)\Lambda=0\ . \quad (3.80)$$

Using the following integrating factor, we may put eq.(3.80) in the standard Stürm-Lioüville eigen-equation form,

$$R(u)=u^{z-1}exp(-2\mu\int\frac{du}{(1-u^{z+2})})\ . \quad (3.81)$$

The Stürm-Lioüville eigen-equation can be written in the following form,

$$(P(u)\Lambda'(u))'+Q(u)\Lambda(u)+\Gamma S(u)\Lambda(u)=0 \quad (3.82)$$

where for the present case, eigenvalue Γ can be identified with the rotation velocity Ω of the super-fluid. This eigenvalue could be obtained by optimising following integral,

$$\Omega=\frac{\int_0^1 du(P(u)(\Lambda'(u))^2-Q(u)\Lambda^2(u))}{\int_0^1 duS(u)\Lambda^2(u)}\ . \quad (3.83)$$

In the most general setting, the Stürm-Lioüville coefficient functions $P(u), Q(u)$ and $S(u)$, for the case of Lifshitz black hole geometry model, are given by,

$$\begin{aligned}P(u)&=u^{z-1}(1-u^{z+2})R(u)\\ Q(u)&=u^{z-1}\Big(\frac{z(z-3)}{u^2}-\frac{2\mu(z-1)}{u}+\frac{2z}{u^{z+1}}-z^2u^z\Big)R(u)\\ S(u)&=-2R(u)\ .\end{aligned} \quad (3.84)$$

Note that the integral in eq.(3.81) can be performed exactly to obtain,

$$R(u)=u^{z-1}exp(-2\mu\ u\ {}_2F_1(1,\frac{1}{z+2};\frac{z+3}{z+2};u^{z+2}))\ . \quad (3.85)$$

${}_2F_1(a,b;c;x)$ is the hypergeometric function given by,

$${}_2F_1(a,b;c;x)=\sum_{n=0}^{\infty}\frac{(a)_n(b)_n}{(c)_n}\frac{x^n}{n!} \quad (3.86)$$

where $(m)_n\equiv m(m+1)...(m+n-1)$.

3.3.5 First Trial Function

In order to proceed further, we have to consider a trial function for $\Lambda(u)$ in eq.(3.83). One good choice for such a trial function may be of the following form,

$$\Lambda_\alpha(u) = (1 - \alpha u^2) \ .$$

This trial function satisfies the required boundary conditions for $\Lambda(u)$ which are given by $\Lambda(0) = 1$ and $\partial_u \Lambda(0) = 0$. Using the trial function in eq.(3.83), we would obtain Ω_α, given in the following equation, which needs to be extremised with respect to α,

$$\Omega_\alpha = \frac{\int_0^1 du(P(u)(\Lambda'_\alpha(u))^2 - Q(u)\Lambda^2_\alpha(u))}{\int_0^1 du S(u)\Lambda^2_\alpha(u)} \ . \tag{3.87}$$

3.3.5.1 Analysis for z=1

We shall first consider the case with the dynamical exponent $z = 1$. In this case, eq.(3.58) shows that bulk spacetime becomes $AdS_{(3+1)}$ black hole spacetime, which is exactly the one that we have analysed in section(3.2). Near the asymptotic AdS boundary $(u \to 0)$, we know that $\Phi(u) \simeq < \mathcal{O} > u\Lambda(u)$, which is the same as in this case with $z = 1$. So we get the following Stürm-Lioüville equation to solve for,

$$(P(u)\Lambda'(u))' + Q(u)\Lambda(u) + \Gamma S(u)\Lambda(u) = 0 \tag{3.88}$$

where eigenvalue $\Gamma = \Omega$ and,

$$\begin{aligned} P(u) &= (1 - u^3)R(u) \\ Q(u) &= -uR(u) \\ S(u) &= -2R(u) \ . \end{aligned} \tag{3.89}$$

The integrating factor in this case can be obtained from eq.(3.85) for $z = 1$,

$$R(u) = exp(-2\mu \ u \ {}_2F_1(1, \frac{1}{3}; \frac{4}{3}; u^3)) \ . \tag{3.90}$$

We may now solve this problem by considering the trial function chosen above. Also, near the asymptotic AdS boundary $u \to 0$, we further approximate integrating factor, $R(u)$, given in eq.(3.90) in the following manner,

$$R(u) \simeq (1 - 2\mu \ u \ {}_2F_1(1, \frac{1}{3}; \frac{4}{3}; u^3)) \ . \tag{3.91}$$

Figure(3.5) shows the variation of extremised values of Ω with the increasing value of imaginary

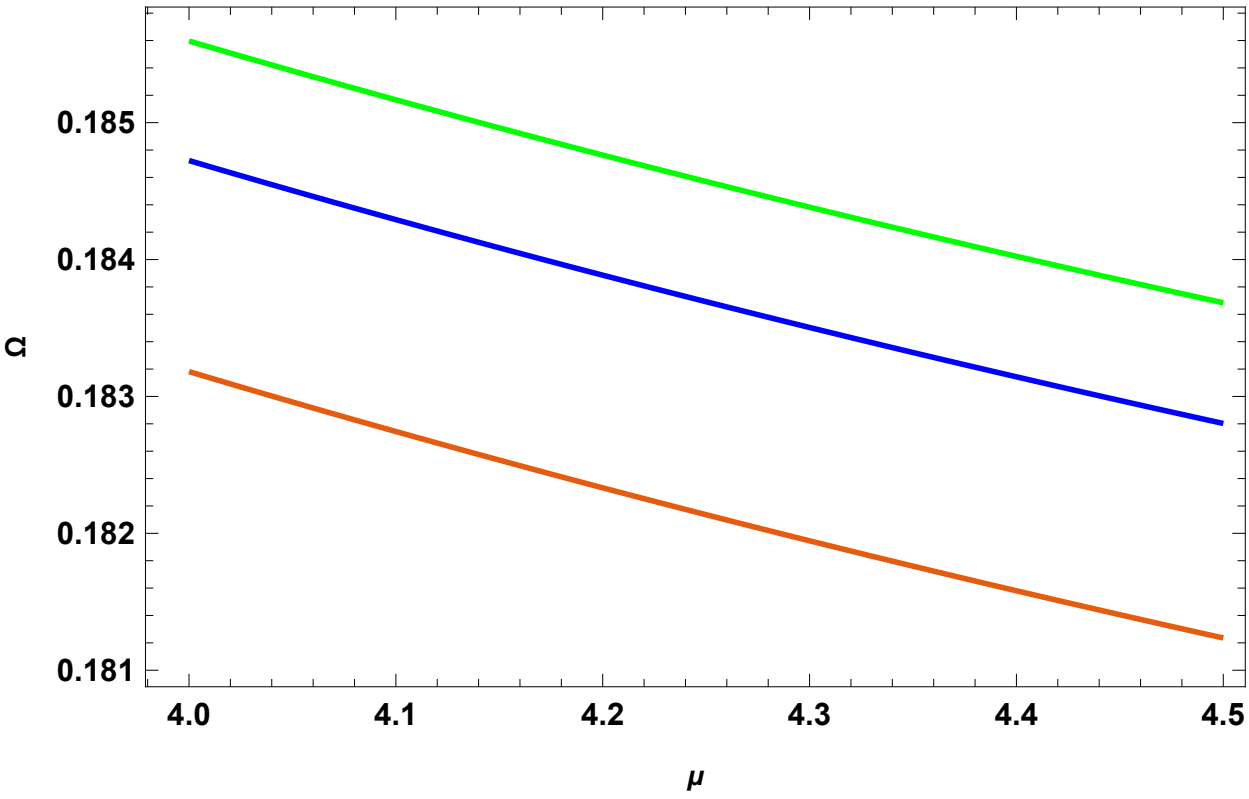

FIGURE 3.5 Ω vs μ for z=1

chemical potential, μ. In this figure, three colour plots represent three different orders upto which we have approximated the hypergeometric function in eq.(3.91) for calculations. Orange plot is obtained with lowest order approximation while blue and green plots result from next consecutive orders of approximation. We shall follow this colour scheme from now onwards. A few essential observations are in order regarding this graph which we shall enumerate below.

1) The graph between Ω and μ shows a decreasing trend, similar to the previous case.

2) Viewed together with the quantisation condition for rotation velocity, that is $\Omega = \frac{p}{R^2}$, this result implies that for an $AdS_{(3+1)}$ holographic superfluid model, analysed near equilibrium, in the presence of imaginary chemical potential, μ, opposes the formation of higher winding number vortices.

3) In gauge/gravity duality, it is well known that vortices in holographic superfluid provide mechanism for external perturbations to decay through black hole horizon and hence represent dissipation in such gravity dual systems. Now graphs in Fig.(3.5) suggest that when dynamical exponent is $z = 1$, because Ω decreases with increase in μ, imaginary chemical potential supports less dissipation in this holographic system.

3.3.5.2 Analysis for z $\neq$1

When the dynamical exponent $z \neq 1$, the Stürm-Lioüville form of the equation is given by eq.(3.82) and the value of z lies in the open interval $(1, 2)$. Here, we have excluded the case with $z \neq 2$ because of the logarithmic divergence of the fields at the boundary $u \to 0$. With the chosen trial function $\Lambda_\alpha(u) = (1 - \alpha u^2)$, we now need to extremise the following eigenvalue integral,

$$\Omega_\alpha = \frac{\int_0^1 du(P(u)(\Lambda'_\alpha(u))^2 - Q(u)\Lambda^2_\alpha(u))}{\int_0^1 du S(u)\Lambda^2_\alpha(u)} \ . \tag{3.92}$$

where

$$\begin{aligned} P(u) &= u^{z-1}(1 - u^{z+2})R(u) \\ Q(u) &= u^{z-1}\Big(\frac{z(z-3)}{u^2} - \frac{2\mu(z-1)}{u} + \frac{2z}{u^{z+1}} - z^2u^z\Big)R(u) \\ S(u) &= -2R(u) \ . \end{aligned} \tag{3.93}$$

In this case, we shall further approximate the integrating factor given in eq.(3.85) in the following form,

$$R(u) = u^{z-1}(1 - 2\mu\ u\ {}_2F_1(1, \frac{1}{z+2}; \frac{z+3}{z+2}; u^{z+2})) \ . \tag{3.94}$$

In Figure(3.6), we have shown the variation of extremised values of Ω against imaginary chemical potential μ for $z = \frac{3}{2}$ again considering three orders of approximation for the hypergeometric function ${}_2F_1(1, \frac{1}{z+2}; \frac{z+3}{z+2}; u^{z+2})$. Colour codes remain same as in the previous case. We may now summarise the key observations from this graph.

1) For $z = \frac{3}{2}$, Ω shows an increasing pattern with μ opposite to the previous case for $z = 1$.

2) This behaviour implies that for a holographic superfluid with Lifshitz geometry and dynamical exponent $z = \frac{3}{2}$, higher winding number solutions are more favourable with increasing value of μ.

3) In terms of dissipation in such a rotating holographic superfluid, we conclude from this result that higher values of μ introduce more dissipation in the presence of Lifshitz fixed points (in gauge/gravity duality Lifshitz geometry of the bulk theory is dual to a boundary theory with Lifshitz fixed point.).

4) Same increasing trend for Ω with μ is obtained for other values of z in the interval $(1, 2)$. Cases with $z = \{1.1, \frac{5}{4}, \frac{7}{4}\}$ are given in **Appendix I**.

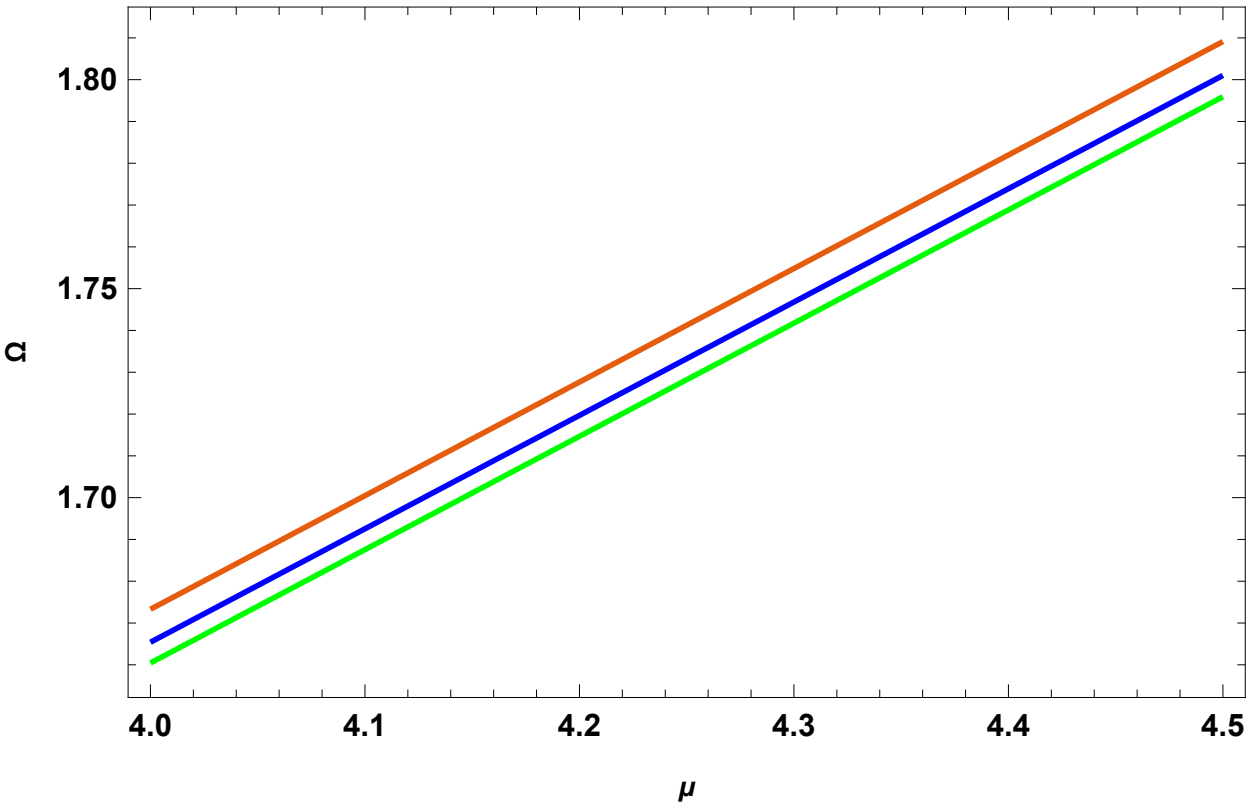

FIGURE 3.6 Ω vs μ for $z = \frac{3}{2}$ with first trial function

3.3.6 Second Trial Function

The Stürm-Liouville eigenvalue approach depends on the choice of a trial function. So, we have also worked with another trial function which is often used in the holographic literature,

$$\Lambda_\alpha(u) = (1 - \alpha u^{(z+1)}) \, .$$

This trial function is also a valid power law function known in holographic literature and satisfies the required boundary conditions. Notice that z may take values in the interval $[1, 2)$. Results obtained with this trial function also show same qualitative difference between relativistic and non-relativistic boundary superfluids. It should be noted that for the case of $z = 1$ both the trial functions become identical and hence results are given in Fig (3.4). However, for other values of z, this trial function differs in power law decay, with variable exponent $(z + 1)$, in comparison to previous trial function where power law decay was fixed with exponent 2. This analysis with second trial function is important for the robustness of our claim regarding behaviour of different boundary superfluid systems. Graphs between Ω and μ using second trial function for $z = \frac{3}{2}$ is shown in Fig.(3.7), which is qualitatively similar to Fig.(3.6). Results for a few other values of z are shown in **Appendix II**.

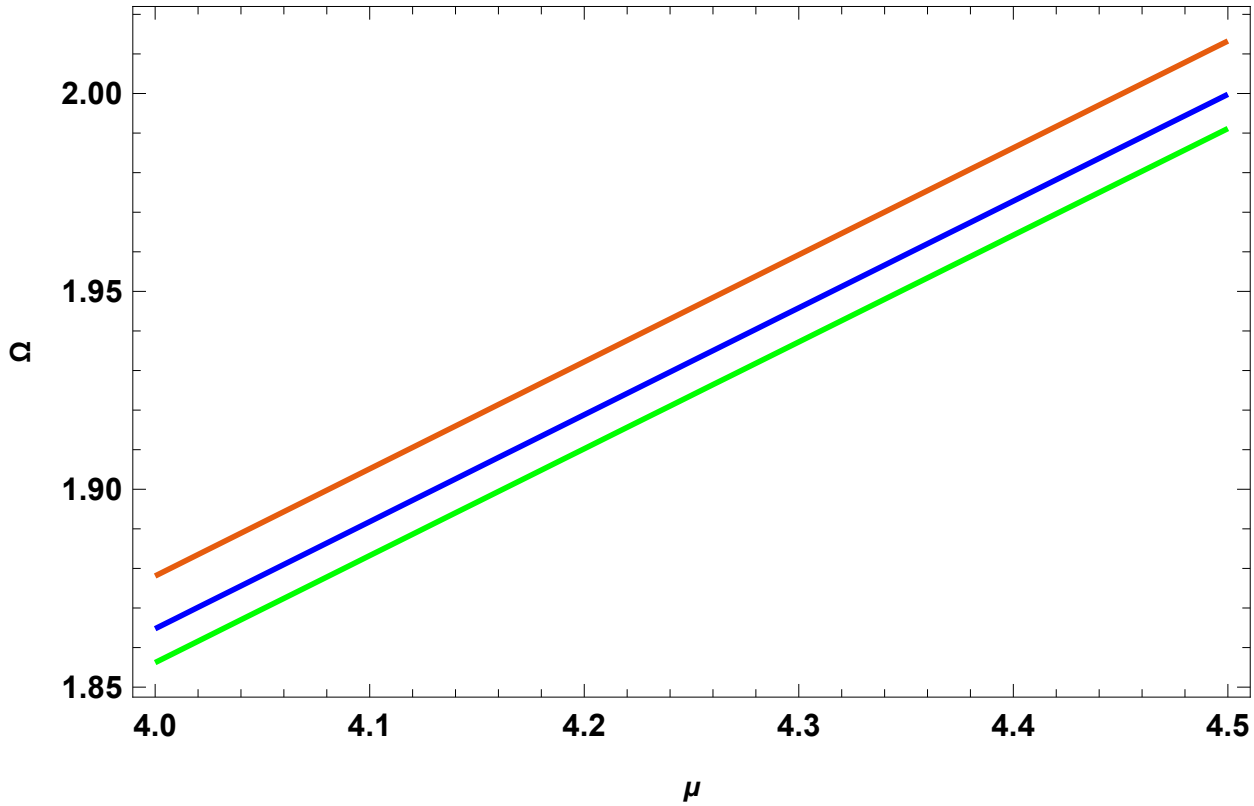

FIGURE 3.7 Ω vs μ for $z = \frac{3}{2}$ with second trial function

3.3.7 Discussion on Results

Let us summarise our findings for holographic vortex analysis in the presence of Lifshitz fixed point. We notice that Lifshitz scaling does not affect equation of motion for matter field on the asymptotic boundary coordinates (r, θ). This implies that structure of vortices on the boundary disc remain unchanged for non-relativistic Lifshitz holographic superfluids (NRLHS). However, in the bulk direction dynamical critical exponent, z, does affect equation of motion for matter field which leads us to surprising result regarding dissipation in the boundary system. Specifically, we have found that for values of $z \neq 1$, increase in the imaginary chemical potential leads to more dissipation in the boundary system unlike in the relativistic case whose results are again recovered in this analysis for $z = 1$. In this work, we have also checked the robustness of our results for two different choices of the trial functions in the Stürm-Liouville analysis as well as we have incorporated approximations of the Gauss hypergeometric function up to three orders. We found that our claims are robust enough under these choices and approximations.

3.4 Conclusions and Remarks

In this chapter, we have studied the formation of vortices in a rotating holographic superfluid near the critical rotation velocity. We were interested in the equilibrium situation where such vortices

are expected to be stable and hence we have ignored any time dependency in the analysis. We found that indeed it is possible to construct such vortex solutions in the holographic setting and in this particular work we have discovered novel single vortex solutions, which were not reported earlier [124, 125]. We have used the method of variable separation to first split the equation of motion for the matter field along bulk direction and on the boundary disc defined by the boundary coordinates (r, θ). We have then analysed the boundary disc equation using Frobenius series solution method and determine explicit expression for vortex solution. It turns out that reasonable choices for the boundary conditions on the boundary disc, for the vortex solutions, provide us with quantisation of the angular velocities associated with the vortices. Also, we were able to deduce a linear relation between angular velocity and the winding number of the vortices for large winding numbers, which seems very similar to Feynman linear relation for large number of vortices in a superfluid [118].

Next, we have studied the solution of the bulk equation for the lowest order of vortex solution given by $(n = 0)$. We have used Stürm-Liouville eigenvalue approach to study this equation and found that for condensate to remain real, we have to consider a purely imaginary chemical potential. We would like to point out that such complex chemical potentials have also been reported in previous studies in holographic QCD [120] and BE condensates [121]. Imaginary chemical potentials have been connected to some sort of dissipations in the systems there. In our work, we have only considered it as a mathematical condition and have not tried to give it a physical meaning. However, we did relate its presence in the superfluid system with a dissipative behaviour. More specifically, we have discovered that an increase in the value of imaginary chemical potential decreases higher winding number vortex solutions in the case of relativistic superfluid (RCHS) on the boundary system [124]. As is well known in holography that vortices allow fluctuations on the boundary to quickly die off inside the black hole and hence presence of vortices may be connected to dissipation in the system [117]. Also, it is expected that higher winding number vortices should be unstable and split in a number of vortices with small winding number. Therefore, possibility of having higher winding number vortices must imply possibility of having more number of vortices with small winding number and in this sense our analysis of relativistic holographic superfluid asserts a decreasing dissipation in the presence of higher values of imaginary chemical potential.

Majority of condensed matter systems are not relativistic in nature and hence it is interesting to understand these systems as well within the gauge/gravity duality. In fact, gravity duals to non-relativistic systems have been constructed in the past and we have studied one such model which is dual to a non-relativistic superfluid with Lifshitz fixed point (NRLHS) [125]. We have utilised analytic calculations of above mentioned RCHS vortex model in this case as well and found that we again get same vortex solutions with quantised angular velocities on the boundary

disc. However, interestingly we discovered an opposite behaviour in terms of dissipation. More specifically, we found that in the case of NRLHS, dissipation through the presence of vortices increases with an increase in the imaginary chemical potential.

In conclusion, we make the following remarks based on the analysis presented in this chapter.

1) Within the gauge/gravity duality, it is possible to built vortex solution for superfluids under rotation.

2) Structure of vortex solution doesn't seem to be changed for either relativistic or non-relativistic superfluid.

3) However, dissipative behaviour of a non-relativistic superfluid differs strongly from relativistic superfluid.

Let us now discuss some open questions that should be pursued in order to understand these holographic systems in more detail. First a free energy analysis is required to further confirm that higher winding number vortices are indeed unstable and should split into multiple small winding number vortices. Then one should be able to figure out vortex lattice structure using these vortex solutions. Also, it should be interesting to incorporate time-dependent analysis of the system which might be able to shed some light of analytic understanding of vortex-antivortex dynamics, which has been studied only numerically in such holographic models so far [117].

Appendix I: First Trial Function

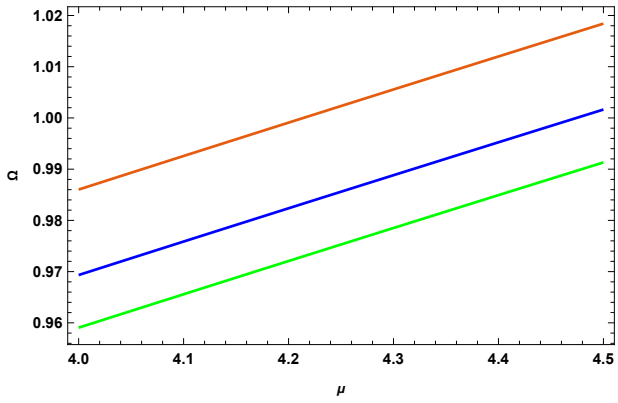

FIGURE 3.8 Ω vs μ for $z = 1.1$

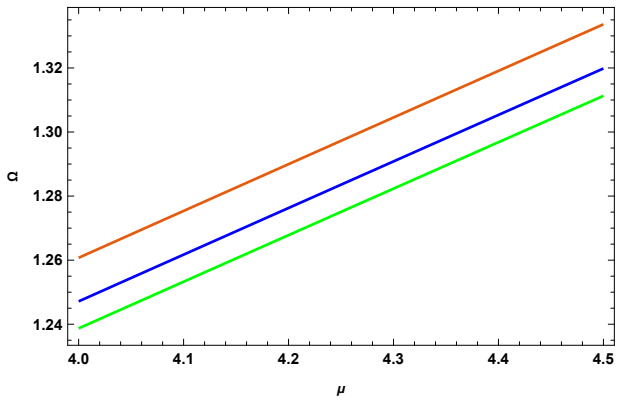

FIGURE 3.9 Ω vs μ for $z = \frac{5}{4}$

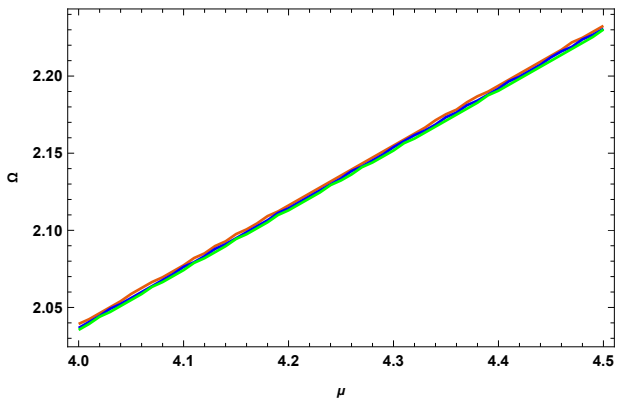

FIGURE 3.10 Ω vs μ for $z = \frac{7}{4}$

Appendix II: Second Trial Function

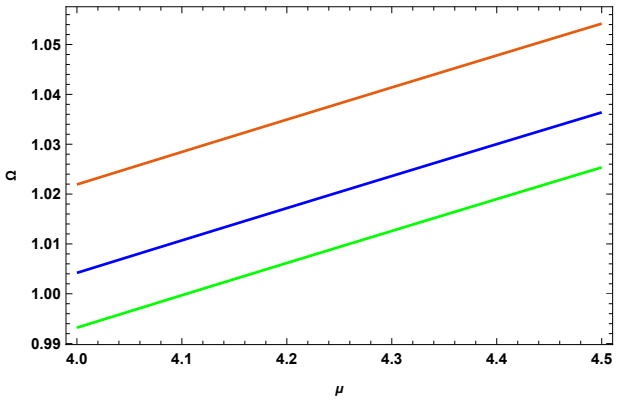

FIGURE 3.11 Ω vs μ for $z = 1.1$

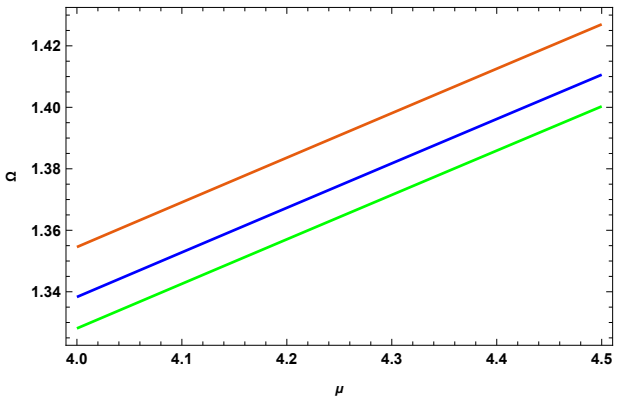

FIGURE 3.12 Ω vs μ for $z = \frac{5}{4}$

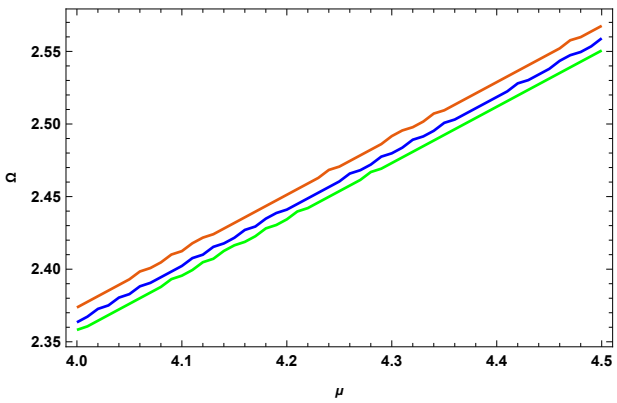

FIGURE 3.13 Ω vs μ for $z = \frac{7}{4}$

CHAPTER 4

Holographic Thermoelectric Coefficients

4.1 Introduction

In previous chapters, we have studied some toy models based on the application of the gauge/gravity duality to understand certain properties of unconventional superfluids and superconductors. As there is no rigorous way to construct these gravity dual models, we are strongly dependent on possible symmetry structure of the boundary dual systems. For example, to understand s-wave superconductivity we had constructed a gravity dual model using scalar field (spin zero) [86]. However, these models are still far from real materials in many aspects and the hope of holographers is to continue building better gravity duals which resemble more closely to reality. One such improvement in holography is to construct a gravity dual model of the boundary systems with some notion of lattice structure. It is well known that all the materials we know of have some underlying lattice and it plays important role in the dynamics of electrons in these materials. Holographic models that we have discussed so far were essentially blind to such lattice structure and hence, were only able to describe properties of the boundary system without any underlying lattice. It turns out that we can indeed built gravity duals with a notion of holographic lattice [126, 127]. In the past, many such models have been studied that were dual to some charged plasma with lattice structure. There are three ways to construct holographic lattices viz. a periodic scalar field (axion models) [128], a periodic chemical potential (ionic models) [129, 130], and massive gravity theories [39].

Effects of lattice are more apparent in the normal state of superconductors and hence, in this chapter, we shall be focusing on the application of the gauge/gravity duality to understand certain properties of the boundary system above superconducting transition (so called strange metallic phase). Let us recall from the phase structure of the Cuprates, discussed in chapter (01), that just above the dome (near optimal doping) lies strange metallic phase which defies conventional Fermi liquid theory. The resistivity (electronic contribution) in these materials scales linearly with temperature

(Linear-T resistivity) unlike conventional Fermi liquid metals, which show a quadratic dependency of resistivity on temperature. It has also been experimentally verified that famous Wiedeman-Franz law is violated in these strange metals. The gauge/gravity duality emerged as an indispensable tool to study these non-Fermi liquid properties. In this thesis, we have extended a model of holographic lattice to obtain the Born-Infeld corrected thermoelectric transport coefficients in terms of black hole horizon data. This chapter is based on the following publication,

1) **A. Srivastav**, S. Gangopadhyay and A. Saha, *Born-Infeld corrections to holographic transport coefficients with spatially modulated chemical potential*, Eur. Phys. J. C 83, 458 (2023).

4.1.1 The Inhomogeneous Holographic Lattice Model

We shall start by considering the simplest action consisting of gravity and gauge sector,

$$\mathcal{S} = \int d^4x\sqrt{-g}\left(R + 6 + \mathcal{L}_{BI}\right) . \tag{4.1}$$

The cosmological constant is taken to be $\Lambda = -3$, the AdS radius to be unity, and $16\pi G = 1$. $\mathcal{L}_{BI}$, that is the Lagrangian density for Born-Infeld electrodynamics [131–133], represents the non-linear gauge sector of the model. It is given by the following expression,

$$\mathcal{L}_{BI} = \frac{1}{b}\left(1 - \sqrt{1 + \frac{b}{2}F^2}\right) . \tag{4.2}$$

Various symbols have their usual interpretation as mentioned in the previous chapters.
The action given in eq.(4.1) leads to the following equations of motion,

$$E_{\mu\nu} \equiv R_{\mu\nu} + 3g_{\mu\nu} - \frac{1}{2}T_{\mu\nu} = 0 \tag{4.3}$$

$$\nabla_\mu\left(\frac{F^{\mu\nu}}{\sqrt{1 + \frac{b}{2}F^2}}\right) = 0 . \tag{4.4}$$

Here $E_{\mu\nu}$ stands for the Einstein tensor and $T_{\mu\nu}$ is the energy-momentum tensor associated with $\mathcal{L}_{BI}$, which is given by [134],

$$T_{\mu\nu} = g_{\mu\nu}\mathcal{L}_{BI} + \frac{F_{\mu\rho}F^{\rho}_{\nu}}{\sqrt{1 + \frac{b}{2}F^2}} . \tag{4.5}$$

We set the background geometry to be the planar-Schwarzschild AdS black hole spacetime, which is given by the following metric,

$$ds^2 = -U(r)dt^2 + \frac{dr^2}{U(r)} + \Sigma(r)(dx^2 + dy^2) . \tag{4.6}$$

In this black hole geometry, the blackhole horizon is at $r = 0$ such that the blackening factor vanishes at the horizon, that is $U(r = 0) = 0$. We may now introduce the spatially modulated chemical potential in the boundary theory along the x-direction, $\mu(x)$, given by [127, 129, 130],

$$\mu(x) = \mu_0 + \bar{\mu}(x) \ . \tag{4.7}$$

In the above equation, μ_0 is the constant part of the chemical potential while $\bar{\mu}(x)$ is the periodic part, that is $\bar{\mu}(x) = \bar{\mu}(x + L)$, with period L along x-direction. According to the holographic dictionary, chemical potential can be introduced in a gravity dual by considering the time component of the gauge field, that is $a_t(r, \mathbf{x})$. As mentioned in the previous chapters, usually it is dependent on the bulk coordinate only at the asymptotic boundary and due to regularity conditions on the horizon, it vanishes. In the present scenario, as boundary chemical potential is periodic along x-direction, we need to consider $a_t(r, x)$ to be periodic along x-direction, with the same period, as well. Now, regularity conditions at the black hole horizon require $a_t(0, x) = 0$. So we can take following ansatz for the gauge fields,

$$A_\mu = (a_t(r, x), 0, 0, 0) \ . \tag{4.8}$$

We may now consider the following near horizon expansions for the gauge-field and the metric coefficients as a power series of bulk coordinate, r, as mentioned in [130],

$$a_t(r, x) = r a_t^{(0)}(x) + r^2 a_t^{(1)}(x) + \mathcal{O}(r^3) \tag{4.9}$$

$$U(r) = 4\pi T r + U^{(1)} r^2 + \mathcal{O}(r^3) \tag{4.10}$$

$$\Sigma(r) = \Sigma^{(0)} + r\Sigma^{(1)} + \mathcal{O}(r^2) \ . \tag{4.11}$$

In the above expansions, T denotes the Hawking temperature of the blackhole. It should be noted here that we have not considered any particular form of the blackening factor. However, there are certain constraints on the choice of this blackening factor; for example, it must recover asymptotic AdS structure at the boundary of spacetime. In general, $\Sigma(r)$ and $U(r)$ should be replaced with $\Sigma(r, x)$ and $U(r, x)$, respectively, for completeness as these should be spatially modulated in the x-direction. However to keep the calculations simple, we have assumed $\Sigma(r)$ and $U(r)$ to be independent of x as considered in [135].

We may now define the electric current densities for the dual field theory at the boundary using following expression,

$$J^a \equiv \left(\frac{\sqrt{-g} F^{ar}}{\sqrt{1 + \frac{b}{2} F^2}} \right) |_{r \to \infty} \ . \tag{4.12}$$

The total charge of the blackhole can be obtained from eq.(4.12) in the following manner,

$$q \equiv \frac{1}{L}\int_0^L dx J^t \tag{4.13}$$

where the integral in x-direction is taken over a period of holographic lattice, L. From now onwards, we would be denoting integral over a lattice period in x-direction using the following notation,

$$\frac{1}{L}\int_0^L dx \equiv \int \ .$$

4.2 The Transport Coefficients

In this section, we shall be calculating the holographic transport coefficients. We shall obtain these transport coefficients, within the linear response of the system, for thermoelectric perturbations to the boundary field theory. We shall now apply an external constant electric field E and a thermal gradient $\zeta \equiv -\frac{\nabla T}{T}$ to the boundary field theory. In the bulk gravity theory, these boundary perturbations could be realised in the form of some perturbations to the bulk gauge fields. However, these perturbations would consequently demand certain perturbations in the background bulk metric itself [130]. Within the linear response regime, we may obtain various thermoelectric coefficients defined in the following matrix equation,

$$\begin{pmatrix} J \\ \mathcal{Q} \end{pmatrix} = \begin{pmatrix} \sigma & \alpha T \\ \bar{\alpha} T & \bar{\kappa} T \end{pmatrix} \begin{pmatrix} E \\ \zeta \end{pmatrix} \ . \tag{4.14}$$

In the above matrix, σ is the electric conductivity, $\bar{\kappa}$ is the thermal conductivity while α and $\bar{\alpha}$ are known as thermoelectric conductivities. J and $\mathcal{Q}$ are electric and heat currents respectively. In general, the following relation is known to hold in real materials,

$$\bar{\alpha} = \alpha$$

which is known as the Onsager relation.

From the t-component of the equations of motion of the gauge fields, that is eq.(4.4), we shall obtain,

$$\nabla_r \left(\frac{F^{rt}}{\sqrt{1+\frac{b}{2}F^2}} \right) = 0.$$

This equation implies that charge, q, remains constant along the AdS direction and hence, one can evaluate it anywhere in the AdS direction including the horizon at $r = 0$. Therefore, using the near horizon expansions given by eqs.(4.9, 4.10, 4.11), we shall be able to obtain the Born-Infeld

corrected expression for charge in terms of the blackhole horizon data upto $\mathcal{O}(r)$,

$$q = \int \Sigma^{(0)} a_t^{(0)} \left(1 + \frac{b}{2}(a_t^{(0)})^2\right) . \tag{4.15}$$

We shall start our analysis with the application of a time independent constant electric field E at the boundary theory, which may be introduced on the bulk side as a linear in time perturbation in the gauge field. Application of such an external perturbation would lead to other perturbations in the gauge fields as well as in the background geometry due to the presence of holographic lattice along x-direction. This situation could be realised from the following perturbations in the metric and the gauge fields [130],

$$\delta ds^2 = \delta g_{tt} dt^2 + \delta g_{rr} dr^2 + \delta g_{xx} dx^2 + \delta g_{yy} dy^2 + 2\delta g_{tr} dt dr + 2\delta g_{tx} dt dx + 2\delta g_{xr} dx dr \tag{4.16}$$

$$\delta A_\mu = (\delta a_t, \delta a_r, \delta a_x - Et, 0) . \tag{4.17}$$

It should be noted that all these perturbations, except electric field term Et, are functions of both x and r coordinates and are periodic in the x-direction with the same period, L, with which chemical potential is modulated in the x-direction. Just like the gauge field and metric coefficients given in eqs.(4.9, 4.10, 4.11), we may consider that these perturbations also admit the following near horizon expansions,

$$\begin{aligned}
&\delta a_t = \delta a_t^{(0)} + \mathcal{O}(r) ; && \delta a_r = \frac{1}{U}(\delta a_r^{(0)} + \mathcal{O}(r)) \\
&\delta a_x = \ln U(\delta a_x^{(0)} + \mathcal{O}(r)) ; && \delta g_{tt} = U(\delta g_{tt}^{(0)} + \mathcal{O}(r)) \\
&\delta g_{rr} = \frac{1}{U}(\delta g_{rr}^{(0)} + \mathcal{O}(r)) ; && \delta g_{xx} = \delta g_{xx}^{(0)} + \mathcal{O}(r) \\
&\delta g_{yy} = \delta g_{yy}^{(0)} + \mathcal{O}(r) ; && \delta g_{tr} = \delta g_{tr}^{(0)} + \mathcal{O}(r) \\
&\delta g_{tx} = \delta g_{tx}^{(0)} + \mathcal{O}(r) ; && \delta g_{xr} = \frac{1}{U}(\delta g_{xr}^{(0)} + \mathcal{O}(r)) .
\end{aligned}$$

Various factors of U in some of the perturbations above are appropriately chosen in such a way that the regularity conditions at the horizon look simple. This shall be apparent in the following subsection.

4.2.1 Regularity Conditions

These perturbations need to be regular at the horizon of the blackhole. Therefore, we switch to ingoing Eddington-Finkelstein (EF)-coordinates in order to discuss the regularity conditions for these perturbations at the blackhole horizon. The ingoing EF-coordinates can be obtained from the

following expression,

$$v = t + \int dr \sqrt{\frac{g_{rr}}{g_{tt}}} \,. \tag{4.18}$$

For the considered background metric given in the eq.(4.6), this leads to $v \simeq t + \frac{lnr}{4\pi T}$ (near the blackhole horizon). Now we require these metric perturbations (δds^2) to be regular at the black hole horizon in EF-coordinates, which leads us to the following constraints,

$$\delta g^{(0)}_{tt} + \delta g^{(0)}_{rr} - 2\delta g^{(0)}_{tr} = 0 \tag{4.19}$$

$$\delta g^{(0)}_{xr} = \delta g^{(0)}_{tx} \,. \tag{4.20}$$

The first constraint, given in the eq.(4.19), is obtained by demanding the regularity of the coefficient of dr^2 at the horizon, while the second constraint, given in the eq.(4.20), comes from requiring regularity of the coefficient of $drdx$. Coefficients of the other metric components do not lead to any further constraints on the perturbations at the leading order in r. Let us now analyse the gauge field perturbations in the similar way. Writing gauge field perturbations in the EF-coordinates and demanding regularity at the blackhole horizon leads to the following constraints on these gauge perturbations,

$$\delta a^{(0)}_r = \delta a^{(0)}_t \tag{4.21}$$

$$\delta a^{(0)}_x = -\frac{E}{4\pi T} \,. \tag{4.22}$$

4.2.2 Gauge Currents

We are now in a position to obtain the expressions for the gauge currents associated with the perturbations defined in eqs.(4.16, 4.17). We shall start with computing the electric current, J, due to the applied electric field, E. From gauge equations of motion, given in eq.(4.4), along r and x directions, we find that

$$\left(\frac{\sqrt{-g} F^{xr}}{\sqrt{1 + \frac{b}{2} F^2}} \right) = constant$$

in both r and x. So we may evaluate this expression anywhere along the AdS-direction, including the blackhole horizon at $r = 0$. It is also clear from eq.(4.12) that the expression mentioned above gives the electric current density at the AdS boundary, that is,

$$J \equiv J^x = \left(\frac{\sqrt{-g} F^{xr}}{\sqrt{1 + \frac{b}{2} F^2}} \right)|_{r \to \infty} \,. \tag{4.23}$$

Up to first order in the perturbations, the electric current density is then given by the following expression,

$$J = \left(1 + \frac{b}{2}\{(\partial_r \delta a_t)^2 + \frac{1}{\Sigma U}(\partial_x \delta a_t)^2\}\right)[U(\partial_x \delta a_r - \partial_r \delta a_x) + (\partial_x a_t)\delta g_{tr} - (\partial_r a_t)\delta g_{tx}] \ . \quad (4.24)$$

Using the near horizon expansions for the perturbations mentioned in eq.(4.24), at the leading order in r, we shall obtain the following expression for J,

$$J = \left(1 + \frac{b}{2}(a_t^{(0)})^2\right)(E + \partial_x \delta a_t^{(0)} - a_t^{(0)} \delta g_{tx}^{(0)}) \ . \quad (4.25)$$

Next, we shall focus on the heat current associated with these perturbations, that is heat current generated due to the application of the constant electric field. We note that under reasonable symmetry considerations as mentioned in [130], one may define the heat current by the following expression,

$$\mathcal{Q} = 2\sqrt{-g}\nabla^r K^x - a_t J \ . \quad (4.26)$$

Here, $K = (\frac{\partial}{\partial t}, 0, 0, 0)$ denotes the Killing vector. To first order in the perturbations, this would further simplify to the following expression,

$$\mathcal{Q} = U^2\left(\partial_r\left(\frac{\delta g_{tx}}{U}\right) - \partial_x\left(\frac{\delta g_{tr}}{U}\right)\right) - a_t J \ . \quad (4.27)$$

Now we shall utilise the near horizon expansions for the perturbations along with considering the leading order in r expression for J from eq.(4.25) in the eq.(4.27) to obtain the following result for heat current at leading order in r,

$$\mathcal{Q} = -4\pi T \delta g_{tx}^{(0)} = constant \ . \quad (4.28)$$

Eq.(4.28) implies that $\delta g_{tx}^{(0)}$ is a constant. Further considering the heat current at sub leading order in r, we may also obtain the following constraint,

$$\partial_x(4\pi T \delta g_{tr}^{(0)}) + \delta g_{tx}^{(0)}\left(2U^{(1)} - (a_t^{(0)})^2\left(1 + \frac{b}{2}(a_t^{(0)})^2\right)\right) + a_t^{(0)}\left(1 + \frac{b}{2}(a_t^{(0)})^2\right)(E + \partial_x \delta a_t^{(0)}) = 0 \ . \quad (4.29)$$

Now using the background (that is for unperturbed metric) Einstein equations (E_{tt} and E_{xx}), we obtain the following condition that relates $U^{(1)}$ to the horizon data for the gauge field, that is $a_t^{(0)}$,

$$2U^{(1)} - (a_t^{(0)})^2\left(1 + \frac{b}{2}(a_t^{(0)})^2\right) = 0 \ . \quad (4.30)$$

We shall now substitute eq.(4.30) in eq.(4.29) and obtain the following condition in terms of the blackhole horizon data only,

$$\partial_x(4\pi T\delta g^{(0)}_{tr}) + a^{(0)}_t\left(1+\frac{b}{2}(a^{(0)}_t)^2\right)(E+\partial_x\delta a^{(0)}_t) = 0\ . \tag{4.31}$$

Using eq.(4.25), we may write eq.(4.31) in the following more useful way,

$$\partial_x(4\pi T\delta g^{(0)}_{tr}) + a^{(0)}_t\left(J + a^{(0)}_t\left(1+\frac{b}{2}(a^{(0)}_t)^2\right)\delta g^{(0)}_{tx}\right) = 0\ . \tag{4.32}$$

Integrating this expression over a period of x, we shall obtaint the following result,

$$J\int a^{(0)}_t = \frac{\mathcal{Q}}{4\pi T}\int (a^{(0)}_t)^2\left(1+\frac{b}{2}(a^{(0)}_t)^2\right)\ . \tag{4.33}$$

It should be noted that we have used eq.(4.28) to replace $\delta g^{(0)}_{tx}$ in terms of $\mathcal{Q}$ to obtain the above result. The term involving $\delta g^{(0)}_{tr}$ in the eq.(4.32) vanishes on integration due to periodicity along x-direction. Also, we may rewrite eq.(4.25) in the following form,

$$\frac{J}{\left(1+\frac{b}{2}(a^{(0)}_t)^2\right)} = E + \partial_x\delta a^{(0)}_t + a^{(0)}_t\frac{\mathcal{Q}}{4\pi T} \tag{4.34}$$

and integrate it over a period of x to get,

$$J\int\frac{1}{\left(1+\frac{b}{2}(a^{(0)}_t)^2\right)} = E + \frac{\mathcal{Q}}{4\pi T}\int a^{(0)}_t\ . \tag{4.35}$$

Some simple manipulations with eqs.(4.33, 4.35) lead to the following expressions for the DC responses due to constant electric field, E,

$$\sigma \equiv \frac{J}{E} = \frac{1}{X_b}\left(1+\frac{(\int a^{(0)}_t)^2}{X}\right) \tag{4.36}$$

$$\bar{\alpha} \equiv \frac{\mathcal{Q}}{TE} = \frac{4\pi\int a^{(0)}_t}{X}\ . \tag{4.37}$$

In the above equations, X_b and X are used to denote following expressions,

$$X_b \equiv \int\frac{1}{\left(1+\frac{b}{2}(a^{(0)}_t)^2\right)} \tag{4.38}$$

$$X \equiv \left[\int (a^{(0)}_t)^2\left(1+\frac{b}{2}(a^{(0)}_t)^2\right)\right]X_b - \left(\int a^{(0)}_t\right)^2\ . \tag{4.39}$$

Let us summarise results obtained so far. We have calculated the linear DC responses to the constant electric field, E, applied on a charged plasma in the presence of spatially modulated chemical potential within the holographic modelling. Next, we shall obtain the linear DC response for this holographic model due to an applied temperature gradient, ζ, at the AdS boundary. Again we shall apply this thermal gradient along x- direction, which may be realised with the following bulk perturbations [130],

$$\delta ds^2 = \delta g_{tt}dt^2 + \delta g_{rr}dr^2 + \delta g_{xx}dx^2 + \delta g_{yy}dy^2 + 2\delta g_{tr}dtdr + 2(\delta g_{tx} - tU\zeta)dtdx + 2\delta g_{xr}dxdr \quad (4.40)$$

$$\delta A_\mu = (\delta a_t, \delta a_r, \delta a_x + t a_t \zeta, 0) \ . \quad (4.41)$$

The above perturbations are chosen appropriately so that time dependency drops out from the gauge currents. Regularity conditions for these perturbations at the horizon impose the following constraints,

$$\delta g^{(0)}_{tt} + \delta g^{(0)}_{rr} - 2\delta g^{(0)}_{tr} = 0 \quad (4.42)$$

$$\delta g^{(0)}_{xr} = \delta g^{(0)}_{tx} \quad (4.43)$$

$$\delta g^{(l)}_{tx} = -\frac{\zeta}{4\pi T} \ . \quad (4.44)$$

The new constraint involving $\delta g^{(l)}_{tx}$ is due to the regularity of the metric coefficient of $dtdx$. $\delta g^{(l)}_{tx}$ appears in the near horizon expansion of δg_{tx} in the following way [130, 136–140],

$$\delta g_{tx} = \delta g^{(0)}_{tx} + \delta g^{(l)}_{tx}(U \ln U) + \mathcal{O}(r) \ .$$

Once again the regularity of the gauge perturbations at the blackhole horizon now leads to the following constraints,

$$\delta a^{(0)}_r = \delta a^{(0)}_t \quad (4.45)$$

$$\delta a^{(0)}_x = 0 \ . \quad (4.46)$$

With these new perturbations, we shall proceed in a similar fashion as before and obtain the following expressions for the gauge currents at leading order in r,

$$J = \left(1 + \frac{b}{2}(a^{(0)}_t)^2\right)(\partial_x \delta a^{(0)}_t - a^{(0)}_t \delta g^{(0)}_{tx}) \quad (4.47)$$

$$\mathcal{Q} = -4\pi T \delta g^{(0)}_{tx} \ . \quad (4.48)$$

However, sub leading order in r expansion of the heat current now leads to the following constraint,

$$\partial_x(4\pi T \delta g^{(0)}_{tr}) + a^{(0)}_t \left(1 + \frac{b}{2}(a^{(0)}_t)^2\right)(\partial_x \delta a^{(0)}_t) + 4\pi T\zeta = 0 \ . \quad (4.49)$$

In order to obtain this equation in terms of the horizon data only, we have utilised eq.(4.30). We may further write it in the following useful form using eq.(4.47),

$$\partial_x(4\pi T\delta g^{(0)}_{tr}) + a^{(0)}_t\left(J + a^{(0)}_t\left(1+\frac{b}{2}(a^{(0)}_t)^2\right)\delta g^{(0)}_{tx}\right) + 4\pi T\zeta = 0. \tag{4.50}$$

After integrating eq.(4.50) over a period of x, we shall obtain the following result,

$$J\int a^{(0)}_t + 4\pi T\zeta = \frac{\mathcal{Q}}{4\pi T}\int (a^{(0)}_t)^2\left(1+\frac{b}{2}(a^{(0)}_t)^2\right) \tag{4.51}$$

where we have used eq.(4.48) to replace $\delta g^{(0)}_{tx}$ in terms of $\mathcal{Q}$. Again using simple mathematical rearrangements in eqs.(4.47, 4.48, 4.51), we could easily obtain the following DC responses to the thermal gradient,

$$\bar{\kappa} \equiv \frac{\mathcal{Q}}{T\zeta} = \frac{(4\pi)^2 T X_b}{X} \tag{4.52}$$

$$\alpha \equiv \frac{J}{T\zeta} = \frac{4\pi\int a^{(0)}_t}{X}\,. \tag{4.53}$$

Notice that we have found $\alpha = \bar{\alpha}$, which is the Onsager relation. We may also define the thermal heat current when all other currents are absent from the system. Therefore, setting $J = 0$ we shall get the following result,

$$\kappa \equiv \frac{\mathcal{Q}}{T\zeta}\bigg|_{J=0} = \frac{(4\pi)^2 T}{\int (a^{(0)}_t)^2\left(1+\frac{b}{2}(a^{(0)}_t)^2\right)}\,. \tag{4.54}$$

We may also obtain the Lorentz factors as below,

$$\bar{l} \equiv \frac{\bar{\kappa}}{\sigma T} = \frac{(4\pi)^2 X_b}{\int (a^{(0)}_t)^2\left(1+\frac{b}{2}(a^{(0)}_t)^2\right)} \tag{4.55}$$

$$l \equiv \frac{\kappa}{\sigma T} = \frac{\bar{l}X}{\int (a^{(0)}_t)^2\left(1+\frac{b}{2}(a^{(0)}_t)^2\right)}\,. \tag{4.56}$$

We note that these Lorentz factors are neither constants nor equal to each other, which is indicative of the strongly coupled boundary theory.

To summarize, we have analytically computed non-trivial Born-Infeld corrections to all the thermoelectric DC responses for the holographic model with spatially modulated chemical potential. We have also given the Born-Infeld corrected expressions for the thermal conductivity in the ab-

sence on any other current as well as the expressions for the Lorentz factors. Next we would briefly discuss the thermal DC responses in a two current model built with two independent Born-Infeld currents in the presence of the spatially modulated chemical potential setting, which could be useful for the holographic modelling of the ultra-clean Graphene near charge neutrality point.

4.3 Two Current Model

Seo et.al. in [135] have proposed a holographic model with two gauge currents that captures some of the properties of an ultra-clean Graphene layer near the Dirac point. With the assumption that the charges associated with both independent gauge currents are proportional to each other, they have shown that their results are in agreement with some experiments. They have worked with a homogeneous holographic lattice model built with the axion fields. Here, we are reconsidering such a two gauge current model with non-linear corrections in the presence of an inhomogeneous holographic lattice built with the spatially modulated chemical potential. In particular, we have incorporated the non linearilty in the gauge currents via Born-Infeld parameters. In this section, we would use the results from the previous sections to briefly discuss this two current model and would obtain the thermoelectric coefficients. We shall also make an assumption about charges as in [135] and list analytical results for all the thermoelectric coefficients, which may be directly compared with the results of the single current model obtained in section (4.2).

We shall start with writing the following action with two Born-Infeld currents,

$$\mathcal{S} = \int d^4x\sqrt{-g}\left(R + 6 + \mathcal{L}_{BI_1} + \mathcal{L}_{BI_2}\right) \tag{4.57}$$

where

$$\mathcal{L}_{BI_i} = \frac{1}{b_i}\left(1 - \sqrt{1 + \frac{b_i}{2}F_i^2}\right); \quad (i = 1, 2)\,.$$

The Faraday tensors for the currents are given by $F_i = \partial_{[\mu}A_{i\nu]}$, where $(i = 1, 2)$. The equations of motion, in this case, are following,

$$E_{\mu\nu} \equiv R_{\mu\nu} + 3g_{\mu\nu} - \frac{1}{2}T^{BI_1}_{\mu\nu} - \frac{1}{2}T^{BI_2}_{\mu\nu} = 0 \tag{4.58}$$

$$\nabla_\mu\left(\frac{F_i^{\mu\nu}}{\sqrt{1 + \frac{b_i}{2}F_i^2}}\right) = 0\,; \;\; (i = 1, 2)\,. \tag{4.59}$$

In the background geometry given by eq.(4.6), following a similar analysis as mentioned in section (4.2) with two constant electric field perturbations, namely E_1 and E_2, and the thermal perturbation,

ζ, we may obtain the following results easily,

$$q_i = \int \Sigma^{(0)} a_{it}^{(0)} \left(1 + \frac{b_i}{2}(a_{it}^{(0)})^2\right) + \mathcal{O}(r)\ ;\ \ (i = 1, 2) \tag{4.60}$$

$$\mathcal{Q} = -4\pi T \delta g_{tx}^{(0)} \tag{4.61}$$

$$J_i = \left(1 + \frac{b_i}{2}(a_{it}^{(0)})^2\right)(E_i + \partial_x \delta a_{it}^{(0)} - a_{it}^{(0)} \delta g_{tx}^{(0)}) \tag{4.62}$$

$$\partial_x(4\pi T \delta g_{tr}^{(0)}) + a_{1t}^{(0)}\left(J_1 + a_{1t}^{(0)}\left(1 + \frac{b_1}{2}(a_{1t}^{(0)})^2\right)\delta g_{tx}^{(0)}\right) + a_{2t}^{(0)}\left(J_2 + a_{2t}^{(0)}\left(1 + \frac{b_2}{2}(a_{2t}^{(0)})^2\right)\delta g_{tx}^{(0)}\right) + 4\pi T\zeta = 0. \tag{4.63}$$

Here q_i, $\mathcal{Q}$, and J_i are charges, heat current and electric currents respectively. It should be noted that these expressions are given in terms of the blackhole horizon data only. In the presence of two currents, heat current given by eq.(4.27) modifies into the following equation,

$$\mathcal{Q} = U^2\left(\partial_r\left(\frac{\delta g_{tx}}{U}\right) - \partial_x\left(\frac{\delta g_{tr}}{U}\right)\right) - a_{1t}J_1 - a_{2t}J_2\ . \tag{4.64}$$

Now with some mathematical rearrangements of eqs.(4.61, 4.62, 4.63) and integrations over a period of x, one may write the following equations,

$$J_1 = \frac{1}{X_{b_1}}\left(1 + \frac{(\int a_{1t}^{(0)})^2}{YX_{b_1}}\right)E_1 + \frac{(\int a_{1t}^{(0)})(\int a_{2t}^{(0)})}{YX_{b_1}X_{b_2}}E_2 + \frac{(4\pi T\int a_{1t}^{(0)})}{YX_{b_1}}\zeta \tag{4.65}$$

$$J_2 = \frac{(\int a_{1t}^{(0)})(\int a_{2t}^{(0)})}{YX_{b_1}X_{b_2}}E_1 + \frac{1}{X_{b_2}}\left(1 + \frac{(\int a_{2t}^{(0)})^2}{YX_{b_2}}\right)E_2 + \frac{(4\pi T\int a_{2t}^{(0)})}{YX_{b_2}}\zeta \tag{4.66}$$

$$\mathcal{Q} = \frac{(4\pi T)\int a_{1t}^{(0)}}{YX_{b_1}}E_1 + \frac{(4\pi T)\int a_{2t}^{(0)}}{YX_{b_2}}E_2 + \frac{(4\pi T)^2}{Y}\zeta \tag{4.67}$$

where

$$X_{b_i} \equiv \int \frac{1}{\left(1 + \frac{b_i}{2}(a_{it}^{(0)})^2\right)}\ ;\quad (i = 1, 2) \tag{4.68}$$

$$Y \equiv \sum_{i=1,2}\left\{\int (a_{it}^{(0)})^2\left(1 + \frac{b_i}{2}(a_{it}^{(0)})^2\right) - \frac{(\int a_{it}^{(0)})^2}{X_{b_i}}\right\}. \tag{4.69}$$

Now we may write the generalized Ohm's law in the presence of two electric perturbations E_1, E_2, and a thermal perturbation ζ as $J_i = \Sigma_{ij}E_j$, with the identifications $J_3 \equiv \mathcal{Q}$ and $E_3 \equiv \zeta$, where Σ_{ij} is given by the following matrix [135],

$$\Sigma\begin{pmatrix} \sigma_1 & \delta & \alpha_1 T \\ \bar{\delta} & \sigma_2 & \alpha_2 T \\ \bar{\alpha}_1 T & \bar{\alpha}_2 T & \bar{\kappa} T \end{pmatrix}\ . \tag{4.70}$$

Using eqs.(4.65, 4.66, 4.67), we may directly read off elements of the matrix Σ, which are given below,

$$\sigma_i = \frac{1}{X_{b_i}}\left(1 + \frac{(\int a_{it}^{(0)})^2}{Y X_{b_i}}\right) \tag{4.71}$$

$$\delta = \frac{(\int a_{1t}^{(0)})(\int a_{2t}^{(0)})}{Y X_{b_1} X_{b_2}} = \bar{\delta} \tag{4.72}$$

$$\alpha_i = \frac{4\pi \int a_{it}^{(0)}}{Y X_{b_i}} = \bar{\alpha}_i \tag{4.73}$$

$$\bar{\kappa} = \frac{(4\pi)^2 T}{Y}\ . \tag{4.74}$$

Here, σ_1 and σ_2 are the electric conductivities and $\bar{\kappa}$ is the heat conductivity, while δ, $\bar{\delta}$, α_i, and $\bar{\alpha}_i$ are thermoelectric conductivities. It should be noted that $\delta = \bar{\delta}$ and $\alpha_i = \bar{\alpha}_i$, which is the Onsager relation in the presence of two currents. The thermal heat conductivity, defined when all other currents vanish, could be obtained by setting $J_1 = 0$ and $J_2 = 0$ in eqs.(4.65, 4.66),

$$\kappa \equiv \frac{\mathcal{Q}}{T\zeta}\bigg|_{J_1=0=J_2} = \frac{(4\pi)^2 T}{\sum_{i=1,2}\left\{\int (a_{it}^{(0)})^2\left(1 + \frac{b_i}{2}(a_{it}^{(0)})^2\right)\right\}}\ . \tag{4.75}$$

It has been mentioned earlier that the two current holographic model proposed in [135] explained the experimental results under the assumption that the two charges q_1 and q_2 are proportional to each other. Hence, in this case, we now make the following ansatz,

$$a_{2t}^{(0)} = g a_{1t}^{(0)} \tag{4.76}$$

$$b_2 = \frac{b_1}{g^2} \tag{4.77}$$

which would imply that $q_2 = g q_1$. With these ansatzs, the thermoelectric DC response obtained for the two current model simplifies to the following results,

$$\sigma_1 = \frac{1}{X_{b_1}}\left(1 + \frac{(\int a_{1t}^{(0)})^2}{(1+g^2)X}\right) \quad ; \quad \sigma_2 = \frac{1}{X_{b_1}}\left(1 + \frac{g^2(\int a_{1t}^{(0)})^2}{(1+g^2)X}\right)$$

$$\delta = \frac{g(\int a_{1t}^{(0)})^2}{(1+g^2)X X_{b_1}} = \bar{\delta}$$

$$\alpha_1 = \frac{4\pi \int a_{1t}^{(0)}}{(1+g^2)X} = \bar{\alpha}_1$$

$$\alpha_2 = g\alpha_1 = \bar{\alpha}_2$$

$$\bar{\kappa} = \frac{(4\pi)^2 T X_{b_1}}{(1+g^2)X}$$

$$\kappa = \frac{(4\pi)^2 T}{(1+g^2)\left\{\int (a_{1t}^{(0)})^2 \left(1+\frac{b_1}{2}(a_{1t}^{(0)})^2\right)\right\}} \,. \tag{4.78}$$

Also it should be noted that under the considered ansatz given by eqs.(4.76, 4.77), $X_{b_1} = X_{b_2}$. In the above expressions for thermoelectric coefficients, X is given by,

$$X = \left[\int (a_{1t}^{(0)})^2 \left(1+\frac{b_1}{2}(a_{1t}^{(0)})^2\right)\right] X_{b_1} - \left(\int a_{1t}^{(0)}\right)^2 .$$

The choice of notation X, in eq.(4.78), is being made to emphasize that these results could directly be compared with the results of the single current model given in sections (4.2). Although, there are no results available in the literature for the two current model for inhomogeneous holographic lattice with Maxwell electrodynamics, we may obtain these by simply taking the limit $b_1 \to 0$ in the above results.

4.4 Conclusions and Remarks

In this part of the thesis, we have obtained the analytical expressions for the DC thermoelectric coefficients for inhomogeneous holographic lattice models with single and two independent gauge currents [141]. In these models, we have studied the role of the non linear gauge sector incorporated in the form of the Born-Infeld (BI) electrodynamics. We found that the presence of BI parameter affects the analytic results non trivially. It has been explicitly shown in both the cases that the Lorentz factors are neither constant nor equal to each other, which indicate towards a strong coupling (non Fermi liquid) regime of the boundary system. Following the analytical methods developed by Donos et.al. [130], we have been able to recover all these transport coefficients in terms of black hole horizon data only. In the holographic model with two independent gauge currents, we found a intriguing result constraining the BI parameters of both the gauge fields once we assumed the proportionality of the charges associated with these gauge fields as considered in [135]. We expect these results to be useful in the case of ultra clean Graphene near the charge neutrality point.

The qualitative similarity of the inhomogeneous holographic lattice results obtained in this chapter with the results in [135], which is based on a homogeneous holographic lattice is also worth noticing. A further extension of the results obtained in this chapter in order to fit the experimental results has been left for future works. Among many phenomenological directions in which we may extend such studies, a comparative analysis of the two current model in all the three possible holographic lattices could shed light on the robustness of these applications of the gauge/gravity duality in real physical systems.

CHAPTER 5

Summary and Future Directions

5.1 Thesis Summary

In this thesis, we have explored some simple bottom-up applications of the gauge/gravity duality in physical systems such as layered HTSCs, unconventional superfluids and Graphene in Dirac fluid regime. We have employed analytic techniques to study these holographic systems and showed various interesting results. Our main focus in this thesis was to study the effects of non-linearities introduced in the holographic models and study exotic properties such as vortex structures.

In our work on the holographic superconductor in the presence of a rotating black hole [86], we found that original holographic superconductor models are robust against this modifications in the sense that we still get condensate below a certain critical temperature. However, we observed that the rotating black hole improves the possibility of condensate formation at higher temperatures in comparison to the non-rotating case of a s-wave holographic superconductor. More specifically, we have noted in this analysis that up to a certain rotation value, rotating holographic superconductor is less favourable but beyond that value of the rotation parameter, possibility of higher critical temperature improves. On the other hand, in case of a p-wave holographic superconductor model [98], we found that presence of the Born-Infeld parameter suppresses such condensation at higher temperatures.

We have also studied exotic properties associated with these systems, where we have discovered novel vortex solutions in a rotating holographic superfluid model [124]. In this application of the gauge/gravity duality, we have further studied the dissipative behaviour of the holographic superfluid in the presence of imaginary chemical potential. Interestingly, we figured out that for relativistic conformal holographic superfluids, imaginary chemical potential suppresses dissipation in the system. We have further showed that these vortex solutions are robust prediction of such holographic systems even in the presence of Lifshitz fixed points instead of conformal fixed point [125]. Holographic systems with Lifshitz fixed points are supposed to be dual to a non-relativistic superfluid system. In our study, we have obtained a remarkable difference between

holographic superfluids with Lifshitz fixed point and conformal fixed point. We found that unlike relativistic conformal holographic superfluids (RCHS), in non-relativistic Lifshitz holographic superfluids (NRLHS) imaginary chemical potential supports dissipation in the system. This observation has been checked for its robustness against different approximation order as well as for different trial functions.

Finally, we have studied a holographic model with two gauge currents, which recently became popular for understanding Graphene in Dirac fluid regime [135, 144, 145]. We have first obtained Born-Infeld corrections to all the thermoelectric transport coefficients holographically in terms of the black hole horizon data for a single current inhomogeneous lattice model [141]. We have employed the obtained results to built a two current holographic model of Graphene at the charge neutrality point where Dirac fluid regime exist. Here also the similarity of obtained results to other such models is noteworthy.

5.2 Future Directions

Applied holography (or gauge/gravity duality) is still an emerging field with a lot of uncharted territories. In fact, so far a lot of holographic models have been constructed to explain only a few parts of the phase diagram of the Cuprates. The larger goal of applied holography is to obtain a universal model to explain this phase diagram completely. There are many directions in which such gravity duals should be explored. We list some of the possible future projects below.

1) In this thesis, we have explored models of s-wave and p-wave layered superconductors only. However, as discussed in the first chapter of this thesis, we have enough evidence that Cuprates show d-wave nature in their ground state and hence, a working model of d-wave holographic superconductors is needed. Although some of such gravity duals have been proposed in the past [146–149], a holographic d-wave superconductor is still a mystery.

2) The BCS gap structure is known to have momentum dependency. In holographic models, this momentum dependent gap structure is not usually captured and only recently a holographic model has been proposed that discusses this momentum dependency in the condensation value [150]. This should be explored for various phenomenological settings as well as it would be interesting to see how different phenomenological parameters affect this momentum dependent gap.

3) In holographic superfluidity, investigation of vortex dynamics is less explored. Especially, this problem has only been studied numerically [117] and an analytical exploration could shed more light into the problem.

4) Applied holographic models to understand Graphene in Dirac fluid regime have been gaining momentum for past few years. Still, only a few results have been explored so far and it would be interesting to investigate this problem more rigorously.

5) Apart from applications in quantum matter, this duality has been useful in cosmology and quantum information theory as well. However, only very few holographic models are available for early Universe cosmology. This could also provide a rich avenue where applied holography could shed some more light.

Bibliography

[1] J. Zaanen et.al., *Holographic Duality in Condensed Matter Physics*, Cambridge University Press, November 2015.

[2] M. Natsuume, *AdS/CFT Duality User Guide*, Springer Japan, January 2015.

[3] nLab: AdS-CFT correspondence.

[4] J. Maldacena, *The Large-N Limit of Superconformal Field Theories and Supergravity*, International Journal of Theoretical Physics 38, 1113–1133 (1999).

[5] S. S. Gubser et.al., *Gauge theory correlators from non-critical string theory*, Phys.Lett.B 428, 105-114 (1998).

[6] E. Witten, *Anti de Sitter space and holography*, Adv. Theor. Math. Phys. 2, 253-291 (1998).

[7] P. Coleman, *Introduction to Many-Body Physics*, Cambridge University Press, December 2015.

[8] A. J. Schofield, *Non-Fermi liquids*, Contemporary Physics 40:2, 95-115 (1999).

[9] S. A. Hartnoll et.al., *Holographic Quantum Matter*, The MIT Press, March 2018.

[10] J. M. Ziman, *Electrons and Phonons: The Theory of Transport Phenomena in Solids*, Oxford University Press, February 2001.

[11] M. I. Kaganov and I. M. Lifshits, *Quasiparticles*, Mir Publishers, 1979.

[12] S. Sachdev, *Quantum Phases of Matter*, Cambridge University Press, March 2023.

[13] J. M. Ziman, *Electrons in metals; a short guide to the Fermi surface*, Taylor & Francis London, 1966.

[14] B. Keimer et.al., *From quantum matter to high-temperature superconductivity in copper oxides*, Nature volume 518, pages179–186 (2015).

[15] D. van Delft and P. Kes, *The discovery of superconductivity*, Physics Today 63 (9), 38–43 (2010).

[16] S. J. Blundell, *Superconductivity: A Very Short Introduction* , Oxford University Press, May 2009.

[17] V. L. Ginzburg, *On Superconductivity and Superfluidity (What I Have and Have Not Managed to Do), as well as on the 'Physical Minimum' at the Beginning of the 21st Century*, ChemPhysChem 5:7, 930-945 (2004).

[18] J. Bardeen et.al., *Theory of Superconductivity*, Phys. Rev. 108, 1175 (1957).

[19] J. G. Bednorz and K. A. Müller, *Possible highT c superconductivity in the Ba−La−Cu−O system*, Z. Physik B - Condensed Matter 64, 189–193 (1986).

[20] A. J. Leggett, *What DO we know about high Tc?*, Nature Phys 2, 134–136 (2006).

[21] K. M. Shen and J. C. S. Davis, *Cuprate high-Tc superconductors*, Materials Today 11:9, 14-21 (2008).

[22] A. Amoretti, *Condensed Matter Applications of AdS/CFT Focusing on Strange Metals*, Springer Theses, July 2017.

[23] D. M. Broun, *What lies beneath the dome?*, Nature Phys 4, 170–172 (2008).

[24] S. Sachdev, *Where is the quantum critical point in the cuprate superconductors?*, Phys. Status Solidi B 247, No. 3, 537–543 (2010).

[25] R. W. Hill et.al., *Breakdown of Fermi-liquid theory in a copper-oxide superconductor*, Nature 414, 711–715 (2001).

[26] J. Crossno et.al., *Observation of the Dirac fluid and the breakdown of the Wiedemann-Franz law in graphene*, Science 351,1058-1061(2016).

[27] A. Lucas et.al., *Transport in inhomogeneous quantum critical fluids and in the Dirac fluid in graphene*, Phys. Rev. B 93, 075426 (2016).

[28] R. A. Cooper et.al., *Anomalous Criticality in the Electrical Resistivity of* $La_{2x}Sr_xCuO_4$, Science323,603-607(2009).

[29] R. Daou et.al., *Linear temperature dependence of resistivity and change in the Fermi surface at the pseudogap critical point of a high-Tc superconductor*, Nature Phys 5, 31–34 (2009).

[30] N. E. Hussey et.al., *Dichotomy in the T-linear resistivity in hole-doped cuprates*, Phil. Trans. R. Soc. A 369, 1626–1639 (2011).

[31] A. Legros et.al. *Universal T-linear resistivity and Planckian dissipation in overdoped cuprates*, Nature Phys 15, 142–147 (2019).

[32] P. W. Phillips et.al, *Stranger than metals*, Science 37, eabh4273(2022).

[33] H. V. Löhneysen et.al., *Non-Fermi-liquid behavior in a heavy-fermion alloy at a magnetic instability*, Phys. Rev. Lett. 72, 3262-3265 (1994).

[34] M. J. Kearney and P. N. Butcher, *Thermal transport in disordered systems*, J. Phys. C: Solid State Phys. 21 L265 (1988).

[35] P. Coleman and A. J. Schofield, *Quantum criticality*, Nature 433, 226–229 (2005).

[36] J. Maldacena, *The gauge/gravity duality*, arXiv:1106.6073v2 [hep-th] (2014).

[37] L. Susskind and J. Lindesay, *An Introduction to Black Holes, Information and the String Theory Revolution The Holographic Universe*, World Scientific, December 2004.

[38] M. Baggioli, *Applied Holography A Practical Mini-Course*, SpringerBriefs in Physics, November 2019.

[39] M. Baggioli, *Gravity, holography and applications to condensed matter*, arXiv:1610.02681v2 [hep-th] (2016).

[40] M. Ammon and J. Erdmenger, *Gauge/Gravity Duality Foundations and Applications*, Cambridge University Press, May 2015.

[41] H. Nastase, *Introduction to the AdS/CFT Correspondence*, Cambridge University Press, September 2015.

[42] L. M. Sokolowski, *The bizarre anti-de Sitter spacetime*, International Journal of Geometric Methods in Modern Physics 13 no.9, 1630016 (2016).

[43] D. Tong, *Holographic Conductivity*, Acta Phys. Pol. B 44, 2579 (2013).

[44] L. Susskind and E. Witten, *The Holographic Bound in Anti-de Sitter Space*, arXiv:hep-th/9805114v1 (1998).

[45] A. W. Peet and J. Polchinski, *UV-IR relations in AdS dynamics*, Phys. Rev. D 59, 065011 (1999).

[46] A. V. Ramallo, *Introduction to the AdS/CFT correspondence*, arXiv:1310.4319v3 [hep-th].

[47] K. Skenderis, *Lecture notes on holographic renormalization*, Class. Quantum Grav. 19 5849 (2002).

[48] Y. Kim et.al., *Holographic QCD: Past, present, and future*, Progress in Particle and Nuclear Physics 68 55-112, (2013).

[49] S. Ryu and T. Takayanagi, *Holographic Derivation of Entanglement Entropy from the anti–de Sitter Space/Conformal Field Theory Correspondence*, Phys. Rev. Lett. 96, 181602 (2006).

[50] H. Nastase and K. Skenderis, *Holography for the very early universe and the classic puzzles of hot big bang cosmology*, Phys. Rev. D 101, 021901(R) (2020).

[51] S. A. Hartnoll et.al., *Building a Holographic Superconductor*, Phys. Rev. Lett. 101, 031601 (2008).

[52] T. Hartman, *Quantum Gravity and Black Holes*, Physics 7661, Spring 2015.

[53] T. Sakai and S. Sugimoto, *Low Energy Hadron Physics in Holographic QCD*, Progress of Theoretical Physics 113:4, 843-882, April 2005.

[54] T. Sakai and S. Sugimoto, *ore on a Holographic Dual of QCD*, Progress of Theoretical Physics 114:5, 1083-1118, November 2005.

[55] J. Kaplan, *Lectures on AdS/CFT from the Bottom Up*, Johns Hopkins University, 2016.

[56] J. Erlich, *An introduction to holographic QCD for nonspecialists*, Contemporary Physics, 56:2, 159-171 (2014).

[57] J. Erlich and C. Westenberger, *Tests of universality in AdS/QCD models*, Phys. Rev. D 79, 066014 (2009).

[58] E. Witten, *Quantum Gravity In De Sitter Space*, arXiv:hep-th/0106109 (hep-th).

[59] A. Strominger, *The dS/CFT correspondence*, JHEP10, 034 (2001).

[60] A. Strominger, *Inflation and the dS/CFT Correspondence*, JHEP11, 049 (2001).

[61] P. McFadden and K. Skenderis, *Holography for cosmology*, Phys. Rev. D 81, 021301(R) (2010).

[62] R. Easther et.al., *Constraining holographic inflation with WMAP*, JCAP09, 030 (2011).

[63] M. Dias, *Cosmology at the boundary of de Sitter space using the dS/QFT correspondence*, Phys. Rev. D 84, 023512 (2011).

[64] N. Afshordi et.al., *From Planck Data to Planck Era: Observational Tests of Holographic Cosmology*,

Phys. Rev. Lett. 118, 041301 (2017).

[65] N. Afshordi et.al., *Constraining holographic cosmology using Planck data*, Phys. Rev. D 95, 123505 (2017).

[66] H. Nastase and K. Skenderis, *Holography for the very early universe and the classic puzzles of hot big bang cosmology*, Phys. Rev. D 101, 021901(R) (2020).

[67] S. Sachdev, *What Can Gauge-Gravity Duality Teach Us About Condensed Matter Physics?*, Annual Review of Condensed Matter Physics 3:1, 9-33 (2012).

[68] S. S. Gubser, *Breaking an Abelian gauge symmetry near a black hole horizon*, Phys. Rev. D 78, 065034 (2008).

[69] R. Cai et.al., *Introduction to holographic superconductor models.*, Sci. China Phys. Mech. Astron. 58, 1–46 (2015).

[70] E. Witten, *Anti-de Sitter space, thermal phase transition, and confinement in gauge theories*, ATMP 2:3, 050-532 (1998).

[71] P. Wittmer, *Application of Black-Hole Physics to Vortex Dynamics in Superfluids*, Dissertation, December 2020.

[72] Y. Kamihara et.al., *Iron-Based Layered Superconductor* $LaO_{1-x}F_xFeAs$ *(*$x = 0.05 - 0.12$*) with* T_c *= 26 K*, . Am. Chem. Soc. 130, 11, 3296–3297 (2008).

[73] R. M. Fernandes et.al., *Iron pnictides and chalcogenides: a new paradigm for superconductivity*, Nature 601, 35–44 (2022).

[74] S. A. Hartnoll et.al., *Holographic Superconductors*, JHEP12, 015 (2008).

[75] C. P. Herzog, *Lectures on holographic superfluidity and superconductivity*, J. Phys. A: Math. Theor. 42, 343001 (2009).

[76] S. A. Hartnoll, *Lectures on holographic methods for condensed matter physics*, Class. Quantum Grav. 26, 224002 (2009).

[77] S. Gangopadhyay and D. Roychowdhury, *Analytic study of properties of holographic superconductors in Born-Infeld electrodynamics*, J. High Energ. Phys. 2012, 2 (2012).

[78] S. Gangopadhyay and D. Roychowdhury, *Analytic study of Gauss-Bonnet holographic superconductors in Born-Infeld electrodynamics*, J. High Energ. Phys. 2012, 156 (2012).

[79] S. Gangopadhyay, *Analytic study of properties of holographic superconductors away from the probe limit*, Phys. Letters B. 724, 1-3 (2013).

[80] D. Ghorai and S. Gangopadhyay, *Higher dimensional holographic superconductors in Born–Infeld electrodynamics with back-reaction*, Eur. Phys. J. C 76, 146 (2016).

[81] G. Siopsis and J. Therrien, *Analytic Calculation of Properties of Holographic Superconductors*, J. High Energ. Phys. 2010, 13 (2010).

[82] S. S. Gubser and S. S. Pufu, *The gravity dual of a p-wave superconductor*, JHEP 11, 033 (2008).

[83] J. D. Bekenstein, *Black hole hair: twenty–five years after*, arXiv:gr-qc/9605059v1 (1996).

[84] J. Sonner, *Rotating holographic superconductor*, Phys. Rev. D 80, 084031 (2009).

[85] K. Lin and E. Abdalla, *Holographic superconductors in a rotating spacetime*, Eur. Phys. J. C 74, 3144 (2014).

[86] A. Srivastav and S. Gangopadhyay, *Analytic investigation of rotating holographic superconductors*, Eur. Phys. J. C 79, 340 (2019).

[87] R. Gregory et.al., *Holographic superconductors with higher curvature corrections*, JHEP10, 010 (2009).

[88] A. Sheykhi, *Charged rotating dilaton black strings in (A)dS spaces*, Phys. Rev. D 78, 064055 (2008).

[89] P. Breitenlohner and D. Z. Freedman, *Stability in gauged extended supergravity*, Annals of Physics 144:2, 249-281 (1982).

[90] P. Breitenlohner and D. Z. Freedman, *Positive energy in anti-de Sitter backgrounds and gauged extended supergravity*, Phys. Letters B 145:3, 197-201 (1982).

[91] B. G. Levi, *In High-T_c Superconductors, is D-Wave the New Wave?*, Physics Today 46 (5), 17–20 (1993).

[92] V. J. Emery, *The search for symmetry*, Nature 370, 598 (1994).

[93] J. R. Kirtley et.al., *Symmetry of the order parameter in the high-T_c superconductor $YBa_2Cu_3O_{7-\delta}$*, Nature 373, 225–228 (1995).

[94] M. Guidry et.al., *The Superconducting Critical Temperature*, Symmetry 13(5), 911 (2021).

[95] N. C. Yeh et.al., *Evidence of Doping-Dependent Pairing Symmetry in Cuprate Superconductors*, Phys. Rev. Lett. 87, 087003 (2001).

[96] E. F. Talantsev et.al., *p-wave superconductivity in iron based superconductors*, Sci Rep 9, 14245 (2019).

[97] R. G. Cai et.al., *A holographic p-wave superconductor model*, J. High Energ. Phys. 2014, 32 (2014).

[98] A. Srivastav et.al., *p-wave holographic superconductors with massive vector condensate in Born–Infeld electrodynamics*, Eur. Phys. J. C 80, 219 (2020).

[99] S. Weinberg, *Superconductivity for Particular Theorists*, PTSP 86, 43-53 (1986).

[100] E. Bergshoeff et.al., *The Born-Infeld action from conformal invariance of the open superstring*, Phys. Letters B 188:1, 70-74 (1987).

[101] R. R. Metsaev et.al., *The born-infeld action as the effective action in the open superstring theory*, Phys. Letters B 193:2-3, 207-212 (1987).

[102] M. Baggioli and O. Pujolas, *On effective holographic Mott insulators*, J. High Energ. Phys. 2016, 107 (2016).

[103] Y. F. Alam and A. Behne, *Review of Born-Infeld electrodynamics*, arXiv:2111.08657v4 [physics.class-ph].

[104] H. S. Jeong et.al., *Collective dynamics and the Anderson-Higgs mechanism in a bona fide holographic superconductor*, J. High Energ. Phys. 2023, 206 (2023).

[105] K. Maeda et.al., *Two pieces of folklore in the AdS/CFT duality*, Phys. Rev. D 82, 046002 (2010).

[106] O. Domenech et.al., *Emergent gauge fields in holographic superconductors*, J. High Energ. Phys. 2010, 33 (2010).

[107] P.J. Silva, *Dynamical gauge fields in holographic superconductors*, Fortsch. Phys. 59, 756 (2011).

[108] O.V. Lounasmaa and E. Thuneberg, *Vortices in rotating superfluid ^3He*, Proc. Natl. Acad. Sci. U.S.A. 96, 7760 (1999).

[109] G. E. Volovik, *Superfluids in rotation: Landau—Lifshitz vortex sheets vs Onsager—Feynman vortices*, Phys.Usp. 58, 897 (2015).

[110] M. Montull et.al., *Holographic Superconductor Vortices*, Phys. Rev. Lett. 103, 091601 (2009).

[111] T. Albash and C. V. Johnson, *A holographic superconductor in an external magnetic field*, JHEP 09, 121 (2008).

[112] T. Albash and C. V. Johnson, *Vortex and droplet engineering in a holographic superconductor*, Phys. Rev. D 80, 126009 (2009).

[113] T. Albash and C. V. Johnson, *Phases of Holographic Superconductors in an External Magnetic Field*, arXiv:0906.0519v1 [hep-th].

[114] X. Li et.al., *Generation of vortices and stabilization of vortex lattices in holographic superfluids*, J. High Energ. Phys. 2020, 104 (2020).

[115] X. Chaun-Yin et.al, *Holographic Abrikosov lattice: Vortex matter from black hole*, Phys. Rev. D 105, L021901 (2022).

[116] J. A. Herrera-Mendoza, *Vortex structure deformation of rotating Lifshitz holographic superconductors*, Phys. Rev. D 106, L081902 (2022).

[117] P. M. Chesler et al., *Holographic Vortex Liquids and Superfluid Turbulence*, Science341,368-372(2013).

[118] X. Chaun-Yin et.al, *Vortex lattice in a rotating holographic superfluid*, Phys. Rev. D 100, 061901(R) (2019).

[119] K. Maeda et.al., *Vortex lattice for a holographic superconductor*, Phys. Rev. D 81, 026002 (2010).

[120] K. Ghoroku et.al., *Extension to imaginary chemical potential in a holographic model*, Phys. Rev. D 102, 046003 (2020).

[121] G. E. Cragg and A. K. Kerman, *Complex Chemical Potential: Signature of Decay in a Bose-Einstein Condensate*, Phys. Rev. Lett. 94, 190402 (2005).

[122] S. Kachru et.al., *Gravity duals of Lifshitz-like fixed points*, Phys. Rev. D 78, 106005 (2008).

[123] Y. Bu, *Holographic superconductors with z = 2 Lifshitz scaling*, Phys. Rev. D 86, 046007 (2012).

[124] A. Srivastav and S. Gangopadhyay, *Novel vortices and the role of a complex chemical potential in a rotating holographic superfluid*, Phys.Rev.D 104:12, 126004 (2021).

[125] A. Srivastav and S. Gangopadhyay, *Vortices in a rotating holographic superfluid with Lifshitz scaling*, Phys.Rev.D 107:8, 086005 (2023).

[126] G. T. Horowitz et.al., *Optical conductivity with holographic lattices*, J. High Energ. Phys. 2012, 168 (2012).

[127] G. T. Horowitz and J. E. Santos, *General relativity and the cuprates*, J. High Energ. Phys. 2013, 87 (2013).

[128] M. Baggioli et.al., *Holographic axion model: A simple gravitational tool for quantum matter*, Sci. China Phys. Mech. Astron. 64, 270001 (2021).

[129] P. Chesler et.al., *Conformal field theories in a periodic potential: Results from holography and field theory*, Phys. Rev. D 89, 026005 (2014).

[130] A. Donos and J. P. Gauntlett, *The thermoelectric properties of inhomogeneous holographic lattices*, J. High Energ. Phys. 2015, 35 (2015).

[131] P. A. M. Dirac, *A Reformulation of the Born-Infeld Electrodynamics*, Proc. R. Soc. Lond. Ser. A Math. Phys. Sci. 257(1288), 32–43 (1960).

[132] R. Banerjee et.al., *Holographic s-wave condensate with nonlinear [132] electrodynamics: A nontrivial boundary value problem*, Phys. Rev. D 87, 104001 (2013).

[133] D. Ghorai and S. Gangopadhyay, *Non-linear effects on the holographic free energy and thermodynamic geometry*, EPL 118 31001 (2017).

[134] J. P. Wu et.al., *Holographic transports from Born–Infeld electrodynamics with momentum dissipation*, Eur. Phys. J. C 78, 900 (2018).

[135] Y. Seo et.al., *Holography of the Dirac Fluid in Graphene with Two Currents*, Phys. Rev. Lett. 118, 036601 (2017).

[136] A. Donos and J. P. Gauntlett, *Holographic Q-lattices*, J. High Energ. Phys. 2014, 40 (2014).

[137] A. Donos and J. P. Gauntlett, *Novel metals and insulators from holography*, J. High Energ. Phys. 2014, 7 (2014).

[138] A. Donos and J. P. Gauntlett, *Thermoelectric DC conductivities from black hole horizons*, J. High Energ. Phys. 2014, 81 (2014).

[139] A. Donos and J. P. Gauntlett, *Navier-Stokes equations on black hole horizons and DC thermoelectric conductivity*, Phys. Rev. D 92, 121901(R) (2015).

[140] E. Banks et.al., *Thermoelectric DC conductivities and Stokes flows on black hole horizons*, . High Energ. Phys. 2015, 103 (2015).

[141] A. Srivastav et.al., *Born–Infeld corrections to holographic transport coefficients with spatially modulated chemical potential*, Eur. Phys. J. C 83, 458 (2023).

[142] Y. Ling, *Holographic lattice in Einstein-Maxwell-dilaton gravity*, J. High Energ. Phys. 2013, 6 (2013).

[143] N. Jokela et.al, *Holographic sliding stripes*, Phys. Rev. D 95, 086006 (2017).

[144] M. Rogatko and K. I. Wysokinski, *Two interacting current model of holographic Dirac fluid in graphene*, Phys. Rev. D 97, 024053 (2018).

[145] M. Rogatko and K. I. Wysokinski, *Conductivity bound of the strongly interacting and disordered graphene from gauge/gravity duality*, Phys. Rev. D 101, 046019 (2020).

[146] F. Benini et.al., *Gauge gravity duality for d-wave superconductors: prospects and challenges*, J. High Energ. Phys. 2010, 137 (2010).

[147] J-W. Chen et.al., *Towards a holographic model of D-wave superconductors*, Phys. Rev. D 81, 106008 (2010).

[148] F. Benini et.al., *Holographic Fermi arcs and a d-wave gap*, Physics Letters B 701:5, 626-629 (2011).

[149] K-Y. Kim and M. Taylor, *Holographic d-wave superconductors*, J. High Energ. Phys. 2013, 112 (2013).

[150] D. Ghorai et.al., *Momentum dependent gap in holographic superconductors revisited*, J. High Energ. Phys. 2022, 98 (2022).